Production and Assessment of Cellulose Nanofibril Films

Alexandrea Maerz

A thesis

submitted in partial fulfillment of the

requirements for the degree of

Master of Science

University of Washington

2024

Committee:

Rick Gustafson

Renata Bura

Anthony Dichiara

Program Authorized to Offer Degree:

School of Environmental and Forest Sciences

©Copyright 2024

Alexandrea Maerz

University of Washington

Abstract

Production and Assessment of Cellulose Nanofibril Films

Alexandrea Maerz

Chair of the Supervisory Committee:

Rick Gustafson

School of Environmental and Forest Sciences

This research was a study on the production and characterization of novel, high (i.e. above 80 wt.%) nanocellulose (CNF) content. These films were successfully created after an established CNF production process (Pascoli, Dichiara, Roumeli, Gustafson, & Bura, 2022) using alkaline pulping and a peracetic acid (PAA) pretreatment was scaled to a kilogram scale. The resulting CNF pulping yield was 68 %, and both chemical and morphological composition of the CNF was maintained from the translation from gram to kilogram scale production. The average CNF fiber diameter was 21.0 nm and the average length weighted was 0.89 mm; high levels of cellulose (100 %) and hemicellulose (92 %) were maintained, contributing to the optical and mechanical properties of the CNF. This CNF was then used in combination with polyvinyl alcohol (PVA) to create film composites at high CNF (i.e. above 80 wt.%) and low PVA (i.e. below 20 wt.%) ratios. These films had unexpectedly impressive optical properties with a

maximum haze of 94.7 % in 100 % CNF films and a maximum light transmittance at 660 nm of 85.7 % at 660 nm in 85 % CNF films. This unique combination of high haze and high light transmittance lends the films to a variety of exciting applications. The composite films were also evaluated for mechanical properties, and 100 % CNF were found to have a high tensile strength of 86.3 MPa with a peak elongation of 4.2 %. These results indicated that the films retain flexibility associated with traditional plastic while benefiting from enhanced mechanical properties associated with CNF. Furthermore, the films were evaluated for mass retention when submerged in moist soil for eleven weeks and for susceptibility to water via contact angle analysis. It was found that the films did not immediately undergo decomposition and remained relatively stable in soil, and they exhibited a decreased susceptibility to water when compared to 100 % PVA control films. The outstanding properties of the film suggest potential applications in solar energy conversion devices, single-use food packaging, or agricultural mulch coverings.

TABLE OF CONTENTS

LIST OF FIGURES ..... **iii**

LIST OF TABLES ..... **iv**

1. Introduction to Plastic Waste, Bioplastics, and Nanocellulose/Polyvinyl Alcohol Films **2**

1.1 THE PROBLEM WITH PLASTIC 2
1.2 BIOPLASTICS SOLUTION 3
1.2.1 Nanocellulose Definitions 3
1.2.2 Properties and Applications of Nanocellulose 4
1.2.3 Production of Nanocellulose 4

2. Research Objectives **6**

2.1 CNF/PVA COMPOSITE FILM PRODUCTION WITH USE OF KILOGRAM SCALE CNF PRODUCTION PROCESS 6

3. Production and Assessment of Cellulose Nanofibril Films **8**

3.1 ABSTRACT 8
3.2 INTRODUCTION 10
3.2 MATERIALS AND METHODS 13
3.2.1 Raw Material 13
3.2.2 Alkaline Peroxide Delignification and Refining 13
3.2.3 Peracetic Acid Pretreatment 13
3.2.4 Nano Lignocellulosic Fibers Production 13
3.2.5 CNF/PVA Composite Films 14
3.2.6 Characterization Techniques 15
3.2.6.1 Mass Yield After Pulping and Pretreatment 15
3.2.6.2 Chemical Composition 15
3.2.6.3 Nano Lignocellulosic Fibrils Characterization 15
3.2.6.4 Composite Film Optical Characterization 16
3.2.6.5 Composite Film Mechanical Characterization 16
3.2.6.6. Composite Film Additional Characterization 16

4. Results and Discussion **18**

4.1 MASS YIELD AND INCREASE FROM GRAM TO KILOGRAM SCALE 18
4.2 EFFECT OF CHEMICAL TREATMENTS ON FIBER CHEMICAL COMPOSITION 19
4.3 NANO LIGNOCELLULOSIC FIBRILS CHARACTERIZATION 20
4.3.1 Fiber Surface Chemistry 20
4.3.2 Fiber Structure and Morphology 21
4.4. CNF/PVA COMPOSITE FILMS CHARACTERIZATION 22

4.4.1 Composite Film Optical Properties 24
4.4.2 Composite Film Mechanical Properties 28
4.4.3 Additional Film Characterization 31

5. Conclusions 37

6. Conclusion and Future Work 38

6.1 CONCLUSION 38
6.2 FUTURE WORK 38

BIBLIOGRAPHY 40

APPENDIX A. SUPPLEMENTARY DATA 45

LIST OF FIGURES

Figure 1. Schematic of the CNF/PVA composite film production process. 18
Figure 2. SEM and FQA fiber analysis. 22
Figure 3. Representative cross-section micrographs of cryo-fractured composite films. 23
Figure 4. Optical data of CNF/PVA composite films. 28
Figure 5. Mechanical data of CNF/PVA composite films. 31
Figure 6. Extended contact angle on CNF/PVA composite films. 33
Figure 7. CNF films for stability testing. 35

LIST OF TABLES

Table 1. Chemical description and mass balance of the agricultural residue (WS), the WS refined pulp, the previously reported CNF produced on a gram scale, and the CNF produced on a kilogram scale in the current study. 20

ACKNOWLEDGEMENTS

This research is supported by the USDA NIFA through the McIntire-Stennis grant and by the Lewis County, WA legislative body. Part of this work was conducted at the Molecular Analysis Facility, a National Nanotechnology Coordinated Infrastructure (NNCI) site at the University of Washington, which is supported in part by funds from the National Science Foundation award NNCI-1542101. Special thanks go to the research advisors and Bura-Gustafson laboratory group members for their unwavering dedication and the invaluable expertise they contributed to this project.

1. Introduction to Plastic Waste, Bioplastics, and Nanocellulose/Polyvinyl Alcohol Films

1.1 THE PROBLEM WITH PLASTIC

The need for sustainable materials is critical across all industries. One material that has been particularly problematic due to our reliance on it combined with its longevity and short-term use is plastic. Approximately 99% of traditional plastic materials are derived from non-renewable fossil fuel sources (Fossil Fuels & Plastic, 2019). To produce plastic, crude oil or natural gas undergo extraction and refinement, both of which are carbon-intensive methods. Next in the process comes polymerization, wherein the monomers from the base molecule transition into polymers—forming extended chains of interconnected monomers that contribute to the desirable, versatile properties of plastic such as durability and flexibility. Further processing, involving mixing with additional substances while in liquid form, yields the plastic material. This liquid mixture is typically solidified into pellets before entering the molding process, ultimately shaping it into a market-ready final plastic product (Zhong, Zhao, Qian, & Zou, 2018).

The recycling of traditional plastics presents further challenges. Complex polymer compositions and the lack of standardized recycling methods contribute to low recycling rates, with a vast majority ending up in landfills or incineration facilities (OCED, 2022). These disposal methods exacerbate environmental issues, releasing harmful gases and toxins into the atmosphere and soil (Qin et al., 2021). Plastic materials are used in so many applications because they are versatile and cheap to produce, but only 9% of plastic globally is ever recycled into another usable form (OCED, 2022). Fossil fuel-based plastics have become a convenient part of our everyday lives, but the negative impact they have on the planet underscores an urgent need to search for alternatives.

1.2 BIOPLASTICS SOLUTION

Bioplastics offer an alternative to synthetic plastics made from fossil fuels. They maintain flexibility and versatility, making them applicable across a range of industries. Cost of production is often recognized as a barrier for bioplastic production, but recent innovations combined with increased consumer demand for sustainable products encourages a trend towards cheaper bioplastic production (Pierobon, Eastin, & Ganguly, 2018). When selecting a material as the basis for a bioplastic, many previous studies focus on nanocellulose (CNF)—a biopolymer made from plants composed of glucose monomers—at low percentages (i.e. below 20 wt.%) combined with polyvinyl alcohol (PVA) —a water-soluble polymer—at high percentages (i.e. above 80 wt.%). This combination of materials is well studied, but there exists a research gap into bioplastics produced with the inverse set of conditions: CNF above 80 wt.% and PVA below 20 wt.%. Thus, the basis for this study is the production of bioplastics with 80 to 100 wt.% CNF content, using PVA as a plasticizer.

1.2.1 Nanocellulose Definitions

Cellulose is a polysaccharide composed of glucose monomers and makes up the main component of plant cell walls. When broken down via either chemical or physical processes—or a combination of the two—cellulose can gain additional properties characteristic of materials that exist in the nano scale. When these fibers have at least one dimension in the range of 1 to 100 nm, they can be considered nanocellulose, abbreviated as NFC or CNF. Depending on the method of production, cellulose nanocrystals or CNC can also be produced. The distinction between CNF and CNC depends on the amount of crystalline or amorphous regions present in the material. CNC has more crystalline regions and are more rigid than CNF, which are fibrous

in structure (Xu et al., 2013). Additionally, bacterial nanocellulose can be produced, although this is via a separate process called biosynthesis (see section 1.2.3).

1.2.2 Properties and Applications of Nanocellulose

Nanocellulose is known for having unique properties related to the material dimension(s) being on the nanoscale. It is widely regarded for its high strength and impressive mechanical properties, large surface area that increases as dimensions decrease, crystallinity that can be manipulated, and high degree of polymerization (Khalid, Al Rashid, Arif, Ahmed, & Arshad, 2021). Additionally, since cellulose is derived from plant material, CNF is made from renewable materials and often has a lower environmental impact than fossil-fuel based counterparts. These properties lend CNF to be a material that can be used across a wide range of applications with the potential to improve sustainability. These applications can include plastics, paper, paint, drug delivery, biosensors, energy storage, and many others (Thomas et al., 2018). The focus of this thesis is on the application of CNF to composite bioplastics.

1.2.3 Production of Nanocellulose

There are many current methods of nanocellulose production that divide into two categories: biosynthesis and mechanical and/or chemical. Biosynthesis can be a method of nanocellulose production (Skiba, Shavyrkina, Skiba, Mironova, & Budaeva, 2023), although it is not the method of choice due to issues associated with maintaining bacteria and cost relative to the quality of nanocellulose produced. Within the category of mechanical and/or chemical, the first of note utilizes TEMPO-oxidation process to produce cellulose nanofibers. This process results in high-quality, high-cost nanofibers that are often used in more specialty applications such as drug delivery (Kaffashsaie et al., 2021). Acid hydrolysis can be used for nanocellulose production, and the dimensions and crystallinity of the nanocellulose produced depend on the specific production method used but can result in CNC or CNF (Pradhan, Jaiswal, & Jaiswal,

2022). The method of CNF production of greatest importance to this thesis is a novel process published by the Bura-Gustafson lab group utilizing alkaline pulping and PAA pretreatment to produce CNF with exceptional properties at low cost (Pascoli, Dichiara, Roumeli, Gustafson, & Bura, 2022).

2. Research Objectives

The primary goal of this research was to develop CNF/PVA composite films using high CNF content and low PVA content. Bioplastics that are currently available have problems related to efficient degradation, high manufacturing costs, and inadequate mechanical and barrier properties. The films in this thesis research were created as a material that has the potential to be used in place of traditional plastics, thereby improving sustainability and offering an alternative to fossil fuel-based plastics.

2.1 CNF/PVA COMPOSITE FILM PRODUCTION WITH USE OF KILOGRAM SCALE CNF PRODUCTION PROCESS

This research centered on the production of thin, flexible, and translucent nanocellulose composite films with low poly(vinyl) alcohol contents (below 20 wt.%) for use as a bioplastic. For this to be attained in an environmentally friendly manner, the availability of sustainably sourced nanocellulose (CNF) was essential for film prototype production and testing. Previously published research on the production of by Danielle Pascoli, a former member of the Bura laboratory group, was scaled from a gram amount basis of production to a kilogram amount basis of production for this purpose. The lignocellulosic nanomaterials needed for bioplastic production also needed to be cost-effective and thus were sourced from the agricultural residue wheat straw. The resulting CNF was thoroughly characterized before being used in the preparation of CNF/PVA composite films. Additional mechanically fibrillated nanofibrils (MCNF) were purchased from the University of Maine and used in the preparation of supplementary composite films for evaluation as a control high MCNF content bioplastic.

These composite films' mechanical, optical, and barrier properties were then thoroughly evaluated for use in various applications. This novel bioplastic proves the potential to replace

petroleum-derived plastics in various industries. Promising applications encompass agriculture such as mulch films, aquaculture including biodegradable nets, and packaging—especially food packaging.

3. Production and Assessment of Cellulose Nanofibril Films

3.1 ABSTRACT

This research was a study on the production and characterization of novel, high (i.e. above 80 wt.%) nanocellulose (CNF) content. These films were successfully created after an established CNF production process (Pascoli, Dichiara, Roumeli, Gustafson, & Bura, 2022) using alkaline pulping and a peracetic acid (PAA) pretreatment was scaled to a kilogram scale. The resulting CNF pulping yield was 68 %, and both chemical and morphological composition of the CNF was maintained from the translation from gram to kilogram scale production. The average CNF fiber diameter was 21.0 nm and the average length weighted was 0.89 mm; high levels of cellulose (100 %) and hemicellulose (92 %) were maintained, contributing to the optical and mechanical properties of the CNF. This CNF was then used in combination with polyvinyl alcohol (PVA) to create film composites at high CNF (i.e. above 80 wt.%) and low PVA (i.e. below 20 wt.%) ratios. These films had unexpectedly impressive optical properties with a maximum haze of 94.7 % in 100 % CNF films and a maximum light transmittance at 660 nm of 85.7 % at 660 nm in 85 % CNF films. This unique combination of high haze and high light transmittance lends the films to a variety of exciting applications. The composite films were also evaluated for mechanical properties, and 100 % CNF were found to have a high tensile strength of 86.3 MPa with a peak elongation of 4.2 %. These results indicated that the films retain flexibility associated with traditional plastic while benefiting from enhanced mechanical properties associated with CNF. Furthermore, the films were evaluated for mass retention when submerged in moist soil for eleven weeks and for susceptibility to water via contact angle analysis. It was found that the films did not immediately undergo decomposition and remained relatively stable in soil, and they exhibited a decreased susceptibility to water when compared to

100 % PVA control films. The outstanding properties of the film suggest potential applications in solar energy conversion devices, single-use food packaging, or agricultural mulch coverings.

3.2 INTRODUCTION

Over the past several decades, it has become clear that there is a critical need for sustainable materials across all industries. One material that has been particularly problematic due to our reliance on it combined with its longevity and short-term use is plastic. Approximately 99% of traditional plastic materials are derived from non-renewable fossil fuel sources (Fossil Fuels & Plastic, 2019). The recycling of traditional plastics presents further challenges. Complex polymer compositions and the lack of standardized recycling methods contribute to low recycling rates, with a vast majority ending up in landfills or incineration facilities (OCED, 2022). These disposal methods exacerbate environmental issues, releasing harmful gasses and toxins into the atmosphere and soil (Qin et al., 2021). Plastic materials are used in so many applications because they are versatile and cheap to produce, but only 9% of plastic globally is ever recycled into another usable form (OCED, 2022). Fossil fuel-based plastics have become a convenient part of our everyday lives, but the negative impact they have on the planet underscores an urgent need to search for alternatives.

Bioplastics, which can be made from renewable resources such as agricultural or forest residues, offer an alternative to fossil fuel-based plastics. Their production emits fewer greenhouse gasses, significantly reducing their carbon footprint when compared to their fossil fuel-based counterparts (Posen, Jaramillo, Landis, & Griffin, 2017). Moreover, bioplastics can be biodegradable, allowing for less harmful disposal and reducing environmental harm in the long-term (Ali et al., 2023; Kibédi-Szabó et al., 2011; Kjeldsen, Price, Lilley, Guzniczak, & Archer, 2018). Their versatility in applications mirrors that of traditional plastics, making them a feasible substitute in various industries (Ingrao et al., 2015; Jones, Speight, Blinco, & O'Hara, 2022; Kibédi-Szabó et al., 2011; Muniyasamy, Ofosu, John, & Anandjiwala, 2016). Cost barriers have

previously prohibited bioplastic production from being an economically viable option (Azapagic, 2014; Li et al., 2023). With innovative manufacturing techniques and increased demand for sustainable products, the cost gap between bioplastics and traditional plastics is narrowing (Pascoli, Dichiara, Roumeli, Gustafson, & Bura, 2022; Pierobon, Eastin, & Ganguly, 2018; Roumeli et al., 2022) Additionally, the potential for job creation and growth of a circular economy integrated with the renewable resource sector further supports the adoption of bioplastics whenever possible (Rosenboom, Langer, & Traverso, 2022).

There is extensive research into what material best suits bioplastic production, and one option is nanocellulose. Nanocellulose (CNF) is a linear polysaccharide comprised of glucose monomers; it is made from plant cellulose fibers and has at least one dimension in the nanoscale. CNF has a large surface area and high degree of polymerization, leading to uniquely tunable optical mechanical properties and high strength (Khalid, Al Rashid, Arif, Ahmed, & Arshad, 2021). Additionally, since cellulose is derived from plant material, CNF is made from renewable materials and often has a lower environmental impact than fossil-fuel based counterparts. Polyvinyl alcohol (PVA) is a biodegradable, hydrophilic polymer, but is known to have inferior mechanical properties compared to synthetic alternatives. When applied as a plastic material, these properties often necessitate the use of additives in conjunction with PVA. CNFs can improve the mechanical performance of PVA composites when added due to CNFs high aspect ratio, large surface area, and good interfacial interactions with PVA (Aslam, Kalyar, & Raza, 2018), and there is a body of research about the use of CNF to reinforce the PVA matrix (Asad et al., 2018; Espinosa et al., 2019; Lee, You, Jin, & Kwak, 2020; Majumdar et al., 2023; Oishi, Nakaya, Matsui, & Hotta, 2015; Srithep, Turng, Sabo, & Clemons, 2012; Xing, Hu, Zhang, Guan, & Gu, 2020). Apart from a few outliers (Forti et al., 2021; Silva et al., 2020), almost all

previous research focuses on films with low percentages of CNF (less than 20%) and high percentages of polymer (greater than 80%). With this research gap identified, this study was designed to explore the inverse of these previous studies: films with 80 to 100% CNF content, using PVA as a plasticizer.

The final problem to address was the cost of materials for CNF film production. CNF is known to be prohibitively expensive, around $1000 USD/kg (Balea et al., 2020; Serra et al., 2017), and is not currently produced at a scale large enough for use in applications like packaging or agriculture where it would be single use. To mitigate this, a novel nanocellulose production process using alkaline peroxide pulping and peracetic acid pretreatment that was previously reported by the Bura-Gustafson lab group was scaled up from a gram scale production to kilogram scale production. As a result, the predicted cost of CNF was reduced to approximately $4 USD/kg, and enough CNF was available to make high CNF, low PVA bioplastics.

3.2 MATERIALS AND METHODS

3.2.1 Raw Material

The swath-cut wheat straw used as the feedstock for nanocellulose production was purchased from Snohomish County, WA.

The polyvinyl alcohol (PVA) had a MW of 89,000-98,000 and was 99+% hydrolyzed, and it was sourced from Sigma-Aldrich. The peracetic acid (PAA) was sourced from Sigma-Aldrich.

3.2.2 Alkaline Peroxide Delignification and Refining

The wheat straw underwent a presoak for 20 minutes at 75 ℃. It was then delignified via alkaline peroxide pulping at 95 ℃ for 150 minutes. Following this reaction, the pulp was washed with deionized water, screened, and refined using a PFI mill for 30,000 revolutions.

3.2.3 Peracetic Acid Pretreatment

The refined pulp was then oxidized using peracetic acid (PAA) following a previously published procedure (Pascoli, Dichiara, Roumeli, Gustafson, & Bura, 2022). with some modifications. The refined pulp was combined with a 4 wt.% PAA solution at 4.8 pH in an IKA HB 10 rotary evaporator. The reaction proceeded at 85 ℃ for 45 minutes. The sample was filtered using a vacuum filtration. The pulp then underwent a 2-step wash with a caustic solution followed by multiple DI water washes.

3.2.4 Nano Lignocellulosic Fibers Production

The PAA treated pulp was suspended to 0.4 % consistency and mechanically fibrillated for 30 minutes using a commercial blender. The resulting product was homogenous in consistency and morphology and can be classified as nanocellulose (CNF) as the morphology of

the fibers had any dimension within the nanoscale from 1 to 100 nm and the fibers produced were composed of cellulose (Khalid, Al Rashid, Arif, Ahmed, & Arshad, 2021). All samples were refrigerated at approximately 2 ℃ to 5 ℃ and kept in glass bottles until use.

For use as a control, mechanically fibrillated nanofibrils (MCNF) were purchased from the University of Maine. Initially measured to have a consistency of 3.15% (Appendix A), this MCNF was diluted to 0.4% for direct comparison with the produced CNF.

3.2.5 CNF/PVA Composite Films

Nanocellulose (CNF)/polyvinyl alcohol (PVA) composite films were prepared using a previously reported, simple solvent casting method (Lu, Wang, & Drzal, 2008). with some modifications. Solid PVA was dissolved at 90 ℃ into DI water at 5 wt.%. This was then combined with either the produced CNF or the purchased MCNF at 0.4 % consistency and additional DI water in a beaker and mixed for approximately 15 minutes. Each film's starting volume was controlled to be 125 mL to achieve about 0.5 g total solids per film. The solution was batch sonicated for 30 minutes before being carefully poured into a deep petri dish 100 mm in diameter. They were then placed in a vacuum oven at -25 “Hg for approximately 48 hours at 60 ℃ to dry. All films were conditioned for approximately 48 h at 25 ℃ and 27 % relative humidity prior to further testing.

These composite films were reinforced with a range of CNF contents. Films were prepared at 95, 90, 85, and 80 wt.% CNF. MCNF was used to prepare control films with the same range of wt.% MCNF contents along with 100 wt.% PVA control films.

3.2.6 Characterization Techniques

3.2.6.1 Mass Yield After Pulping and Pretreatment

After alkaline pulping and fiber screening, the mass yield was calculated gravimetrically based on the oven dry weight of the fibers after each processing step compared to the feedstock oven dry weight.

3.2.6.2 Chemical Composition

To understand how each chemical treatment affected the produced fibers, the chemical composition of the wheat straw feed stock, the refined pulp, and the PAA pretreated pulp were evaluated. Following previously established methods (Dou, Bura, Ewanick, & Morales-Vera, 2019; Dou, Marcondes, Djaja, Bura, & Gustafson, 2017; Horhammer, Dou, Suko, Gustafson, & Bura, 2018; Pascoli, Suko, Gustafson, Gough, & Bura, 2021), the cellulose, hemicellulose, and lignin (both acid-soluble and acid-insoluble) content were quantified via Klason analysis. Ash analysis was performed gravimetrically (Sluiter et al., 2008). Water and ethanol Soxhlet extraction was used to find extractives content with a 12 h reflux time (Sluiter, Ruiz, Scarlata, Sluiter, & Templeton, 2008). Ultimately, the percentage extractives associated with ethanol were negligible, so extraction calculations for CNF were based solely on water Soxhlet extraction.

3.2.6.3 Nano Lignocellulosic Fibrils Characterization

A conductometric titration previously described (Besbes, Alila, & Boufi, 2011) was used with minor modifications to assess the charge density of the fibers.

Fiber morphology of the CNF and MCNF was assessed using scanning electron microscope (SEM) and fiber quality analysis (FQA). For imaging, samples were coated with approximately 2 nm Platinum and an Apero-S SEM was used to obtain images. For FQA, all

fibers (CNF and MCNF) were subjected to a 4 minutes of batch sonication at 100 % amplitude to ensure no bundles were present during the time of analysis.

3.2.6.4 Composite Film Optical Characterization

The optical transmittance and haze of the films was characterized using a PerkinElmer UV/VIS/NIR Spectrometer Lambda 750 ranging from 400 nm to 780 nm. The light transmittance of these films was further evaluated using the percent transmittance at the chosen point of 660 nm.

3.2.6.5 Composite Film Mechanical Characterization

To serve as a benchmark for industry comparison and to ensure consistency across composite films produced, the thickness of all films was evaluated using a Thwing-Albert electronic thickness tester.

The tensile strength, peak elongation, and Young's modulus were found using a Thwing-Albert EJA Vantage-10 (standard method TAPPI T494) at a gauge length of 42 mm. A minimum of seven specimens per sample were tested.

3.2.6.6. Composite Film Additional Characterization

The air permeability of the composite films was evaluated using the Jinan Xhinghua Instrument Co., LTD Air Permeability Tester.

To visualize and confirm dispersion of PVA and CNF within the films, the edge of the composite films was imaged using SEM. To do this, the films were subjected to liquid nitrogen and cryo-fractured, then the fractured surface was coated with approximately 2 nm Platinum and imaged using SEM.

To evaluate the wettability of the composite films, the static and dynamic contact angle of water on the surface of each film composition was evaluated using drop shape analysis with

FTÅ200. For the static contact angle, an image was taken immediately after a drop of water was added to the surface of each film. This was repeated three times to attain the average static contact angle. Then, to evaluate the stability of the film surface in contact with water over an extended period of time, a drop of water was added to a new sample of each film, and this recorded for 10 minutes with a static contact angle being calculated every 30 seconds. For the dynamic contact angle, water was pumped onto the surface of another new film sample for 10 seconds, then retracted until the water droplet had disconnected from the dispersion nozzle. Then, the contact angle hysteresis was calculated as the receding angle subtracted from the advancing angle.

The composite films were evaluated for stability using a previously described procedure (Roumeli et al., 2022) with some modifications. Five samples of composite films of each composition, each approximately 2 cm x 2cm, were subjected to soil and constant humidity over the course of 11 weeks. Each week, the samples were removed from the soil, dried in an oven at 65°C, then weighed on an O.D. basis.

4. Results and Discussion

4.1 MASS YIELD AND INCREASE FROM GRAM TO KILOGRAM SCALE

Figure 1 shows the kilogram scale CNF production process and the CNF/PVA composite film production process. The previously described CNF production process was successfully increased from a gram scale to a kilogram scale (from now on referred to as the gram scale CNF in reference to the previous research (Pascoli, Dichiara, Roumeli, Gustafson, & Bura, 2022) and the kilogram scale CNF in reference to the current study). This process resulted in an average pulping yield of 68 % (see Table A3) and an average yield of 55 % after screening (see Table A4).

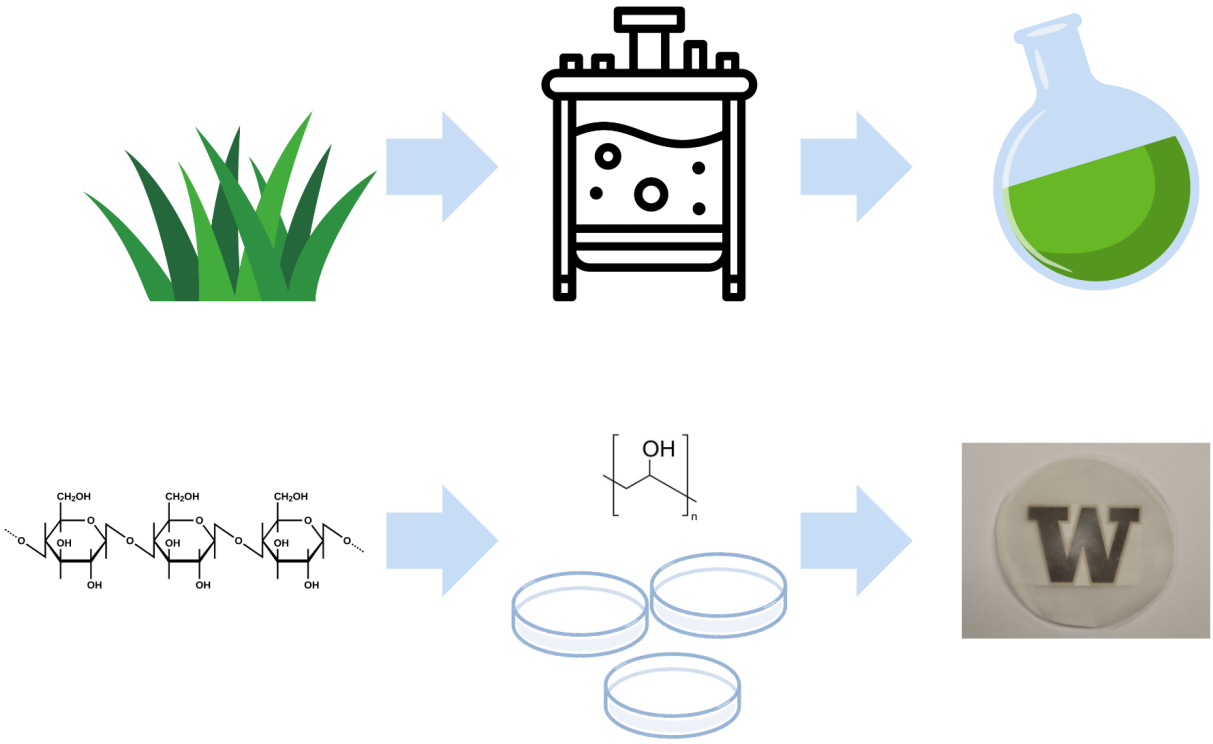


Figure 1. Schematic of the CNF/PVA composite film production process.

4.2 EFFECT OF CHEMICAL TREATMENTS ON FIBER CHEMICAL COMPOSITION

Table 1 presents changes in chemical composition throughout the process, including cellulose, hemicellulose, and lignin recovery related to the original wheat straw (WS). Chemical and morphological values for the gram scale CNF were previously quantified by Danielle Pascoli, a former member of the Bura lab group (Pascoli, Dichiara, Roumeli, Gustafson, & Bura, 2022). The ash and extractives content of the wheat straw refined pulp produced on a kilogram scale (1 % and 5 %, respectively) were comparable to that which was previously reported at a gram scale (2 % and 3 %, respectively). The pulping conditions resulted in pulp with only 26 % lignin at a kilogram scale. In contrast, the cellulose and hemicellulose were mostly recovered in the kilogram scale refined pulp at 100 % and 73 %, respectively. This demonstrates a low sugar loss throughout the pulping reaction. After the wheat straw had been sufficiently delignified, it was subjected to a peracetic acid (PAA) pretreatment procedure. At the kilogram scale, the PAA pretreatment resulted in a high cellulose (100 %) and hemicellulose (92 %) recovery, while some lignin (9 %) was also retained (Table 1) as PAA is a relatively mild delignification process. This further demonstrates the success of the alkaline pulping and PAA pretreatment when translated from gram to kilogram scale.

Table 1. Chemical description and mass balance of the agricultural residue (WS), the WS refined pulp, the previously reported CNF produced on a gram scale, and the CNF produced on a kilogram scale in the current study.

	Chemical composition (%)				
Biomass	**Cellulose**	**Hemicellulose**	**Lignin**	**Ash***	**Extractives***
Agricultural residue (WS)	39.9 ± 1.0	23.4 ± 0.9	22.8 ± 1.3	7.9 ± 0.6	13.9 ± 0.5
Gram scale WS refined pulp	57.7 ± 0.7	26.6 ± 0.3	8.2 ± 0.1	1.9 ± 0.1	2.7 ± 0.1
Kilogram scale WS refined pulp	64.8 ± 0.6	25.1 ± 1.1	8.7 ± 1.4	1.4 ± 0.4	5.4 ± 0.5
Gram scale CNF[1]	67.1 ± 0.5	25.5 ± 1.0	7.0 ± 0.4	0.3 ± 0.0	0.0 ± 0.0
Kilogram scale CNF	72.0 ± 1.6	24.8 ± 1.7	2.3 ± 0.4	-	-

	Mass balance			
Biomass	**Mass yield (%)**	**Cellulose recovery (%)**	**Hemicellulose recovery (%)**	**Lignin recovery (%)**
Gram scale WS refined pulp	65.8	99.9	79.6	19.2
Kilogram scale WS refined pulp	68.3	99.9	73.3	26.1
Gram scale CNF[1]	52.9	99.7	61.3	13.2
Kilogram scale CNF	59.5	99.9	92.3	8.8

**Note that ash and extractive analysis was not performed on kilogram scale CNF as both were previously reported to be about zero when evaluated for gram scale CNF. Additional information related to calculations for this table are available in the appendix Tables A4, A10, A11, and A12).*

4.3 NANO LIGNOCELLULOSIC FIBRILS CHARACTERIZATION

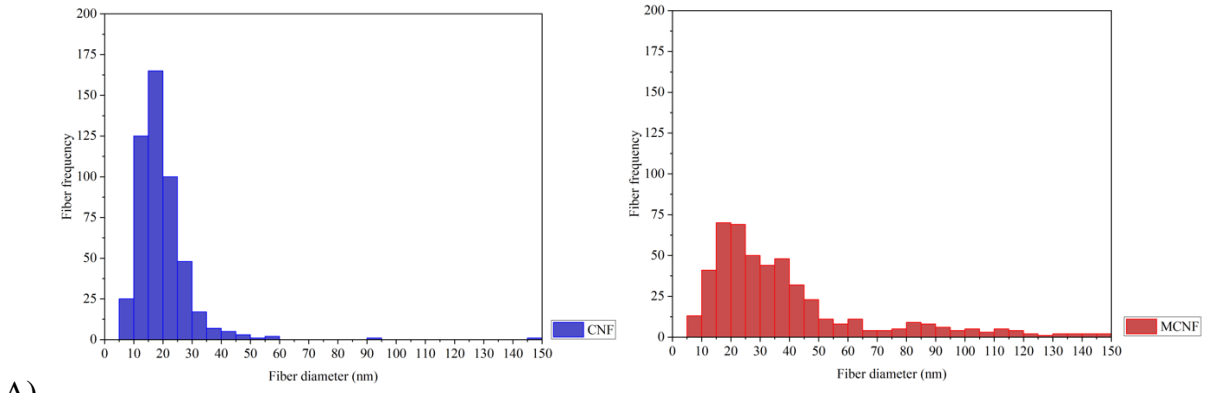
4.3.1 Fiber Surface Chemistry

The charge density (CD) of the CNF and MCNF was measured using conductometric titration. The CNF average CD was measured to be 139 mmol/g, and the average CD of the MCNF 163 mmol/g (see Table A13 and Figures A1 through A18). The gram scale CD was

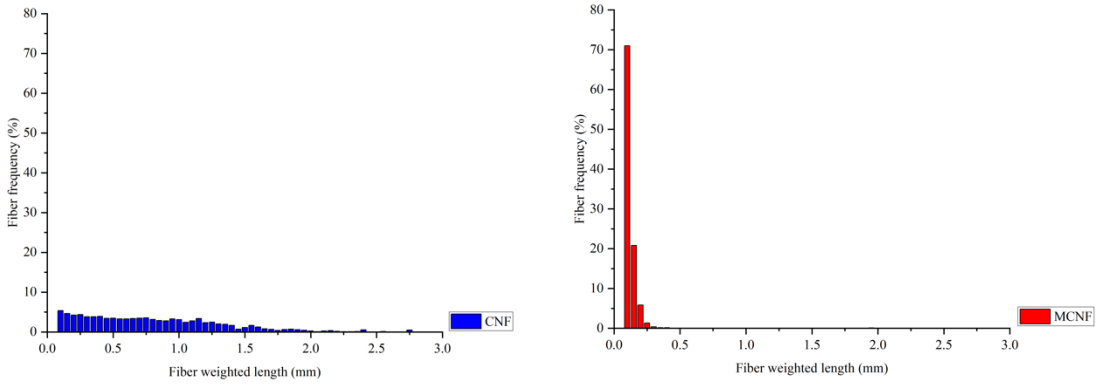
previously reported to range from 105 to 266 mmol/g (Pascoli, Dichiara, Roumeli, Gustafson, & Bura, 2022). The low CD can be attributed to the PAA oxidation mechanism only targeting the reducing end-groups in polysaccharides.

4.3.2 Fiber Structure and Morphology

To confirm that the morphology of CNF fibers produced at a kilogram scale was the same as those produced at a gram scale, the previously reported diameter of gram scale CNF was compared to the kilogram scale CNF. The kilogram scale CNF was found to be 21.0 nm, similar to the gram scale CNF diameter of 16.4 nm.



A)



B)

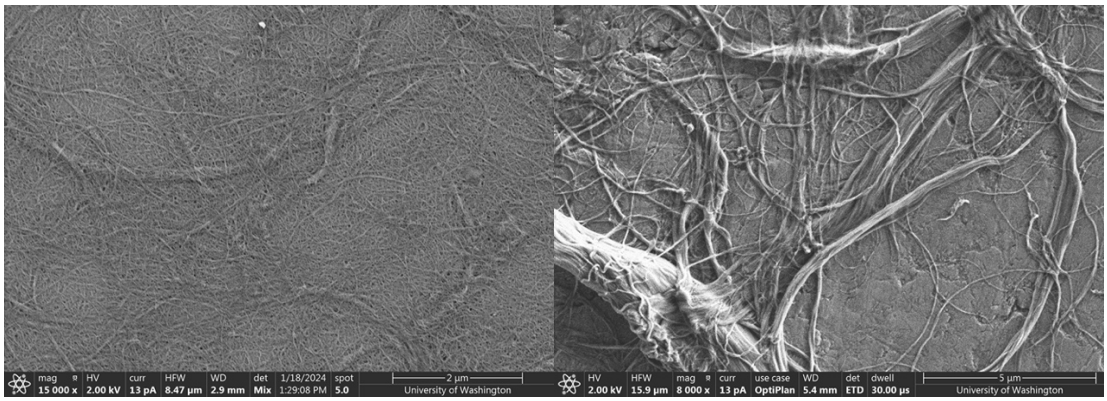
C) 

Figure 2. SEM and FQA fiber analysis.

A) SEM fiber distribution showing the diameter of CNF fibers (left) and the diameter of MCNF fibers (right). B) FQA fiber distribution showing the length of CNF fibers (left) and the length of MCNF fibers (right). C) SEM image of CNF fibers (left) and MCNF fibers (right).

Figure 2 shows the distribution of CNF and MCNF fiber diameters collected using SEM (A), the distributions of CNF and MCNF fiber lengths collected using FQA (B), and SEM images of both. After confirmation that the gram scale CNF morphology was the same as the kilogram scale CNF, the kilogram scale CNF was then compared to the MCNF control using SEM to evaluate fiber diameter and FQA to evaluate fiber length. Kilogram scale CNF had a diameter of 21.0 nm and a length of 0.89 mm (see Tables A8 and A9). Comparatively, the MCNF was found to have a much larger fiber diameter of 45.3 nm and length of 0.23 mm.

Qualitatively, the distribution of kilogram scale CNF diameter is much narrower compared to MCNF, and the distribution of kilogram scale CNF length is much wider compared to MCNF. A potential explanation is that the MCNF was exceedingly short from fiber cutting due to its mechanical production, compared to kilogram scale CNF where there was minimal mechanical treatment.

4.4. CNF/PVA COMPOSITE FILMS CHARACTERIZATION

Novel composite films with a low percent polymer composition were successfully produced using a simple solvent casting method. The resulting flexible, strong plastics were extensively

characterized and found to have an extraordinarily high percent haze and percent light transmittance along with improved mechanical properties as compared to 100 % PVA films.

Figure 3 shows SEM images of the edge of films with compositions 100 % PVA, 100 % CNF, 80 % CNF and 85 % CNF. To ensure that the nanocellulose (either CNF or MCNF) and PVA were well dispersed throughout the film, a portion of each film was cryo-frozen, fractured, and evaluated using SEM. These images confirmed a good distribution of PVA throughout CNF and MCNF, indicating a successful integration of the two compounds in the composite material.

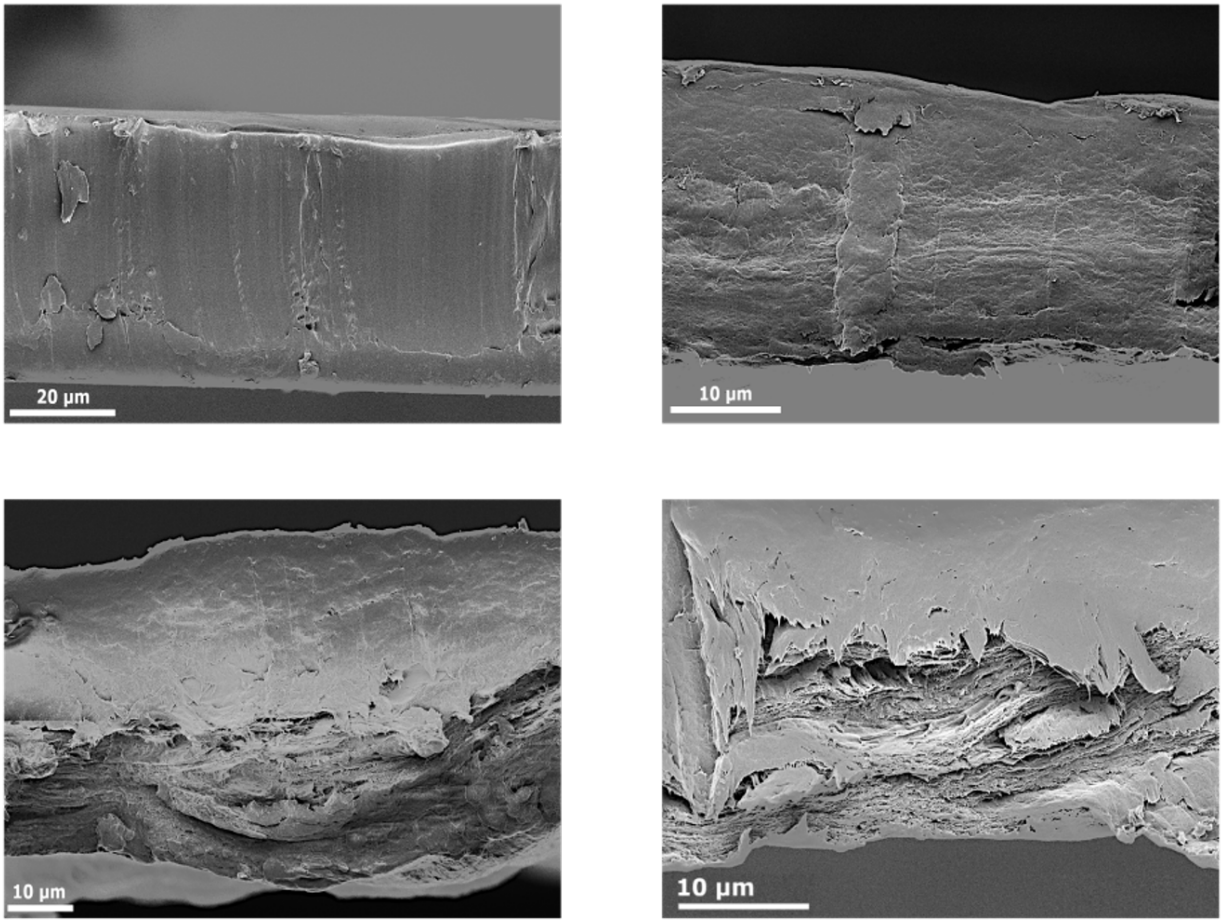


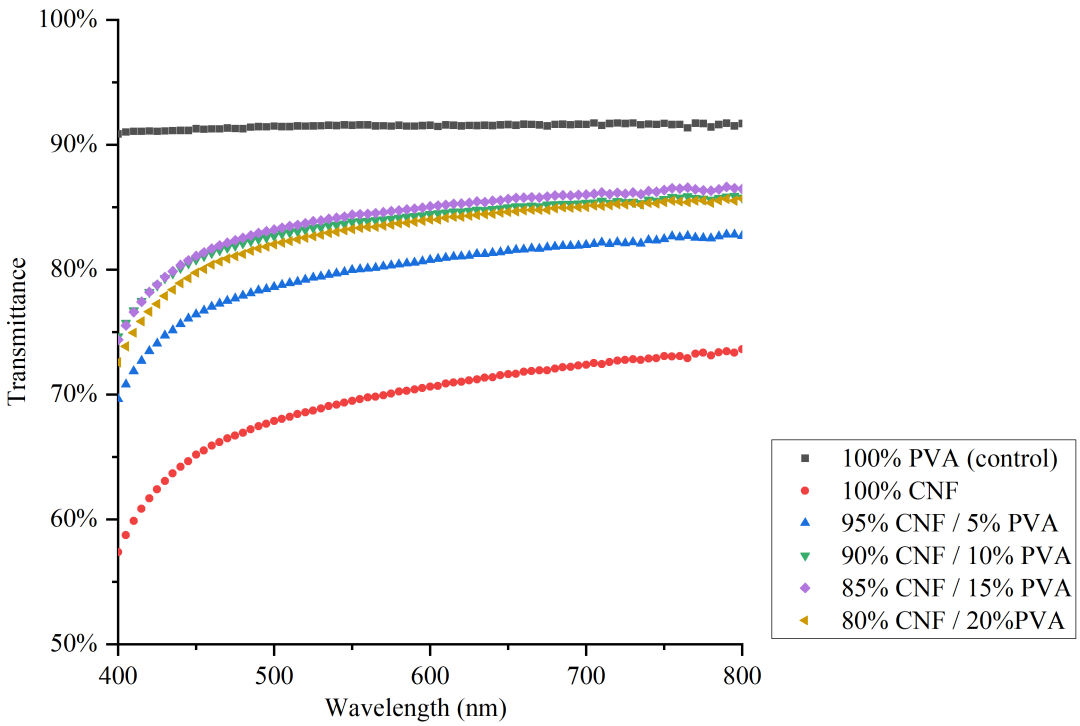
Figure 3. Representative cross-section micrographs of cryo-fractured composite films. Films were prepared at CNF/PVA mass ratio of A) 0/100, B) 100/0, C) 80/20, and D) 85/15.

4.4.1 Composite Film Optical Properties

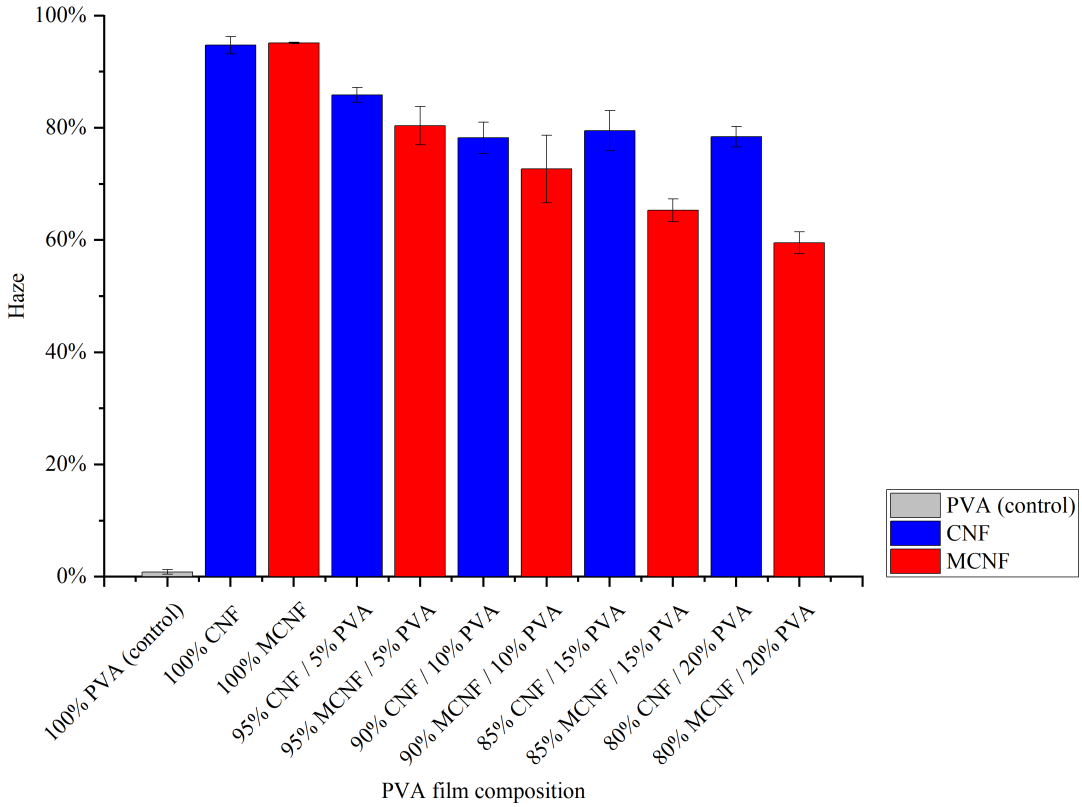
Figure 4 shows A) the percent light transmittance of the composite films from 400 to 800 nm, B) the percent haze of the composite films, C) a comparison of the two and D) a qualitative explanation of these properties. The PVA control films had expectedly the highest transmittance of 91 % at the chosen light transmittance of 660 nm (see Table A18). Surprisingly, the CNF films maintained a very high transmittance at this point as well around 72 %. As the amount of PVA increased in the films, the light transmittance also increased in almost all instances; 80% CNF films had a light transmittance of 85 % at 660 nm. This holds true for films made with MCNF as well.

When evaluated for haze, the PVA control had a very low haze of 0.8 %, which was expected. The haze of 100% CNF films was approximately 95 % (see Table A19), and this was unexpectedly high. As the amount of PVA increased in the films, the haze also decreased in almost all instances; 80% CNF films had a haze of 78 %. This trend held true for films made with MCNF as well.

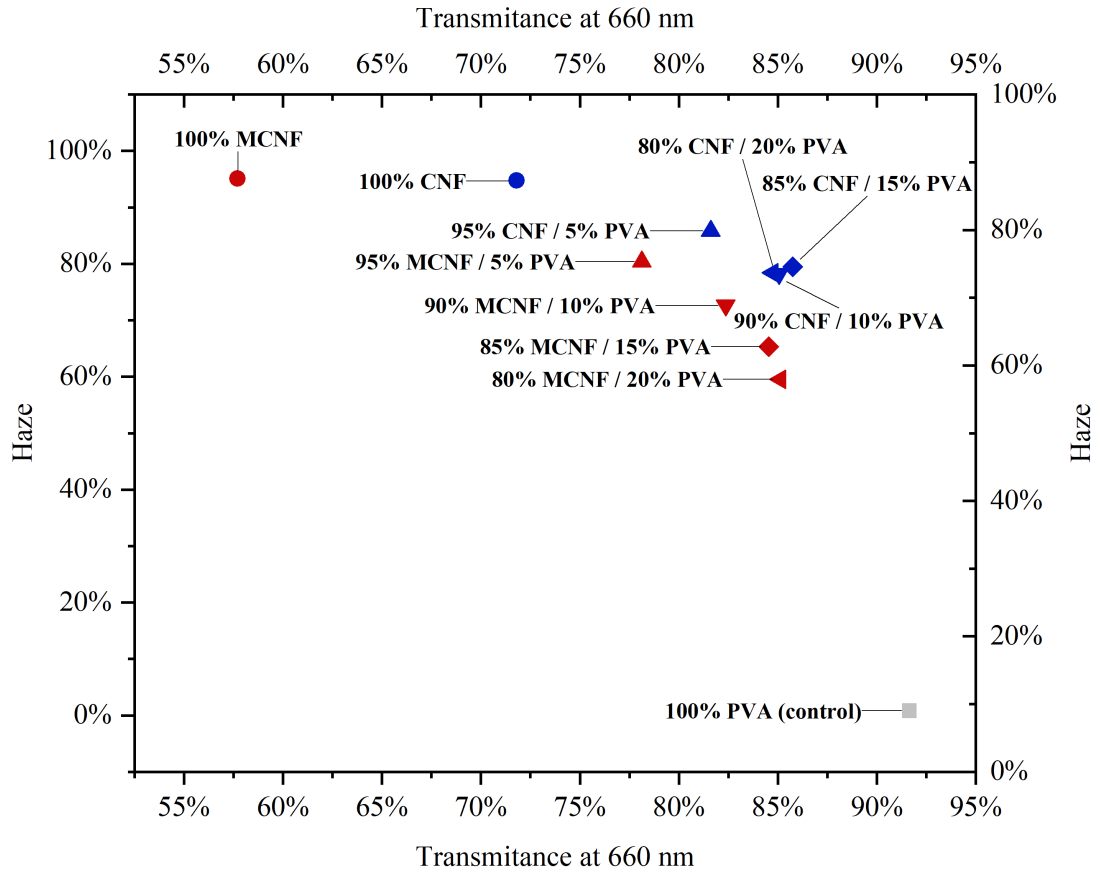
The optical properties of the composite films imply that a wide range of exciting applications are possible and improved values compared to previous literature. For example, one previous study into the haze and transparency of nanocellulose reported a light transmittance of 90 % and a haze of 47 % (Chen, Song, & Xu, 2018). The results of the current study are excellent because typically materials with high haze have low light transmittance, inverse also being true. Because of this, the novel bioplastics produced can be considered desirable properties for use in solar conversion. Furthermore, the composites could be integrated with other paperboard materials to create transparent biodegradable food packaging with optical properties superior to currently available options.


100%
90%
80%
70%
60%
50%
Transmittance
400
500
600
700
800
Wavelength (nm)
100% PVA (control)
100% CNF
95% CNF / 5% PVA
90% CNF / 10% PVA
85% CNF / 15% PVA
80% CNF / 20%PVA

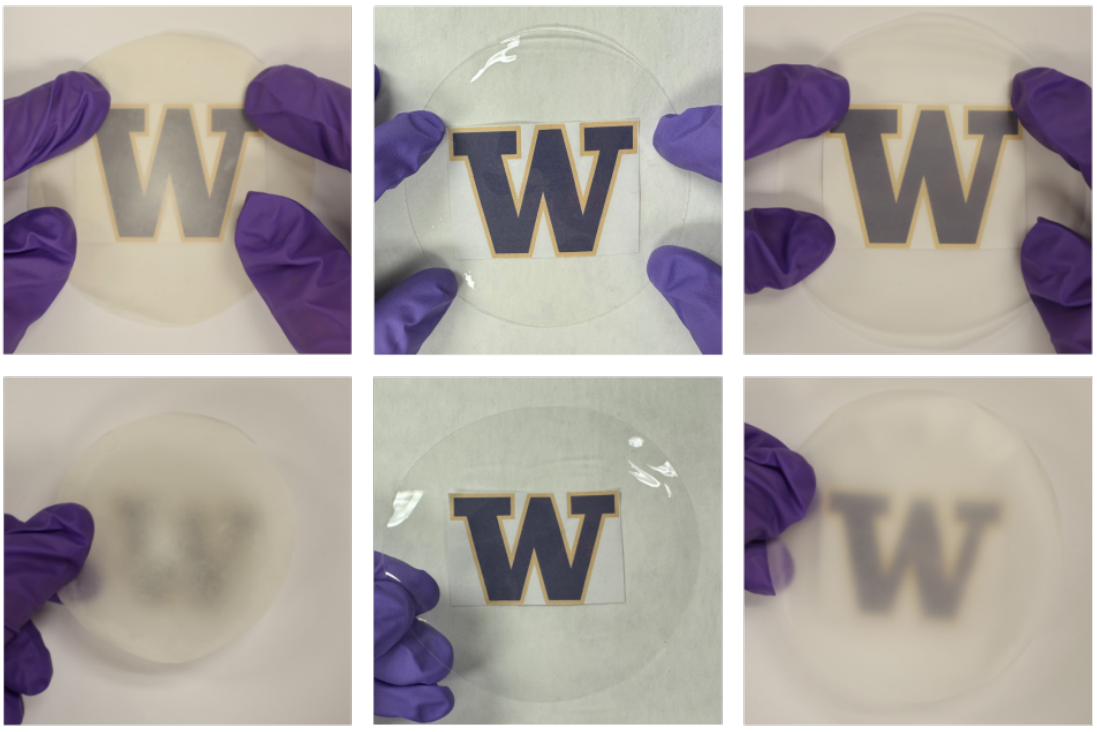
A)


100%
80%
60%
40%
20%
0%
Haze
PVA (control)
CNF
MCNF
100% PVA (control)
100% CNF
100% MCNF
95% CNF / 5% PVA
95% MCNF / 5% PVA
90% CNF / 10% PVA
90% MCNF / 10% PVA
85% CNF / 15% PVA
85% MCNF / 15% PVA
80% CNF / 20% PVA
80% MCNF / 20% PVA
PVA film composition

B)


Transmitance at 660 nm
55%
60%
65%
70%
75%
80%
85%
90%
95%
100%
80%
60%
40%
20%
0%
Haze
100% MCNF
100% CNF
95% CNF / 5% PVA
95% MCNF / 5% PVA
90% MCNF / 10% PVA
85% MCNF / 15% PVA
80% MCNF / 20% PVA
80% CNF / 20% PVA
85% CNF / 15% PVA
90% CNF / 10% PVA
100% PVA (control)

C)



D)

Figure 4. Optical data of CNF/PVA composite films.

A) Percent light transmittance of CNF/PVA composite films from 400 to 800 nm. B) Haze of CNF/PVA composite films compared to MCNF/PVA composite films. C) Haze and light transmittance of CNF/PVA composite films compared to MCNF/PVA composite films. D) Demonstration of the haze of select composite films. The films were pressed against a blank background (first row), then raised 2 cm off the background (second row). The films shown, from left to right, are 100 % CNF, 100 % PVA, and 80 % CNF / 20 % PVA.

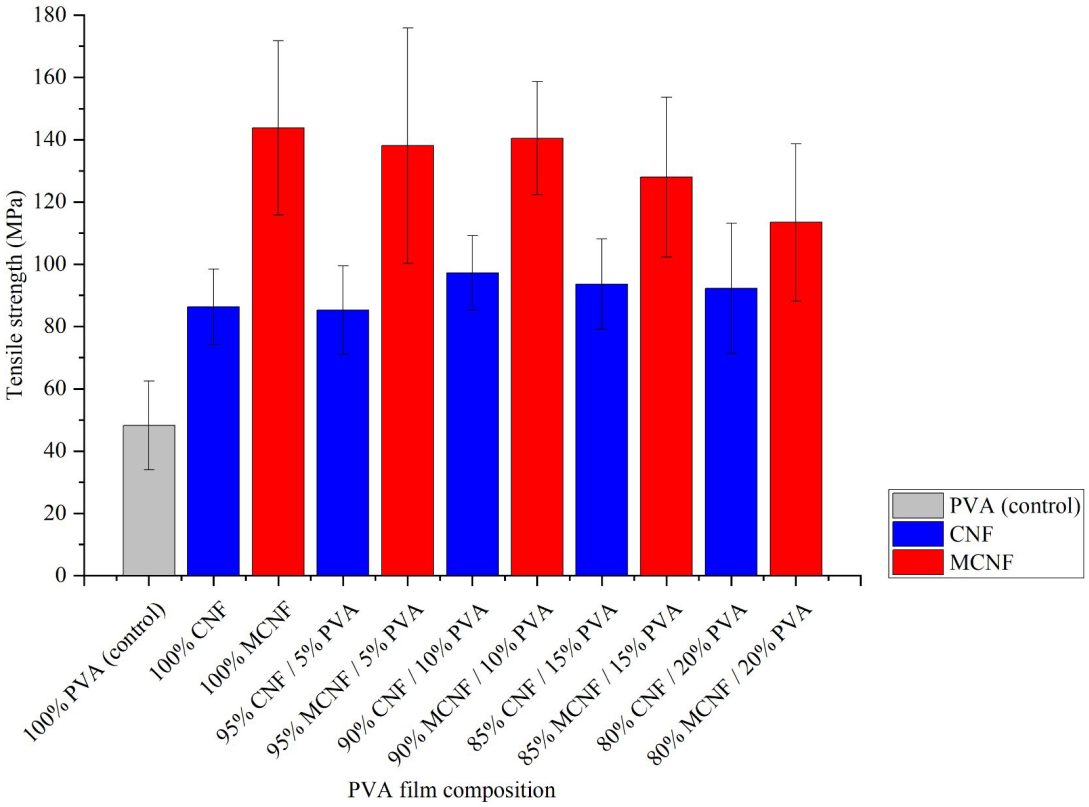
4.4.2 Composite Film Mechanical Properties

Composite films were prepared with the goal of a final total solids of approximately 0.5 g per film. The thickness of each film was evaluated and found to be in the range of 53 mm to 63 mm, on average. Neat PVA films had a thickness of 30 mm (see Table A15).

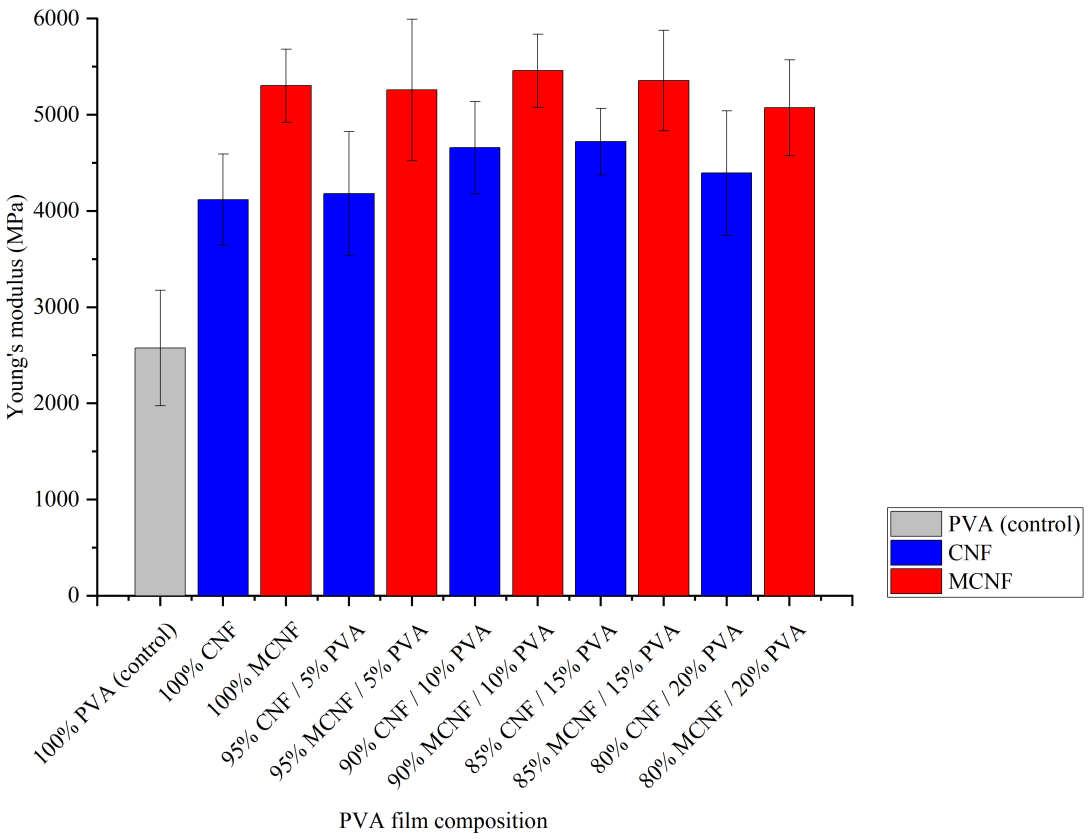
Figure 5 shows the results of the A) tensile strength, B) Young's modulus, and C) peak elongation of the composite films. 100 % PVA films had an expectedly low tensile strength at 48.2 MPa. 100 % CNF had an increased strength of 86.3 MPa, and this strength is retained as PVA is added to the composite films. The same increase with MCNF is observed as well. The Young's modulus of the neat PVA films was expectedly lower at 2575.3 MPa, indicating higher flexibility compared to CNF (4118.4 MPa) and MCNF (5303.2 MPa) films. Finally, the peak elongation of the PVA was low at 2.9 %, but this can be attributed to the low tensile strength leading the film to break before stretching very far. Similarly, the CNF and MCNF had low peak elongation of 4.2 % and 7.7%.

These values are comparable to those present in literature. For example, in one study 100 % CNF films were evaluated to have a tensile strength of 96.3 MPa and Young's modulus of approximately 4000 MPa (Li, Skolrood, Aytug, Tekinalp, & Ozcan, 2019). In another study of oxygen-delignified CNF films, they were found to have a modulus of 10,000 MPa and peak elongation of 2.0 mm (Ferrer et al., 2012).

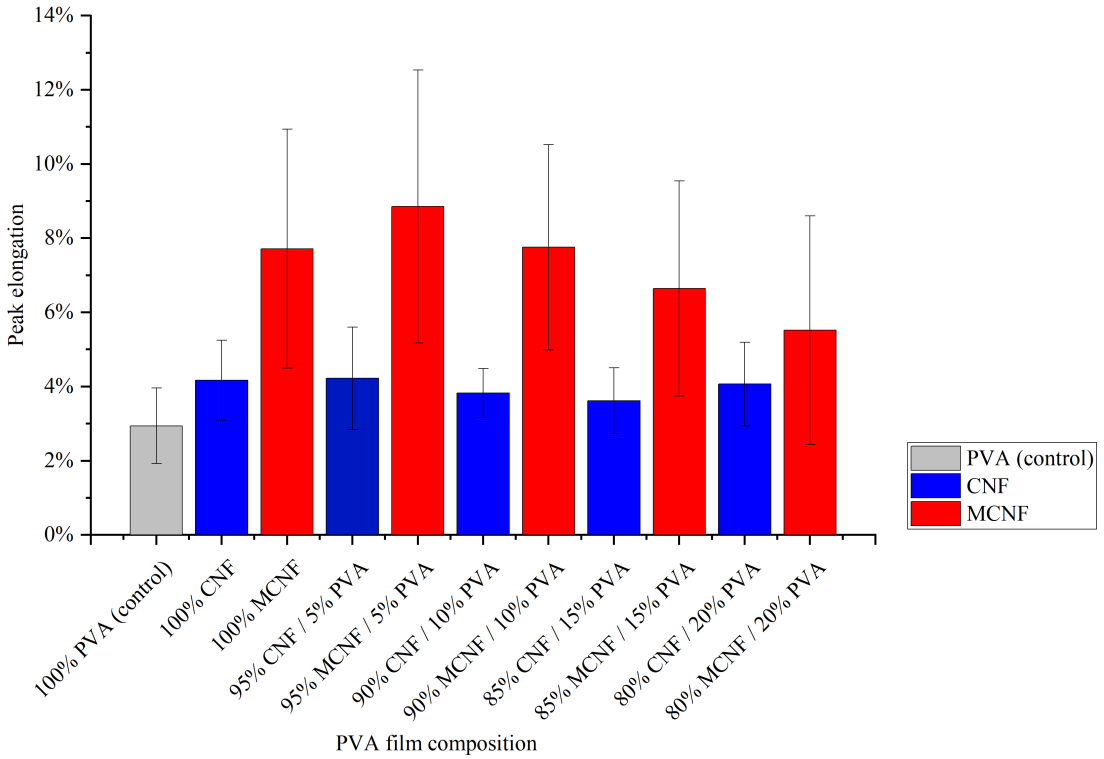
The tensile strength of the composite films compared to 100 % PVA films demonstrates their superior strength when compared to traditional plastics. Additionally, the comparable values of peak elongation and Young's Modulus indicate that these novel bioplastic composites are stiff but have maintained flexibility, indicating their use in a broad range of applications.



A)


Young's modulus (MPa)
6000
5000
4000
3000
2000
1000
0
100% PVA (control)
100% CNF
100% MCNF
95% CNF / 5% PVA
95% MCNF / 5% PVA
90% CNF / 10% PVA
90% MCNF / 10% PVA
85% CNF / 15% PVA
85% MCNF / 15% PVA
80% CNF / 20% PVA
80% MCNF / 20% PVA
PVA film composition
PVA (control)
CNF
MCNF

B)


Peak elongation
14%
12%
10%
8%
6%
4%
2%
0%
100% PVA (control)
100% CNF
100% MCNF
95% CNF / 5% PVA
95% MCNF / 5% PVA
90% CNF / 10% PVA
90% MCNF / 10% PVA
85% CNF / 15% PVA
85% MCNF / 15% PVA
80% CNF / 20% PVA
80% MCNF / 20% PVA
PVA film composition
PVA (control)
CNF
MCNF

C)

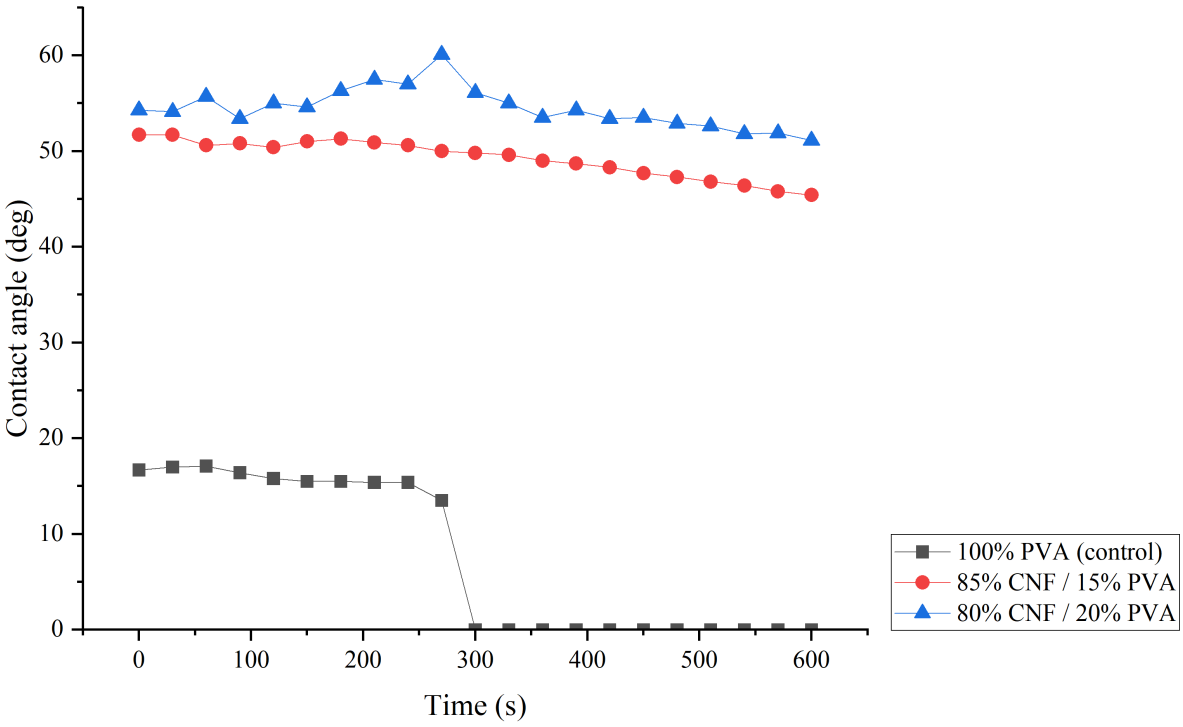
Figure 5. Mechanical data of CNF/PVA composite films.

A) Tensile strength of composite films. B) Young's modulus of composite films. C) Peak elongation of composite films.

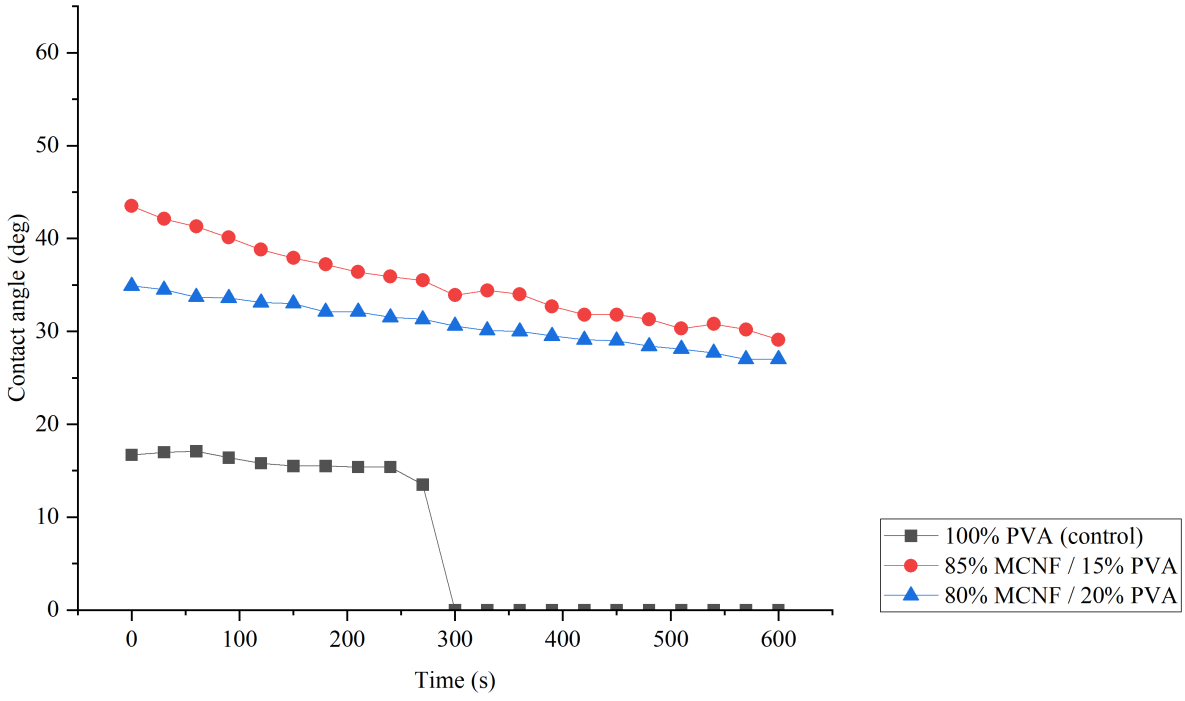
4.4.3 Additional Film Characterization

The air permeability of the composite films was evaluated but found to be above the machine limit of 10 KPa of pressure, demonstrating the lack of permeability in these films that is conducive for use in applications such as food packaging.

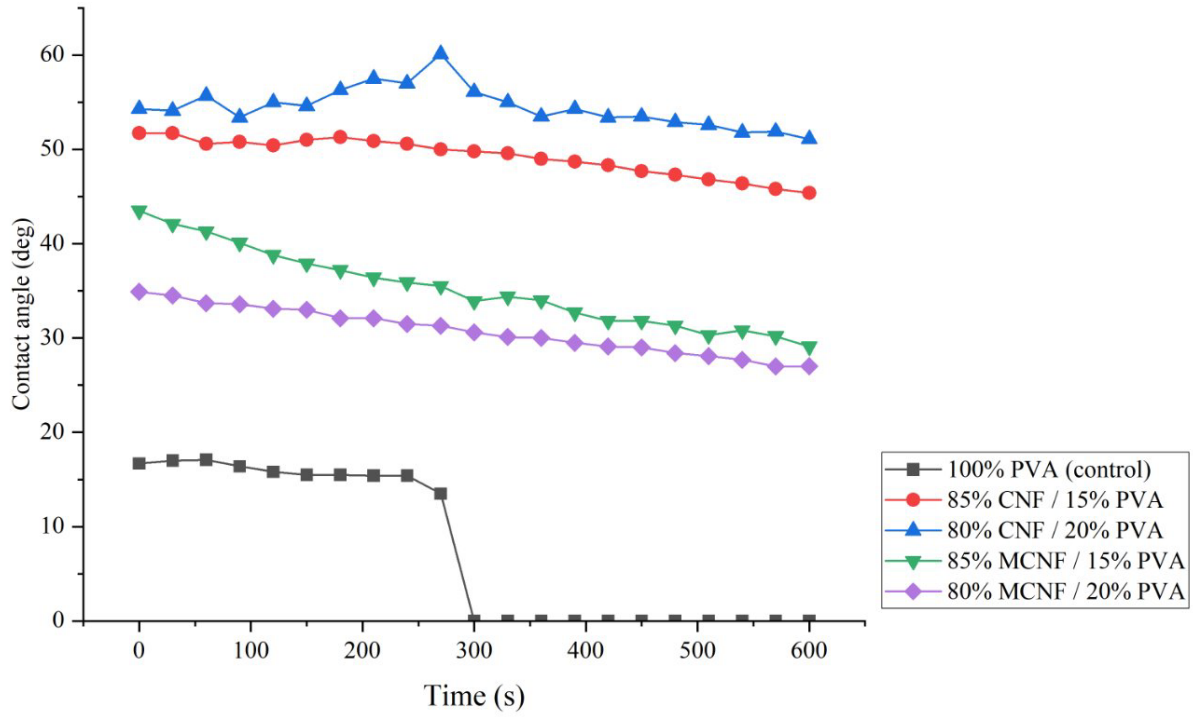
The contact angle of water on the surface of each composite film was evaluated in three ways: static contact angle, dynamic contact angle, and the static contact angle over an extended period of time. For static contact angle, it was found that 100 % PVA films had an average static contact angle of 20° compared to 100 % CNF films which had an average contact angle of 55° (similar to 100% MCNF with a contact angle of 52°; see Table A25). For dynamic contact angle, it was found that 100 % PVA films expectedly became completely wettable, and the contact angle dropped to 0°. The contact angle hysteresis (CAH) of the 100 % CNF film was calculated to be 21° and 100 % MCNF CAH was 25° (see Table A26).


Contact angle (deg)
Time (s)
0
10
20
30
40
50
60
0
100
200
300
400
500
600
100% PVA (control)
85% CNF / 15% PVA
80% CNF / 20% PVA

A)


Contact angle (deg)
Time (s)
0
10
20
30
40
50
60
0
100
200
300
400
500
600
100% PVA (control)
85% MCNF / 15% PVA
80% MCNF / 20% PVA

B)



C)

Figure 6. Extended contact angle on CNF/PVA composite films.

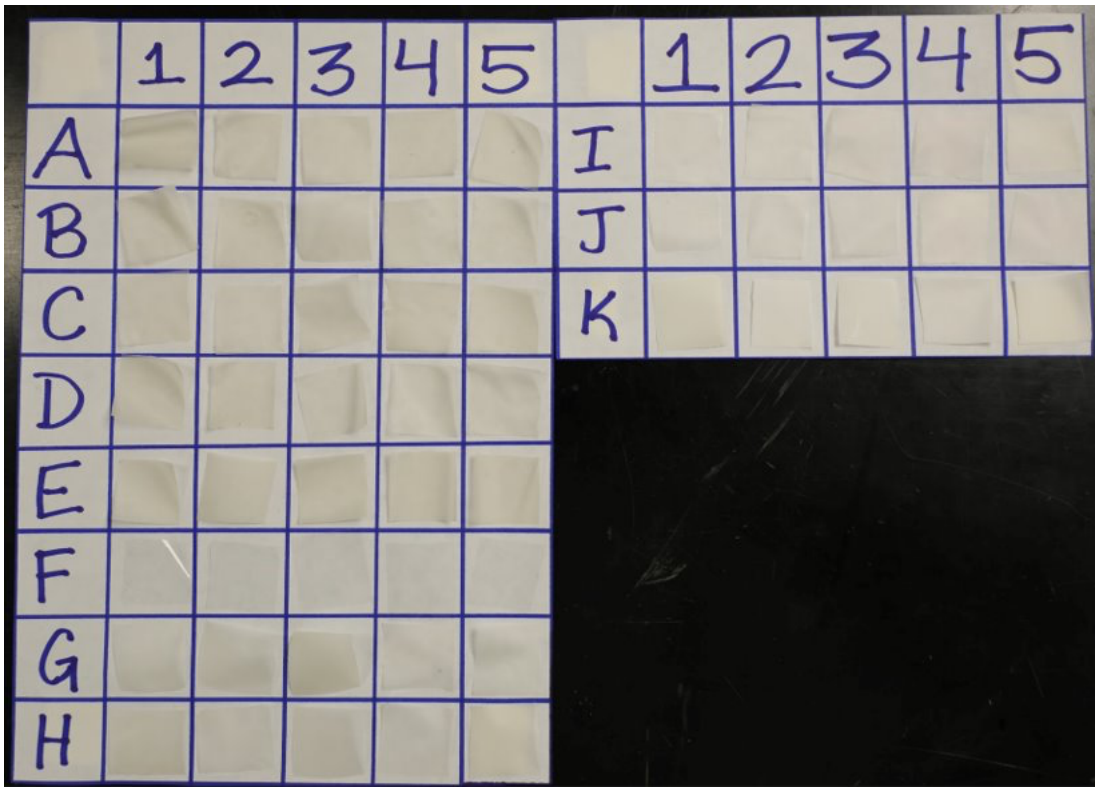
A) Extended contact angle on CNF/PVA composite films. B) Extended contact angle on MCNF/PVA composite films. C) Compilation of A and B.

Figure 6 shows the results of recording the static contact angle of the CNF films over an extended period of time. A drop of water was added to each composite film and observed over 10 minutes with a contact angle measurement taken every 30 seconds. From 0 seconds to 600 seconds, the contact angle of 100 % PVA dropped from 16.7° to 0.0°, resulting in complete wetting after approximately 5 minutes. It was seen that the composite films prepared with CNF maintained a higher contact angle over a longer time, remaining qualitatively stable. From 0 seconds to 600 seconds, the contact angle of 100 % CNF dropped from 56.0° to 41.6°, a difference of 14.4°. From 0 seconds to 600 seconds, the contact angle of 100 % MCNF dropped from 46.2° to 35.6°, a difference of 10.6°. All films prepared with either MCNF or CNF experienced a decreased wettability as compared to 100 % PVA, and films prepared with CNF

appeared to be more stable over time. This increased resistance to water with the addition of nanocellulose (either CNF or MCNF) ideal for applications of these films in areas such as food packaging or agricultural mulch coverings.

The composite films were then subjected to stability testing. Five samples of each film composition were submerged in soil at a constant humidity for eleven weeks. Each week, the samples were removed and dried, and the mass lost was measured on an O.D. basis. Figure 8 shows these films before at the beginning and end of this test. 100 % PVA films were found to have an average mass decrease of 12 % over eleven weeks. It was observed that 100 % CNF composite films experienced an average mass decrease of 24 %. 100 % MCNF samples lost an average of 12 % mass. Additionally, as the amount of PVA present in the film composition increased, the average percent mass lost increased as well. These results show that the CNF composite films are stable enough against soil and humidity for eleven weeks to remain mostly intact with most of the mass remaining. These results are encouraging in that the materials created will not remain permanently in the environment like fossil fuel-based plastics, but they will remain intact for long enough to fulfil their purpose in applications like food packaging or agricultural mulch covering.

A)



B)

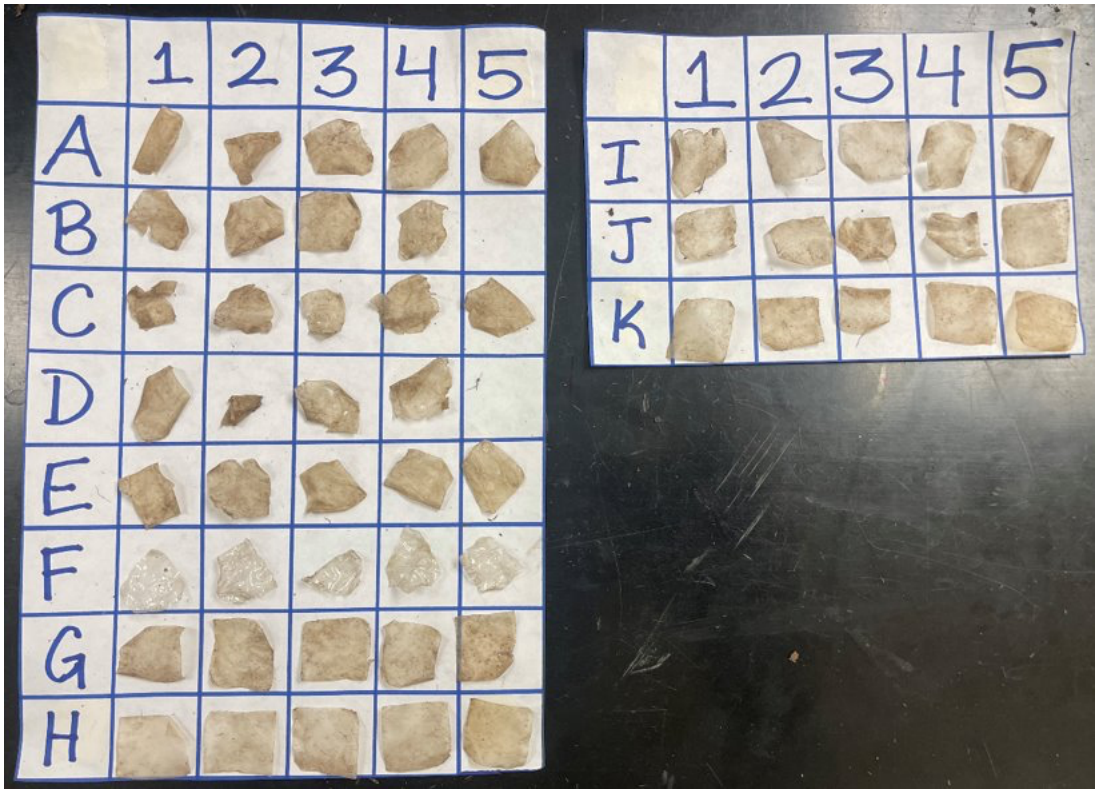


Figure 7. CNF films for stability testing.

A) CNF films prior to stability testing and B) after eleven weeks.

5. Conclusions

This work proved the robustness of the previously published CNF production process using alkaline pulping and PAA pretreatment. CNF was able to be produced on a kilogram scale with a 68 % pulping yield. The fibers produced were evaluated and shown to be chemically and morphologically identical to those previously produced at a gram scale. With an average fiber diameter of 21.0 nm and average fiber length of 0.89 mm, the kilogram scale CNF also maintained high levels of cellulose (100 %) and hemicellulose (92 %), which contributed to the observed optical and mechanical characteristics.

The CNF produced was effectively used in the creation of CNF/PVA film composites. These films were evaluated and found to have a maximum haze of 94.7 % in 100 % CNF films and a maximum light transmittance of 85.7 % at 660 nm in the 85 % CNF films; the simultaneous high light transmittance and high haze of these films is a unique property that lends this bioplastic to a broad range of applications. Furthermore, a high tensile strength of 86.3 MPa combined with a peak elongation of 4.2 % shows that CNF/PVA composite films prepared using CNF were able to retain a significant amount of flexibility associated with traditional plastic films while gaining increased strength and mechanical properties associated with CNF. Lastly, these films were proven to begin to break down in soil over time but not at once, and they have a decreased wettability as compared to 100 % PVA film controls. These properties show the viability of applications such as single-use food packaging, agricultural mulch covering, or solar energy conversion devices.

6. Conclusion and Future Work

6.1 CONCLUSION

The ability to adjust the Bura-Gustafson lab group nanocellulose production process from a gram scale production basis to a kilogram scale production shows the robustness of the process. With an increase in scale comes optimized economic potential for this material. Therefore, the direct use of CNF in the creation of bioplastics allows for applications of these plastics in industrial sectors previously unavailable due to the prohibitive cost of CNF. Based on optical, mechanical and other barrier properties evaluated throughout this thesis, it was shown that these novel bioplastics can replace many fossil fuel-based plastics across a range of applications.

Historically, bioplastics have been composed of mostly polymers reinforced with a small amount of renewable fibers or similar material. The composite films engineered by the Bura-Gustafson lab group do the opposite; the main component of these plastics come from renewable fibers with a fraction of the film coming from a polymer, placing the emphasis on sustainability.

6.2 FUTURE WORK

There is proven viability in the production of CNF at a kilogram scale using alkaline pulping and PAA pretreatment to decrease potential environmental impacts and economic limitations associated with other methods of nanocellulose production. There is potential for further adjustment to the chemistry and energy requirements of this CNF production process to optimize CNF yield, decrease chemistry and energy input requirements, and further improve economic feasibility. A full Life Cycle Analysis (LCA) is called for were this process to continue to scale up to an industrial level.

This project indicates a need for further research on degradable composite films made with more CNF than polymer. With the promising results of the novel bioplastic made using over 80 wt.% CNF, there are many applications that will greatly benefit from a basis in sustainability and renewable products. As the sustainability of these plastics is improved with most film components originating from renewable materials, further work is called for to explore direct applications of this material.

BIBLIOGRAPHY

Ali, S. S., Abdelkarim, E. A., Elsamahy, T., Al-Tohamy, R., Li, F., Kornaros, M., … Sun, J. (2023). Bioplastic production in terms of life cycle assessment: A state-of-the-art review. *Environmental Science and Ecotechnology*, *15*, 100254. doi:10.1016/j.ese.2023.100254

Asad, M., Saba, N., Asiri, A. M., Jawaid, M., Indarti, E., & Wanrosli, W. D. (2018). Preparation and characterization of nanocomposite films from oil palm pulp nanocellulose/poly (vinyl alcohol) by casting method. *Carbohydrate Polymers*, *191*, 103–111. doi:10.1016/j.carbpol.2018.03.015

Aslam, M., Kalyar, M. A., & Raza, Z. A. (2018). Polyvinyl Alcohol: A Review of Research Status and use of polyvinyl alcohol based nanocomposites. *Polymer Engineering & Science*, *58*(12), 2119–2132. doi:10.1002/pen.24855

Azapagic, A. (2014). Sustainability considerations for integrated biorefineries. *Trends in Biotechnology*, *32*(1), 1–4. doi:10.1016/j.tibtech.2013.10.009

Balea, A., Fuente, E., Monte, M. C., Merayo, N., Campano, C., Negro, C., & Blanco, A. (2020). Industrial application of Nanocelluloses in papermaking: A review of challenges, technical solutions, and Market Perspectives. *Molecules*, *25*(3), 526. doi:10.3390/molecules25030526

Besbes, I., Alila, S., & Boufi, S. (2011). Nanofibrillated cellulose from tempo-oxidized eucalyptus fibres: Effect of the carboxyl content. *Carbohydrate Polymers*, *84*(3), 975–983. doi:10.1016/j.carbpol.2010.12.052

British Plastics Federation. (n.d.). How is plastic made? A simple step-by-step explanation. Retrieved from http://www.bpf.co.uk/plastipedia/how-is-plastic-made.aspx

Chen, S., Song, Y., & Xu, F. (2018). Highly transparent and hazy cellulose Nanopaper simultaneously with a self-cleaning superhydrophobic surface. *ACS Sustainable Chemistry & Engineering*, *6*(4), 5173–5181. doi:10.1021/acssuschemeng.7b04814

Dou, C., Bura, R., Ewanick, S., & Morales-Vera, R. (2019). Blending short rotation coppice poplar with wheat straw as a biorefinery feedstock in the state of Washington. *Industrial Crops and Products*, *132*, 407–412. doi:10.1016/j.indcrop.2019.02.033

Dou, C., Marcondes, W. F., Djaja, J. E., Bura, R., & Gustafson, R. (2017). Can we use short rotation coppice poplar for sugar based biorefinery feedstock? bioconversion of 2-year-old poplar grown as short rotation coppice. *Biotechnology for Biofuels*, *10*(1). doi:10.1186/s13068-017-0829-6

Espinosa, E., Bascón-Villegas, I., Rosal, A., Pérez-Rodríguez, F., Chinga-Carrasco, G., & Rodríguez, A. (2019). PVA/(Ligno)nanocellulose biocomposite films. effect of residual

lignin content on structural, mechanical, barrier and antioxidant properties. *International Journal of Biological Macromolecules*, *141*, 197–206. doi:10.1016/j.ijbiomac.2019.08.262

Ferrer, A., Quintana, E., Filpponen, I., Solala, I., Vidal, T., Rodríguez, A., … Rojas, O. J. (2012). Effect of residual lignin and heteropolysaccharides in nanofibrillar cellulose and nanopaper from wood fibers. *Cellulose*, *19*(6), 2179–2193. doi:10.1007/s10570-012-9788-z

Forti, E. S., Awad, S. M., Ng, X. Y., Cho, W., Schueneman, G. T., Moon, R. J., … Youngblood, J. (2021). *Mechanical Enhancement of Cellulose Nanofibril (CNF) Films through the Addition of Water-Soluble Polymers*. doi:10.21203/rs.3.rs-162652/v1

Fossil Fuels & Plastic. (2019). Retrieved from https://www.ciel.org/issue/fossil-fuels-plastic/

Hörhammer, H., Dou, C., Gustafson, R., Suko, A., & Bura, R. (2018). Removal of non-structural components from Poplar whole-tree chips to enhance hydrolysis and fermentation performance. *Biotechnology for Biofuels*, *11*(1). doi:10.1186/s13068-018-1219-4

Ingrao, C., Tricase, C., Cholewa-Wójcik, A., Kawecka, A., Rana, R., & Siracusa, V. (2015). Polylactic acid trays for fresh-food packaging: A Carbon Footprint Assessment. *Science of The Total Environment*, *537*, 385–398. doi:10.1016/j.scitotenv.2015.08.023

Jones, R. E., Speight, R. E., Blinco, J. L., & O'Hara, I. M. (2022). Biorefining within food loss and waste frameworks: A Review. *Renewable and Sustainable Energy Reviews*, *154*, 111781. doi:10.1016/j.rser.2021.111781

Kaffashsaie, E., Yousefi, H., Nishino, T., Matsumoto, T., Mashkour, M., Madhoushi, M., & Kawaguchi, H. (2021). Direct conversion of raw wood to tempo-oxidized cellulose nanofibers. *Carbohydrate Polymers*, *262*, 117938. doi:10.1016/j.carbpol.2021.117938

Khalid, M. Y., Al Rashid, A., Arif, Z. U., Ahmed, W., & Arshad, H. (2021). Recent advances in nanocellulose-based different biomaterials: Types, properties, and emerging applications. *Journal of Materials Research and Technology*, *14*, 2601–2623. doi:10.1016/j.jmrt.2021.07.128

Kibédi-Szabó, C. Z., Stroescu, M., Stoica-Guzun, A., Jinga, S. I., Szilveszter, S., Jipa, I., & Dobre, T. (2011). Biodegradation behavior of composite films with poly (vinyl alcohol) matrix. *Journal of Polymers and the Environment*, *20*(2), 422–430. doi:10.1007/s10924-011-0391-4

Kjeldsen, A., Price, M., Lilley, C., Guzniczak, E., & Archer, I. (2018). A review of standards for biodegradable plastics. *Industrial Biotechnology Innovation Centre*, *33*(1).

Lee, H., You, J., Jin, H.-J., & Kwak, H. W. (2020). Chemical and physical reinforcement behavior of dialdehyde nanocellulose in PVA composite film: A comparison of nanofiber and Nanocrystal. *Carbohydrate Polymers*, *232*, 115771. doi:10.1016/j.carbpol.2019.115771

Li, C., Yan, W., Wang, B., Xu, T., Lin, C. S., Zou, X., & Du, C. (2023). Integrated biorefineries for the co-production of biofuels and high-value products. *Handbook of Biofuels Production*, 513–541. doi:10.1016/b978-0-323-91193-1.00014-7

Li, K., Skolrood, L. N., Aytug, T., Tekinalp, H., & Ozcan, S. (2019). Strong and tough cellulose nanofibrils composite films: Mechanism of synergetic effect of hydrogen bonds and ionic interactions. *ACS Sustainable Chemistry & Engineering*, *7*(17), 14341–14346. doi:10.1021/acssuschemeng.9b03442

Lu, J., Wang, T., & Drzal, L. T. (2008). Preparation and properties of microfibrillated cellulose polyvinyl alcohol composite materials. *Composites Part A: Applied Science and Manufacturing*, *39*(5), 738–746. doi:10.1016/j.compositesa.2008.02.003

Majumdar, R., Mishra, U., Mahata, N., Shah, M. P., Mondal, A., & Bhunia, B. (2023). Preparation, characterization, and performance evaluation of composite films of polyvinyl alcohol/ cellulose nanofiber extracted from Imperata cylindrica. *Chemosphere*, *337*, 139370. doi:10.1016/j.chemosphere.2023.139370

Muniyasamy, S., Ofosu, O., John, M. J., & Anandjiwala, R. D. (2016). Mineralization of poly(lactic acid) (PLA), poly(3-hydroxybutyrate-co-valerate) (PHBV) and PLA/PHBV blend in compost and soil environments. *Journal of Renewable Materials*, *4*(2), 133–145. doi:10.7569/jrm.2016.634104

OCED. (2022). *Global Plastics Outlook: Economic Drivers, Environmental Impacts and Policy Options*. doi:10.1787/de747aef-en

Oishi, Y., Nakaya, M., Matsui, E., & Hotta, A. (2015). Structural and mechanical properties of cellulose composites made of isolated cellulose nanofibers and poly(vinyl alcohol). *Composites Part A: Applied Science and Manufacturing*, *73*, 72–79. doi:10.1016/j.compositesa.2015.02.026

Pascoli, Danielle U., Dichiara, A., Roumeli, E., Gustafson, R., & Bura, R. (2022). Lignocellulosic nanomaterials production from Wheat Straw via peracetic acid pretreatment and their application in Plastic Composites. *Carbohydrate Polymers*, *295*, 119857. doi:10.1016/j.carbpol.2022.119857

Pascoli, Danielle Uchimura, Suko, A., Gustafson, R., Gough, H. L., & Bura, R. (2021). Novel ethanol production using biomass preprocessing to increase ethanol yield and reduce overall costs. *Biotechnology for Biofuels*, *14*(1). doi:10.1186/s13068-020-01839-0

Pierobon, F., Eastin, I. L., & Ganguly, I. (2018). Life cycle assessment of residual lignocellulosic biomass-based jet fuel with activated carbon and lignosulfonate as co-products. *Biotechnology for Biofuels*, *11*(1). doi:10.1186/s13068-018-1141-9

Posen, I. D., Jaramillo, P., Landis, A. E., & Griffin, W. M. (2017). Greenhouse gas mitigation for U.S. plastics production: Energy first, feedstocks later. *Environmental Research Letters*, *12*(3), 034024. doi:10.1088/1748-9326/aa60a7

Pradhan, D., Jaiswal, A. K., & Jaiswal, S. (2022). Emerging technologies for the production of nanocellulose from lignocellulosic biomass. *Carbohydrate Polymers*, *285*, 119258. doi:10.1016/j.carbpol.2022.119258

Qin, M., Chen, C., Song, B., Shen, M., Cao, W., Yang, H., … Gong, J. (2021). A review of biodegradable plastics to biodegradable microplastics: Another ecological threat to soil environments? *Journal of Cleaner Production*, *312*, 127816. doi:10.1016/j.jclepro.2021.127816

Rosenboom, J.-G., Langer, R., & Traverso, G. (2022). Bioplastics for a circular economy. *Nature Reviews Materials*, *7*(2), 117–137. doi:10.1038/s41578-021-00407-8

Roumeli, E., Hendrickx, R., Bonanomi, L., Vashisth, A., Rinaldi, K., & Daraio, C. (2022). Biological matrix composites from cultured plant cells. *Proceedings of the National Academy of Sciences*, *119*(15). doi:10.1073/pnas.2119523119

Serra, A., González, I., Oliver-Ortega, H., Tarrès, Q., Delgado-Aguilar, M., & Mutjé, P. (2017). Reducing the amount of catalyst in tempo-oxidized cellulose nanofibers: Effect on properties and cost. *Polymers*, *9*(11), 557. doi:10.3390/polym9110557

Silva, E. L., Reis, C. A., Vieira, H. C., Santos, J. X., Nisgoski, S., Saul, C. K., & Muñiz, G. I. (2020). Evaluation of poly(vinyl alcohol) addition effect on nanofibrillated cellulose films characteristics. *CERNE*, *26*(1), 1–8. doi:10.1590/01047760202026012654

Skiba, E. A., Shavyrkina, N. A., Skiba, M. A., Mironova, G. F., & Budaeva, V. V. (2023). Biosynthesis of bacterial nanocellulose from low-cost cellulosic feedstocks: Effect of microbial producer. *International Journal of Molecular Sciences*, *24*(18), 14401. doi:10.3390/ijms241814401

Sluiter, A., Hames, B., Ruiz, R. O., Scarlata, C., Sluiter, J., Templeton, D., & Kreft, J.-U. (2008). *Determination of Ash in Biomass: Laboratory Analytical Procedure (LAP)*. doi:TP-510-42622

Sluiter, A., Ruiz, R., Scarlata, C., Sluiter, J., & Templeton, D. (2008). *Determination of Extractives in Biomass: Laboratory Analytical Procedure (LAP)*. doi:NREL/TP-510-42619

Srithep, Y., Turng, L.-S., Sabo, R., & Clemons, C. (2012). Nanofibrillated cellulose (NFC) reinforced Polyvinyl Alcohol (PVOH) nanocomposites: Properties, solubility of carbon dioxide, and foaming. *Cellulose*, *19*(4), 1209–1223. doi:10.1007/s10570-012-9726-0

Thomas, B., Raj, M. C., B, A. K., H, R. M., Joy, J., Moores, A., … Sanchez, C. (2018). Nanocellulose, a versatile green platform: From Biosources to materials and their applications. *Chemical Reviews*, *118*(24), 11575–11625. doi:10.1021/acs.chemrev.7b00627

Xing, L., Hu, C., Zhang, W., Guan, L., & Gu, J. (2020). Biodegradable cellulose I (ii) nanofibrils/poly(vinyl alcohol) composite films with high mechanical properties, improved thermal stability and excellent transparency. *International Journal of Biological Macromolecules*, *164*, 1766–1775. doi:10.1016/j.ijbiomac.2020.07.320

Xu, X., Liu, F., Jiang, L., Zhu, J. Y., Haagenson, D., & Wiesenborn, D. P. (2013). Cellulose nanocrystals vs. cellulose Nanofibrils: A comparative study on their microstructures and effects as polymer reinforcing agents. *ACS Applied Materials & Interfaces*, *5*(8), 2999–3009. doi:10.1021/am302624t

Zhong, X., Zhao, X., Qian, Y., & Zou, Y. (2018). Polyethylene Plastic Production Process. *Insight - Material Science*, *1*(1), 1. doi:10.18282/ims.v1i1.104

APPENDIX A. SUPPLEMENTARY DATA

Replicate	Wet sample weight (g)	Dry sample weight (g)	Moisture content	Consistency (g/g)
1	6.99	0.22	0.97	0.032
2	8.57	0.27	0.97	0.032
3	12.28	0.39	0.97	0.032
4	9.66	0.30	0.97	0.031
5	15.02	0.47	0.97	0.031
Summary				
Average consistency (%)			**Standard deviation**	
3.16			0.05	

Table A1. Measured consistency of the MCNF purchased from the University of Maine.

Pulping replicate	Wheat straw moisture content (%)	Wheat straw weight O.D. (g)	Wheat straw weight including moisture (g)	Measured wheat straw weight (g)
Pulp 1	7.05	300.00	322.75	324.90
Pulp 2	7.10	300.00	322.75	322.70
Pulp 3	7.10	300.00	322.93	322.90

Table A2. Calculations and measurements prior to alkaline peroxide pulping reaction.

Pulping replicate	Pulp weight (g)	Pulp moisture content (%)	Pulp weight O.D. (g)	Pulping yield (%)	Black liquor pH
Pulp 1	1634.90	87.55	203.56	67.85	11.36
Pulp 2	1580.30	87.14	203.16	67.72	-
Pulp 3	1640.80	87.31	208.28	69.43	-
Summary					
Average pulping yield (%)			**Standard deviation**		
68.33			0.95		

Table A3. Calculations and measurements following the alkaline peroxide pulping reaction.

Pulping replicate	Accepts weight (g)	Accepts moisture content (%)	Rejects weight (g)	Rejects moisture content (%)	Accepts weight O.D. (g)	Rejects weight O.D. (g)	Accepts and rejects weight O.D. (g)	Accepts (%)	Rejects (%)	Screening yield (%)
Pulp 1	1248.13	87.37	89.52	92.91	157.64	6.35	163.99	96.13	3.87	54.67
Pulp 2	969.30	82.79	33.74	78.29	166.85	7.33	174.17	95.79	4.21	58.06
Pulp 3	3706.00	95.97	53.66	91.82	149.52	4.35	153.87	97.17	2.83	51.29
Summary										
Average screening yield (%)					**Standard deviation**					
54.67					3.39					

Table A4. Calculations and measurements following pulp screening.

Pulping replicate	Dewatered accepts moisture content (%)	Calculated accepts needed for each 30g O.D. refining batch (g)	Water weight from biomass (g)	Calculated added water needed to reach 10% consistency (mL)	Refined accepts moisture content (%)
Pulp 1	87.37	237.53	207.53	62.47	82.65
Pulp 2	82.79	174.28	144.28	125.72	90.19
Pulp 3	85.51	207.05	177.05	92.95	88.61

Table A5. Calculations and measurements for pulp refining.

PAA reaction replicate	Calculated pulp weight (g)	Measured pulp weight (g)	Calculated PAA stock weight (g)	Measured PAA stock weight (g)	Calculated DI water weight (g)	Measured DI water weight (g)	Initial PAA pH	Volume of 10M NaOH added (mL)	Neutralized PAA pH
PAA 1.1	115.30	115.31	18.75	18.78	260.67	260.70	1.84	7.60	4.78
PAA 2.1	203.90	203.95	23.08	23.08	202.84	202.88	1.60	8.80	4.78
PAA 3.1	175.60	175.51	23.08	23.00	212.71	212.80	2.98	38.00	4.77
PAA 3.2	175.60	175.68	23.08	23.08	212.71	212.72	1.52	9.75	4.79
PAA 3.3	175.60	175.66	23.08	23.14	212.71	212.64	1.61	12.20	4.79
PAA 3.4	175.60	175.66	23.08	23.11	212.71	212.67	1.64	9.50	4.77
PAA 3.5	175.60	175.60	23.08	23.08	212.71	212.84	1.62	9.60	4.77
PAA 3.6	175.40	175.44	18.75	18.89	215.2	215.44	1.93	7.55	4.78

Table A6. Calculations and measurements prior to peracetic acid (PAA) delignification.

PAA reaction replicate	Filtrate pH after reaction	Filtrate conductivity after reaction (mS)	Filtrate pH after washing	Filtrate conductivity after washing (µS)
PAA 1.1	4.45	9.65	6.25	15.31
PAA 2.1	4.38	11.4	6.42	23.96
PAA 3.1	4.43	10.36	5.64	23.64
PAA 3.2	4.39	6.25	5.79	19.40
PAA 3.3	4.37	6.82	6.01	4.09
PAA 3.4	4.37	7.15	5.8	5.86
PAA 3.5	4.41	6.41	5.18	7.11
PAA 3.6	4.45	11.02	7.19	25.8

Table A7. Measurements following peracetic acid (PAA) delignification.

Biomass	Average fiber diameter (nm)	Standard deviation	Skewness
CNF gram scale	16.40	5.10	-
CNF 1.1	15.69	4.07	0.76
CNF 2.1	27.00	17.30	3.02
CNF 3.1	20.10	13.70	3.81
CNF 3.2	22.43	11.73	4.74
CNF 3.3	19.68	9.94	5.81
MCNF	45.29	57.77	6.13
Summary			
Biomass	**Average fiber diameter (nm)**	**Standard deviation**	**Skewness**
CNF gram scale	16.40	5.10	-
CNF	20.98	12.71	4.25
MCNF	45.29	57.77	6.13

Table A8. Measurements of fiber width from SEM imaging.

Biomass	Fiber count	Fiber frequency (EPS)	Average length weighted (mm)
CNF 1	5000	32.89	0.784
CNF 3	5000	43.86	0.819
CNF 3	5000	40.00	1.145
CNF 4	5000	39.37	0.816
MCNF 1	930	5.00	0.247
MCNF 2	1650	11.15	0.307
MCNF 3	1893	12.97	0.161
MCNF 4	1807	12.82	0.209
Summary			
Biomass	**Average length weighted (mm)**	**Standard deviation**	
CNF	0.89	0.17	
MCNF	0.23	0.06	

Table A9. Measurements of fines content, fiber length, and fiber width of CNF and MCNF. A minimum of three replicates were used to calculate the average of each.

Biomass	Ash content replicate 1 (%)	Ash content replicate 2 (%)	Ash content replicate 3 (%)	Average ash content (%)	Standard deviation
Wheat straw	7.21	8.39	8.20	7.94	0.63
Pulp 1 accepts	1.76	1.98	2.03	1.92	0.14
Pulp 1 rejects	1.61	1.50	1.62	1.57	0.07
Pulp 2 accepts	1.19	1.18	1.12	1.17	0.04
Pulp 2 rejects	1.41	1.36	1.23	1.33	0.09
Pulp 3 accepts	1.21	1.17	1.16	1.18	0.02
Pulp 3 rejects	1.57	-	-	1.57	-
Summary					
Biomass		**Average ash content (%)**		**Standard deviation**	
Wheat straw		7.94		0.63	
Pulp accepts		1.42		0.38	
Pulp rejects		1.47		0.14	

Table A10. Ash content of the wheat straw biomass, pulping accepts, and pulping rejects.

Biomass	Post water extractives (g)	Post water extractives (%)	Average post water extractives (%)	Standard deviation
Wheat straw replicate 1	0.66	13.39	13.92	0.47
Wheat straw replicate 2	0.68	14.08		
Wheat straw replicate 3	0.57	14.30		
Pulp 1 accepts replicate 1	0.28	5.66	5.88	0.30
Pulp 1 accepts replicate 2	0.31	6.09		
Pulp 2 accepts replicate 1	0.22	4.42	4.91	0.44
Pulp 2 accepts replicate 2	0.25	5.02		
Pulp 2 accepts replicate 3	0.27	5.28		
Pulp 3 accepts replicate 1	0.27	5.61	5.52	0.13
Pulp 3 accepts replicate 3	0.27	5.42		
Summary				
Biomass	**Average post water extractives (%)**	**Standard deviation**		
Wheat straw	13.92	0.47		
Pulp accepts	5.36	0.53		

Table A11. Water extractive content of the wheat straw biomass, pulping accepts, and pulping rejects. Note, ethanol Soxhlet extraction was also performed, however no post ethanol extractives were measured. Thus, it is reasonable to assume that there are no ethanol extractives.

Biomass	Glucose (%)	Xylose (%)	Total sugars (%)	Acid-insoluble lignin (%)	Acid-soluble lignin (%)	Total lignin (%)	Sum of total sugars and total lignin (%)
Wheat straw	39.89	23.37	63.26	20.43	2.33	22.75	86.02
Pulp 1 accepts	64.97	26.15	91.11	7.58	1.00	8.58	99.69
Pulp 1 rejects	56.42	26.89	83.31	9.15	1.29	10.44	93.75
Pulp 2 accepts	64.10	23.95	88.05	8.80	1.11	9.92	97.97
Pulp 2 rejects	49.03	26.43	75.46	15.97	1.51	17.48	92.94
Pulp 3 accepts	65.24	25.14	90.39	6.05	1.14	7.18	97.57
Pulp 3 rejects	50.95	27.48	78.43	12.18	1.68	13.87	92.29
PAA 1.1	74.08	26.24	100.32	1.77	0.82	2.59	102.91
PAA 2.1	72.57	23.93	96.50	1.27	0.84	2.11	98.60
PAA 3.4	71.03	26.90	97.93	1.33	0.82	2.15	100.08
PAA 3.5	70.03	22.77	92.80	1.06	0.77	1.83	94.63
PAA 3.6	72.46	24.39	96.85	2.05	0.90	2.95	99.80

Summary

Biomass	Average glucose (%)	Standard deviation	Average xylose (%)	Standard deviation	Average total sugars (%)	Standard deviation	Average total lignin (%)	Standard deviation
Wheat straw	39.89	-	23.37	-	63.26	-	22.75	-
Pulp accepts	64.77	0.60	25.08	1.10	89.85	1.60	8.56	1.37
Pulp rejects	52.13	3.83	26.93	0.53	79.07	3.96	13.93	3.52
PAA	72.03	1.56	24.85	1.70	96.88	2.73	2.33	0.44

Table A12. Klason analysis results of wheat straw, alkaline peroxide pulp, and PAA reacted pulp.

Replicate	Charge density (µM/g)
CNF PAA 1.1 replicate 1	183.61
CNF PAA 1.1 replicate 2	184.71
CNF PAA 1.1 replicate 3	204.92
CNF PAA 2.1 replicate 1	146.04
CNF PAA 2.1 replicate 2	147.85
CNF PAA 2.1 replicate 3	217.87
CNF PAA 3.4 replicate 1	127.60
CNF PAA 3.4 replicate 2	98.62
CNF PAA 3.4 replicate 3	84.52
CNF PAA 3.5 replicate 1	97.60
CNF PAA 3.5 replicate 2	100.36
CNF PAA 3.5 replicate 3	120.62
CNF PAA 3.6 replicate 1	112.94
CNF PAA 3.6 replicate 2	120.64
CNF PAA 3.6 replicate 3	133.82
MCNF replicate 1	160.94
MCNF replicate 2	161.75
MCNF replicate 3	164.86

Summary		
Sample	**Average charge density (µM/g)**	**Standard deviation**
CNF	138.78	41.48
MCNF	162.52	2.07

Table A13. Summary of calculated charge densities of CNF and MCNF.

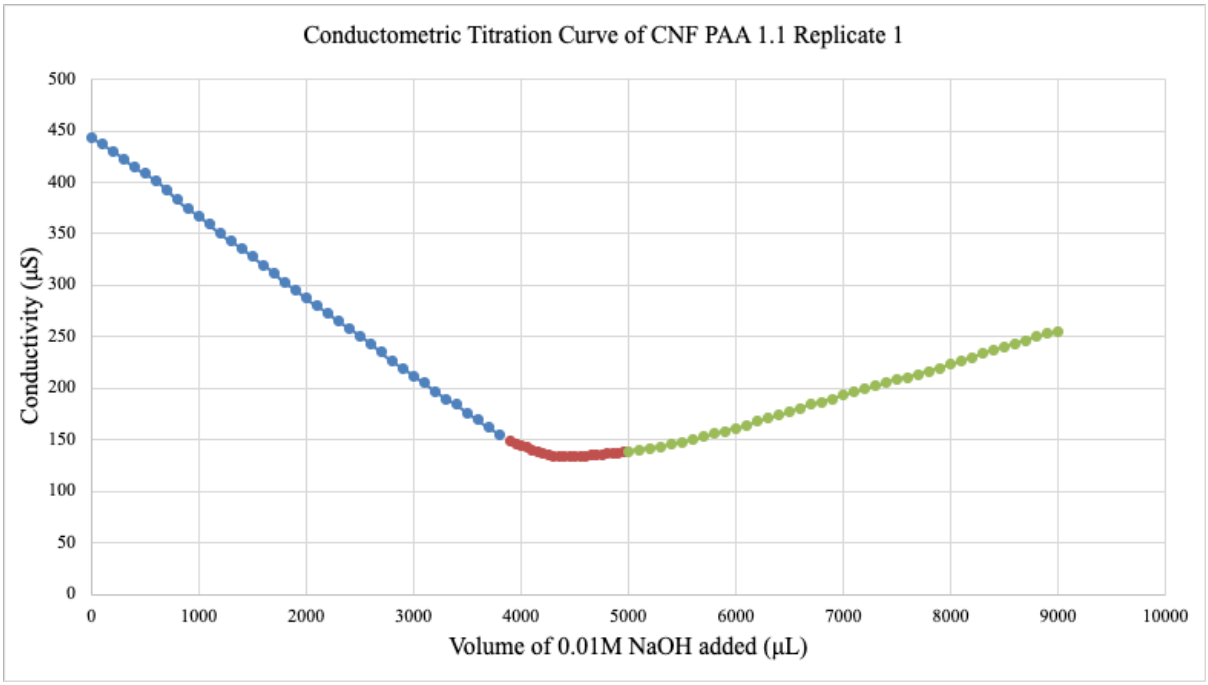


Figure A1. First replicate of conductometric titration curves used to calculate charge density of CNF from PAA reaction 1.1. It was calculated to be 183.61 µM/g.

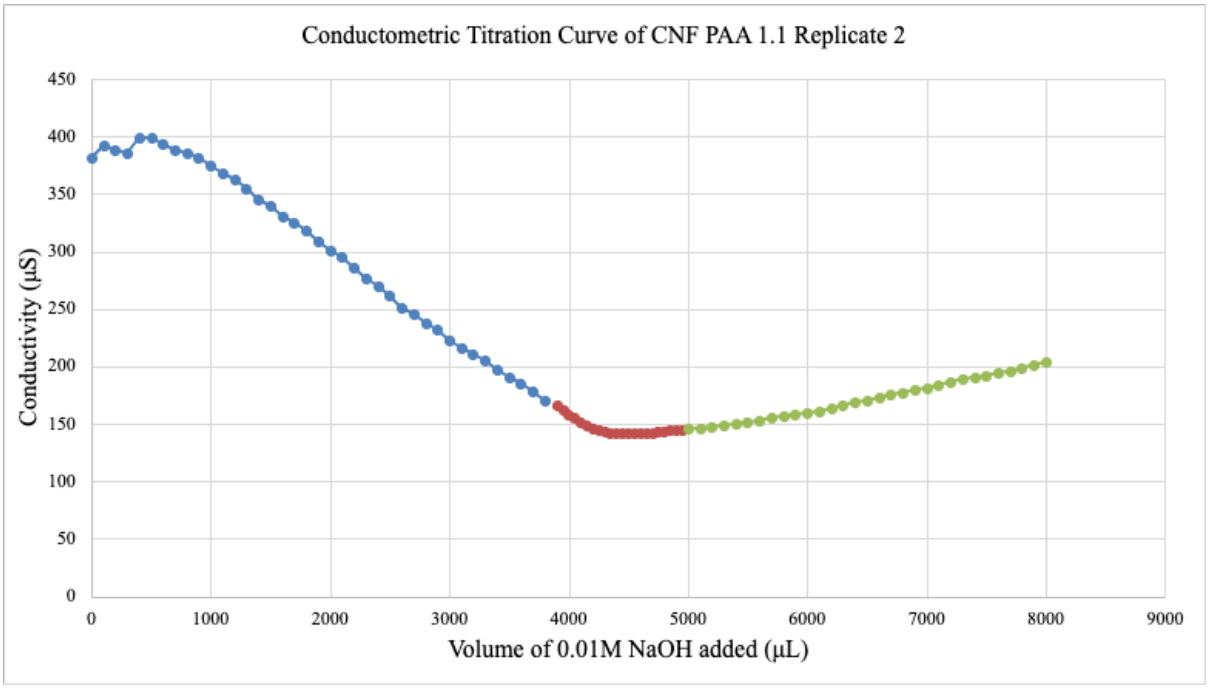


Figure A2. The second replicate of conductometric titration curves is used to calculate charge density of CNF from PAA reaction 1.1. It was calculated to be 184.71 µM/g.

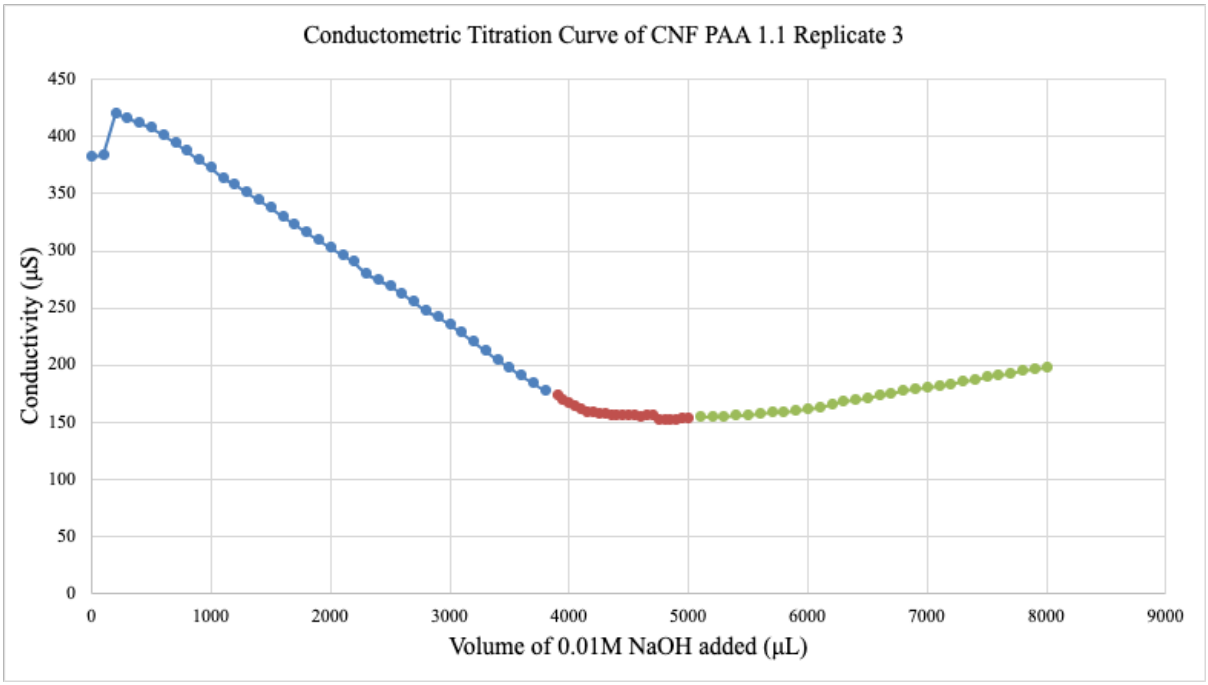


Figure A3. Third replicate of conductometric titration curves used to calculate charge density of CNF from PAA reaction 1.1. It was calculated to be 204.92 µM/g.

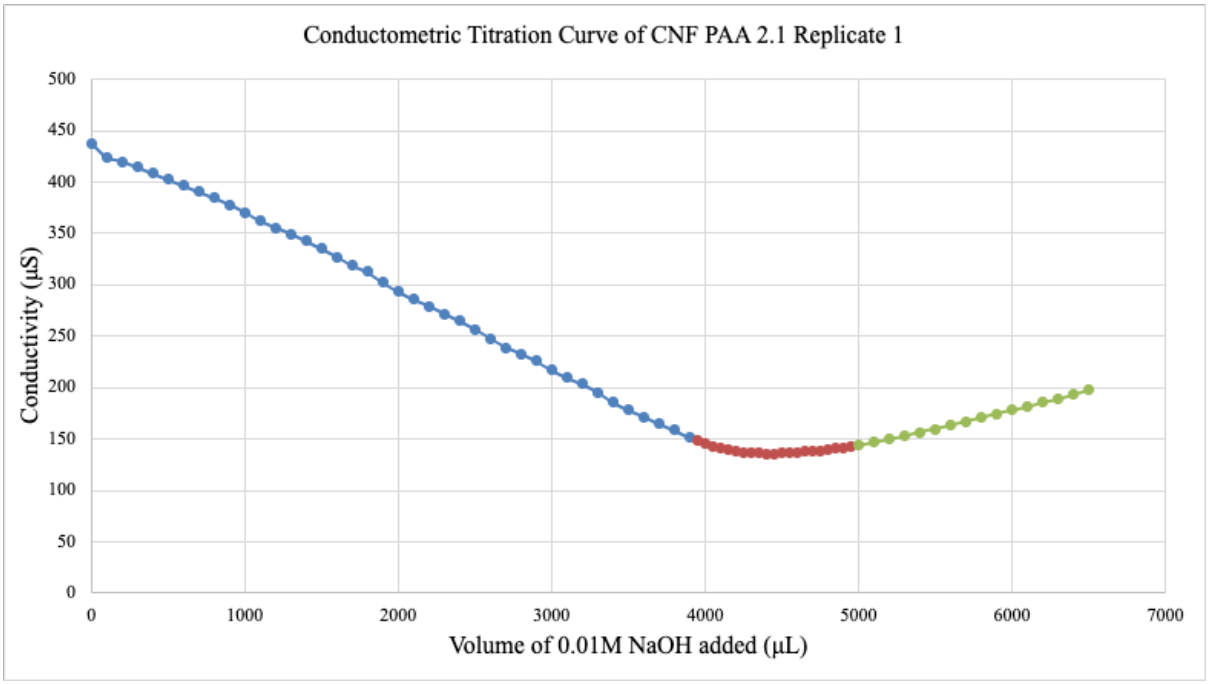


Figure A4. First replicate of conductometric titration curves used to calculate charge density of CNF from PAA reaction 2.1. It was calculated to be 146.04 µM/g.

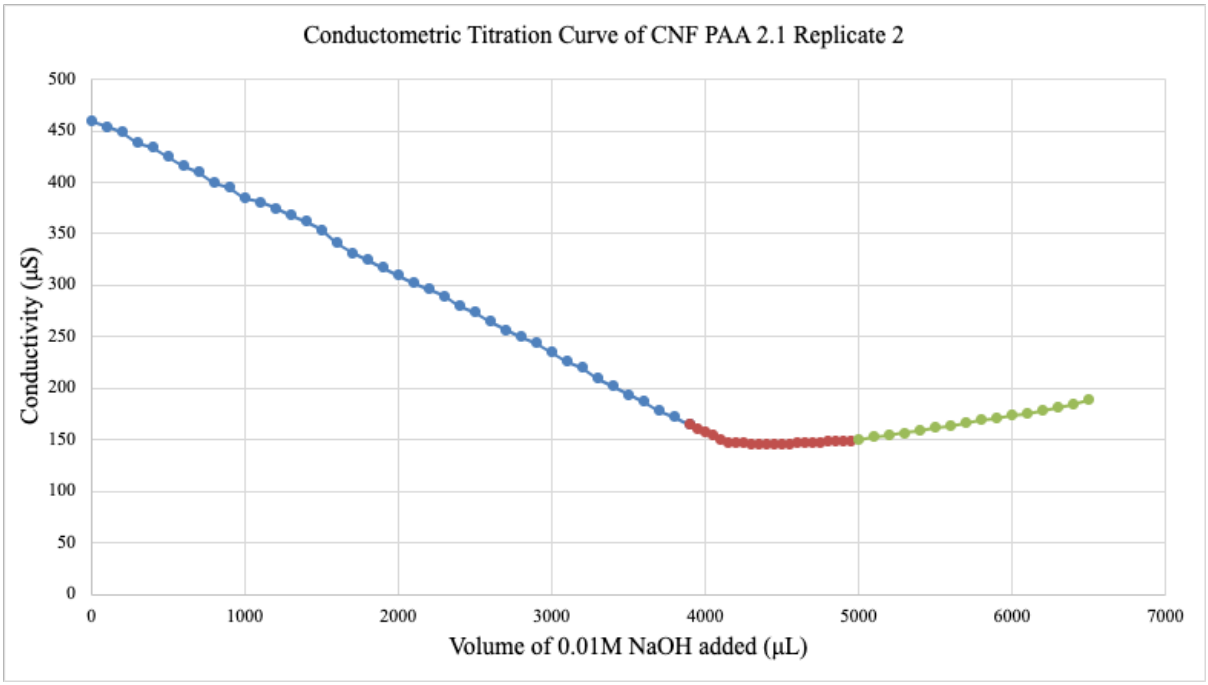


Figure A5. Second replicate of conductometric titration curves used to calculate charge density of CNF from PAA reaction 2.1. It was calculated to be 147.85 µM/g.

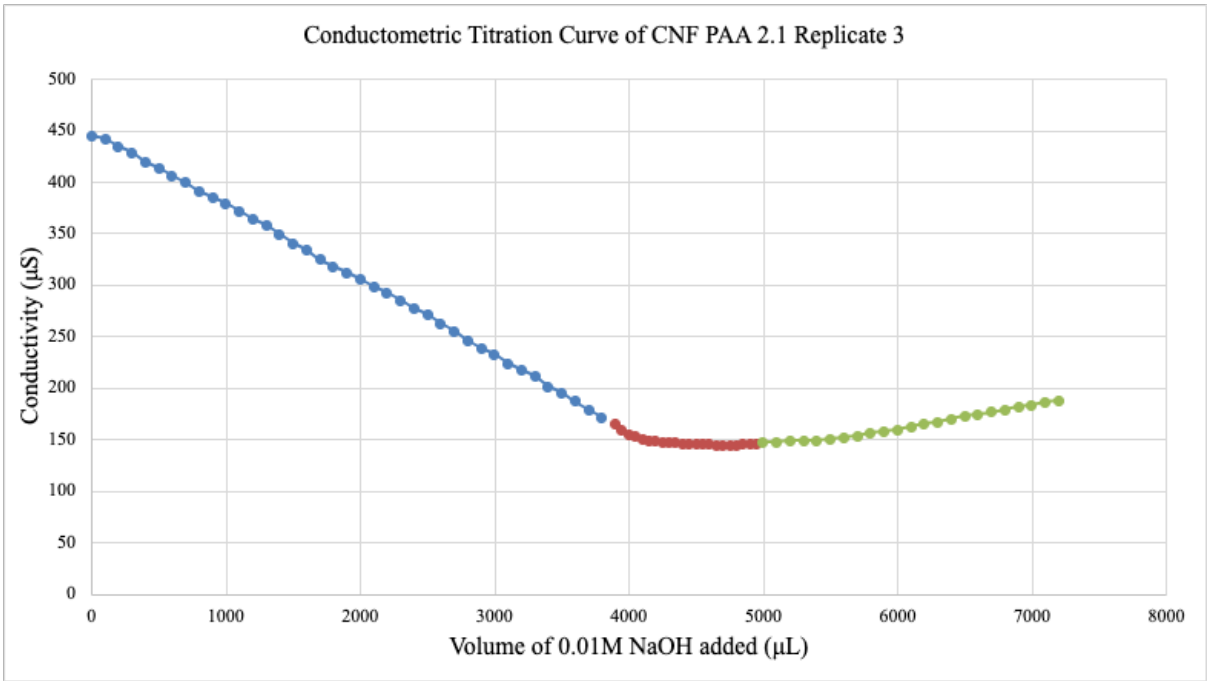


Figure A6. Third replicate of conductometric titration curves used to calculate charge density of CNF from PAA reaction 2.1. It was calculated to be 217.87 µM/g.

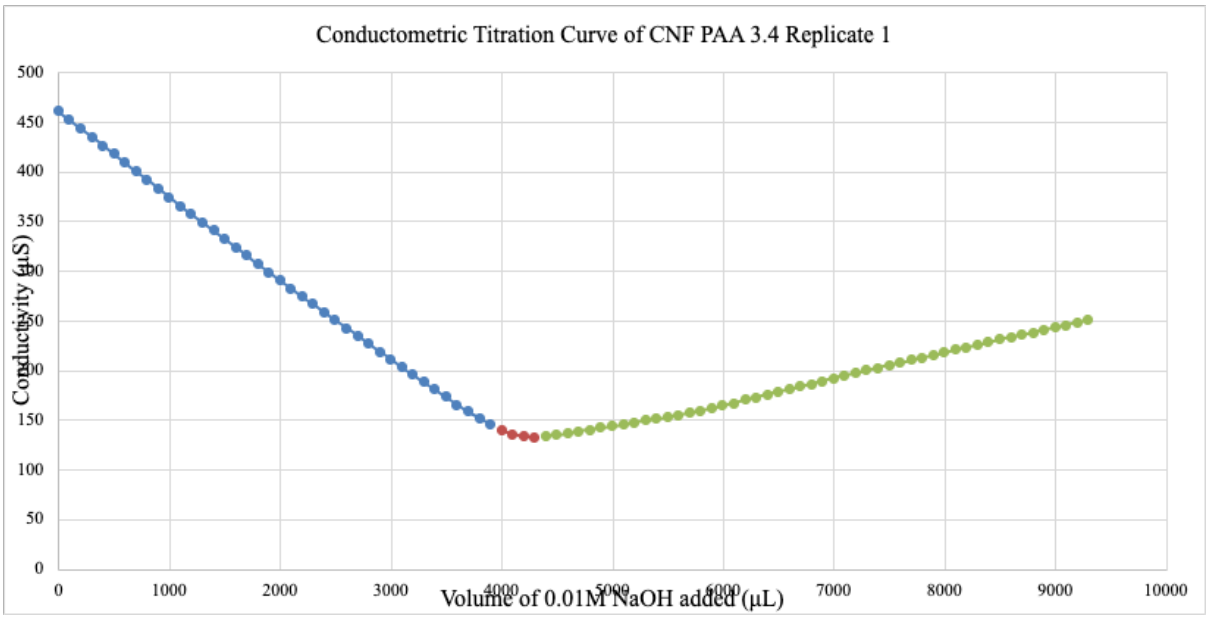


Figure A7. First replicate of conductometric titration curves used to calculate charge density of CNF from PAA reaction 3.4. It was calculated to be 127.60 µM/g.

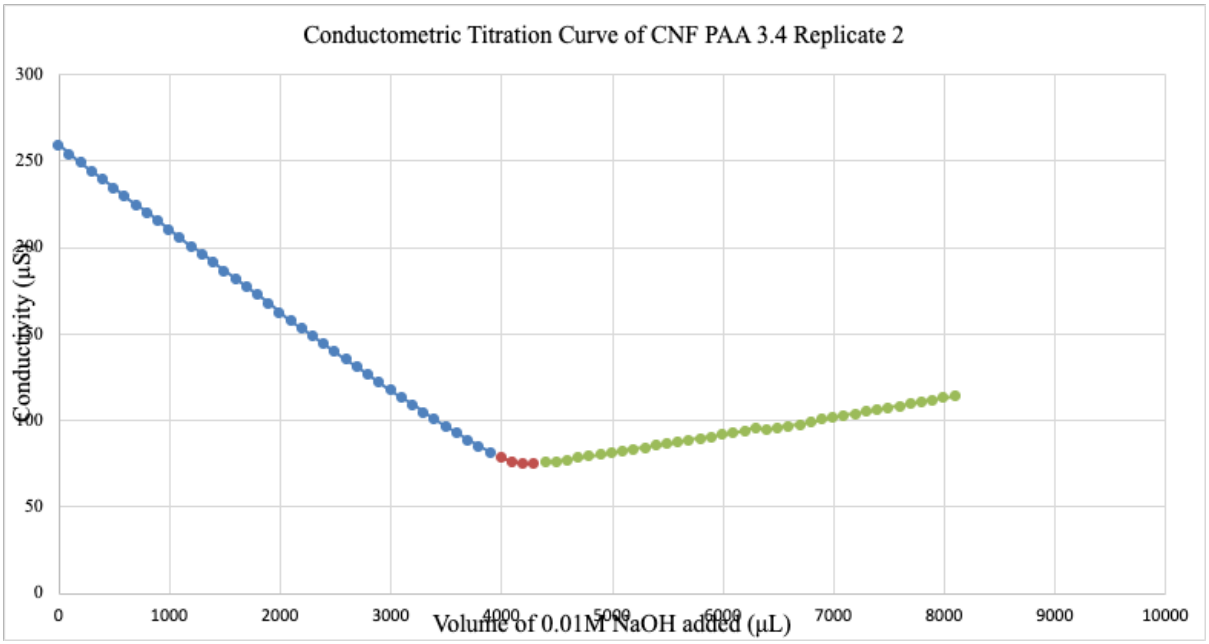


Figure A8. Second replicate of conductometric titration curves used to calculate charge density of CNF from PAA reaction 3.4. It was calculated to be 98.62 µM/g.

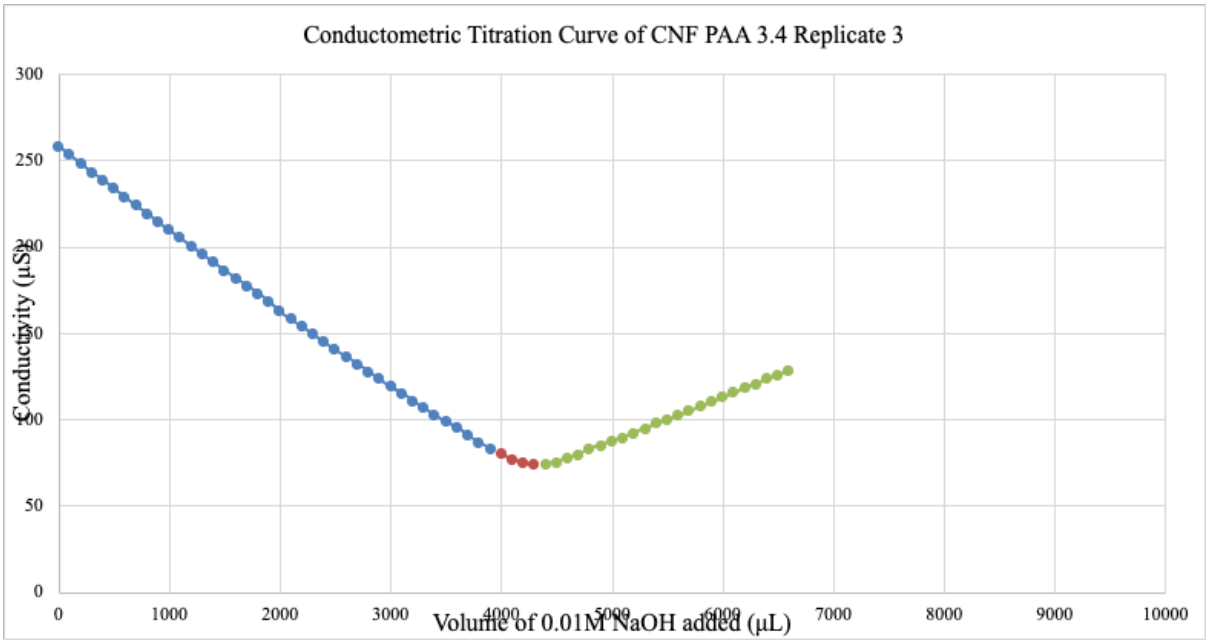


Figure A9. Third replicate of conductometric titration curves used to calculate charge density of CNF from PAA reaction 3.4. It was calculated to be 84.52 µM/g.

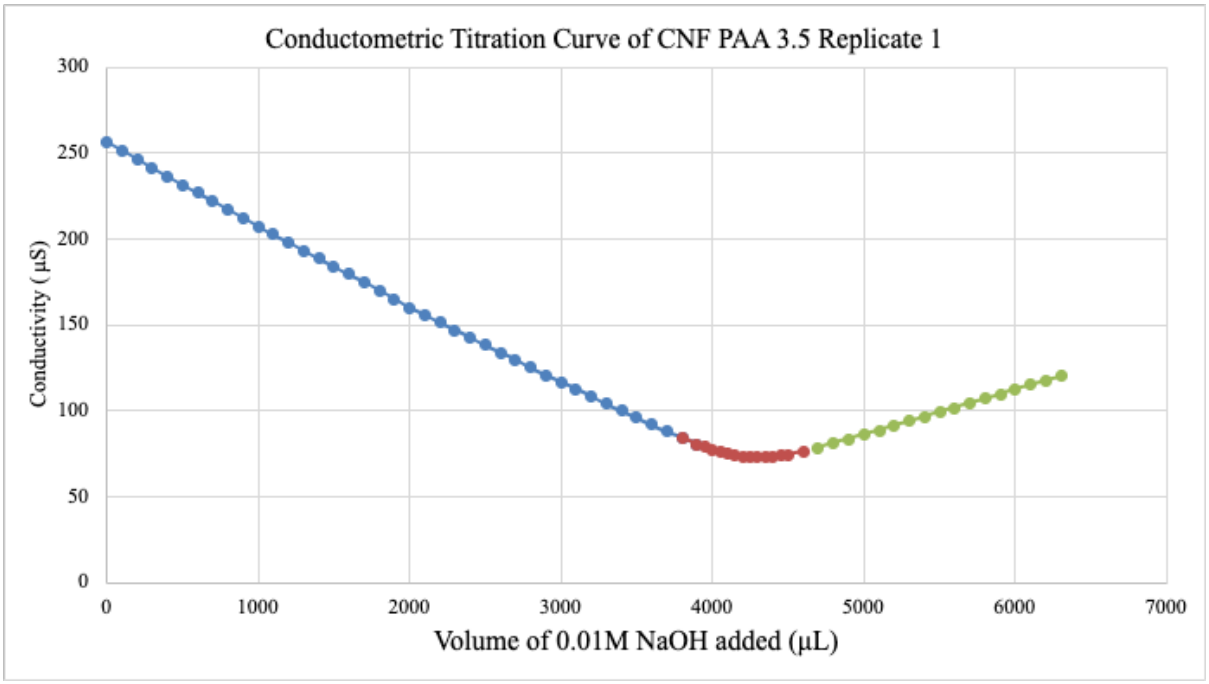


Figure A10. First replicate of conductometric titration curves used to calculate charge density of CNF from PAA reaction 3.5. It was calculated to be 97.60 µM/g.

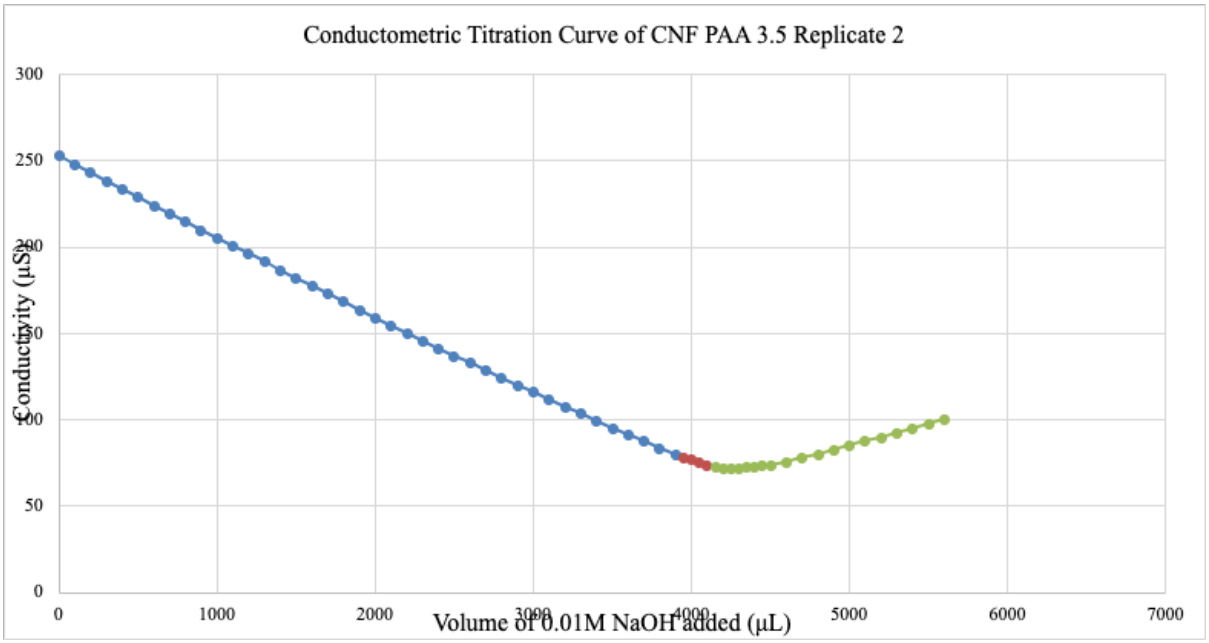


Figure A11. Second replicate of conductometric titration curves used to calculate charge density of CNF from PAA reaction 3.5. It was calculated to be 100.36 µM/g.

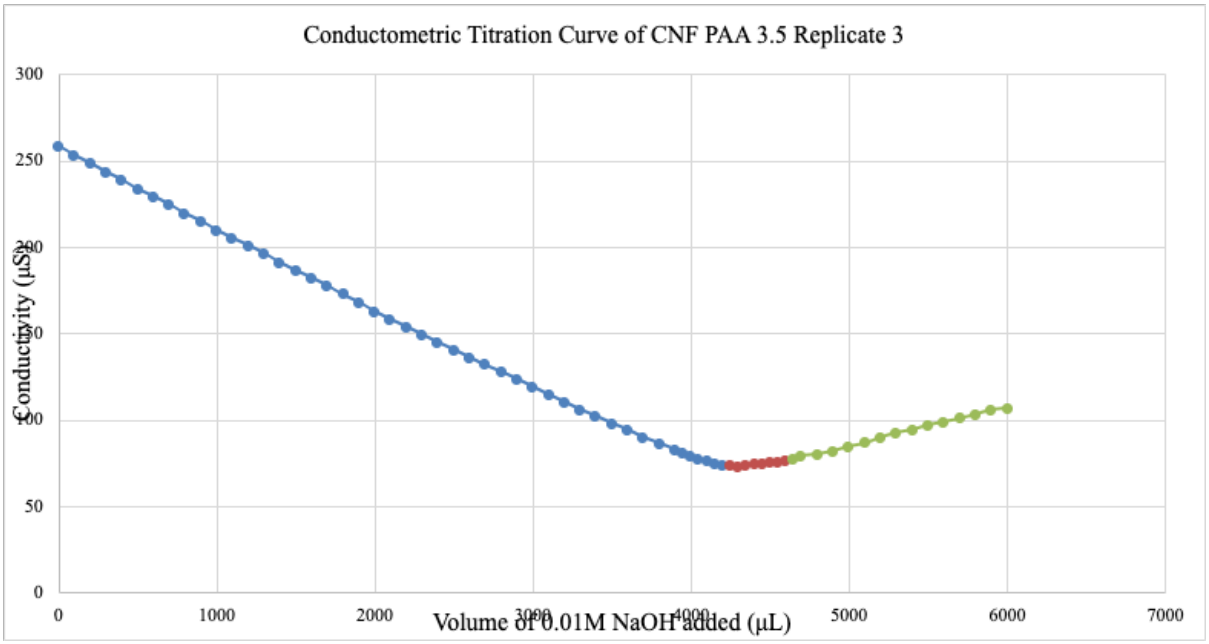


Figure A12. Third replicate of conductometric titration curves used to calculate charge density of CNF from PAA reaction 3.5. It was calculated to be 120.62 µM/g.

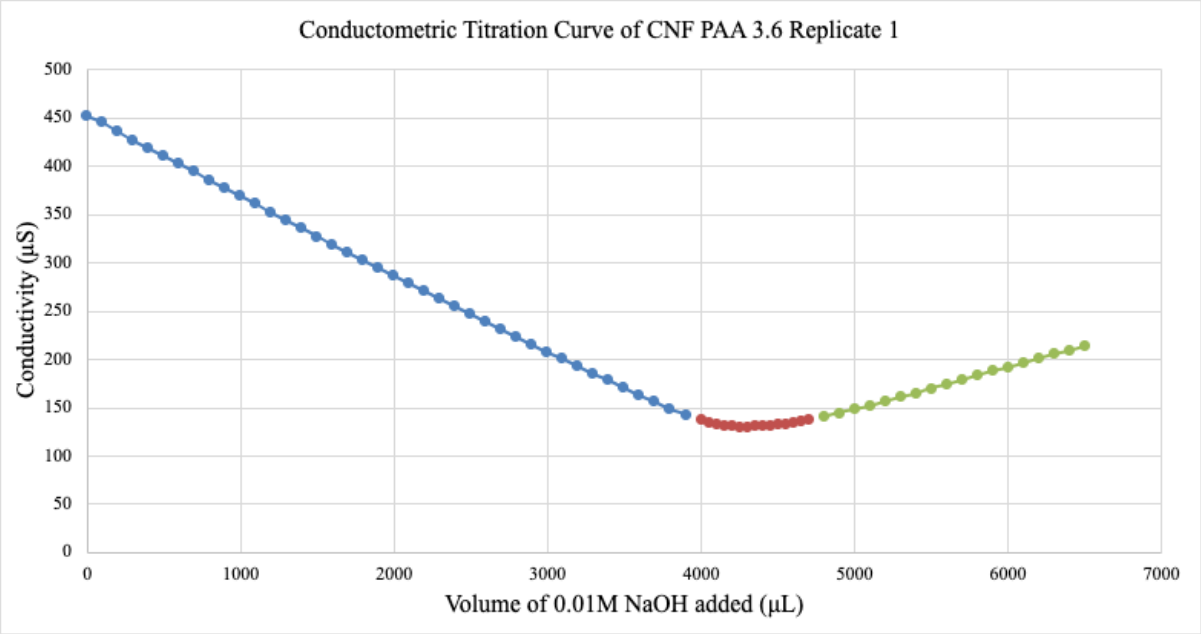


Figure A13. First replicate of conductometric titration curves used to calculate charge density of CNF from PAA reaction 3.6. It was calculated to be 112.94 µM/g.

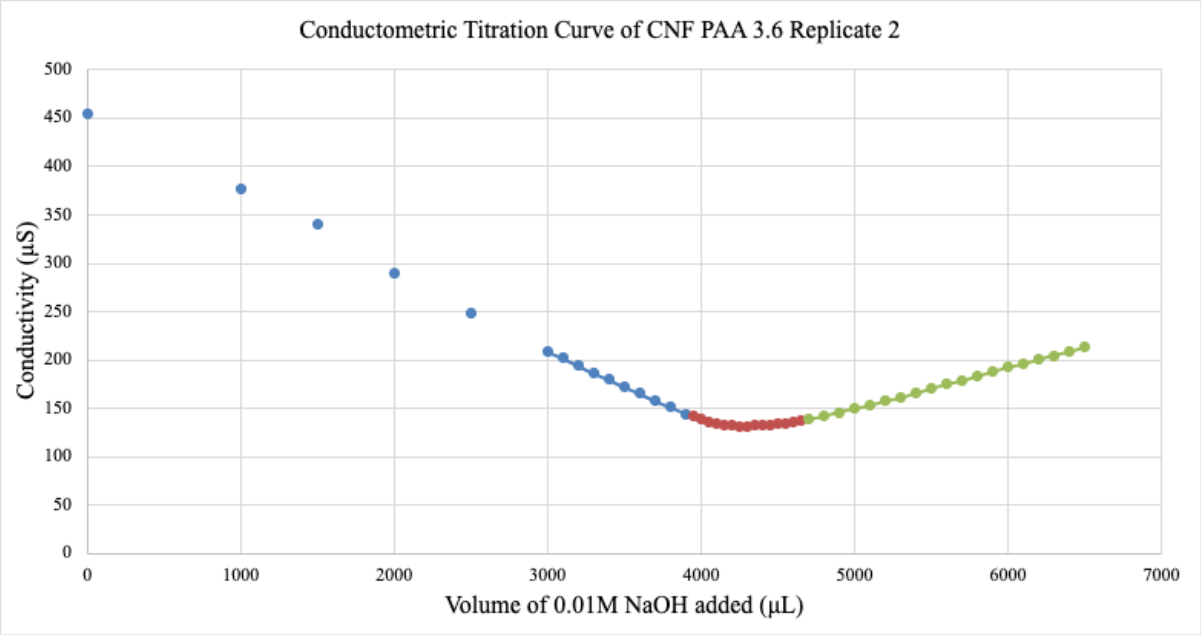


Figure A14. The second replicate of conductometric titration curves is used to calculate charge density of CNF from PAA reaction 3.6. It was calculated to be 120.64 µM/g.

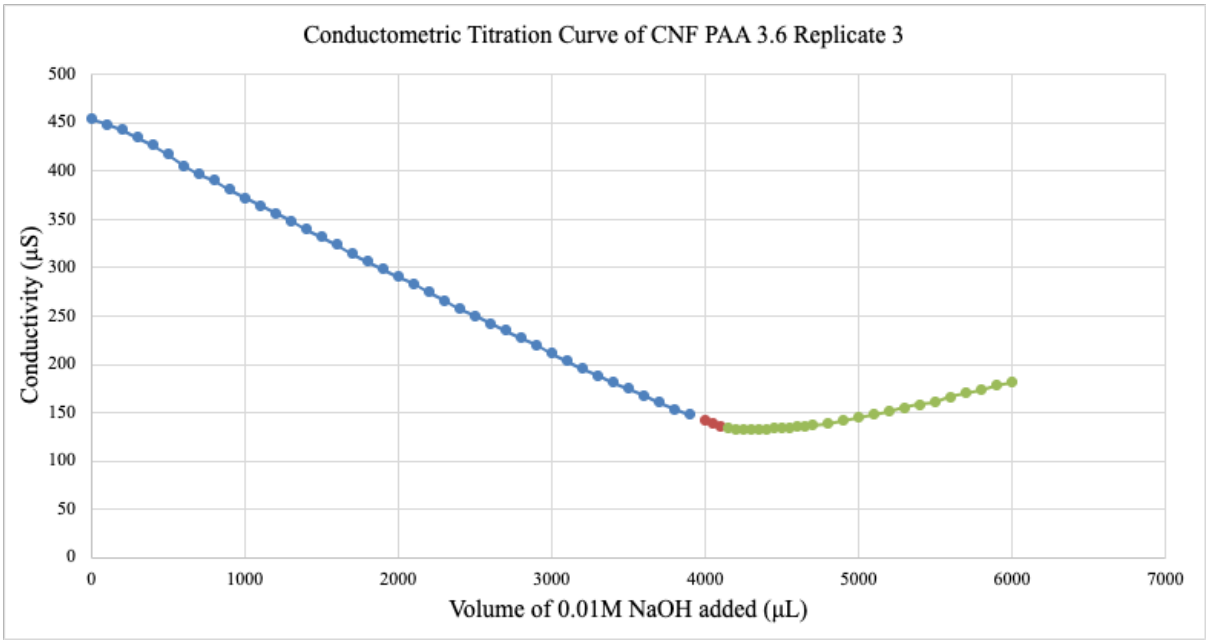


Figure A15. Third replicate of conductometric titration curves used to calculate charge density of CNF from PAA reaction 3.6. It was calculated to be 133.82 µM/g.

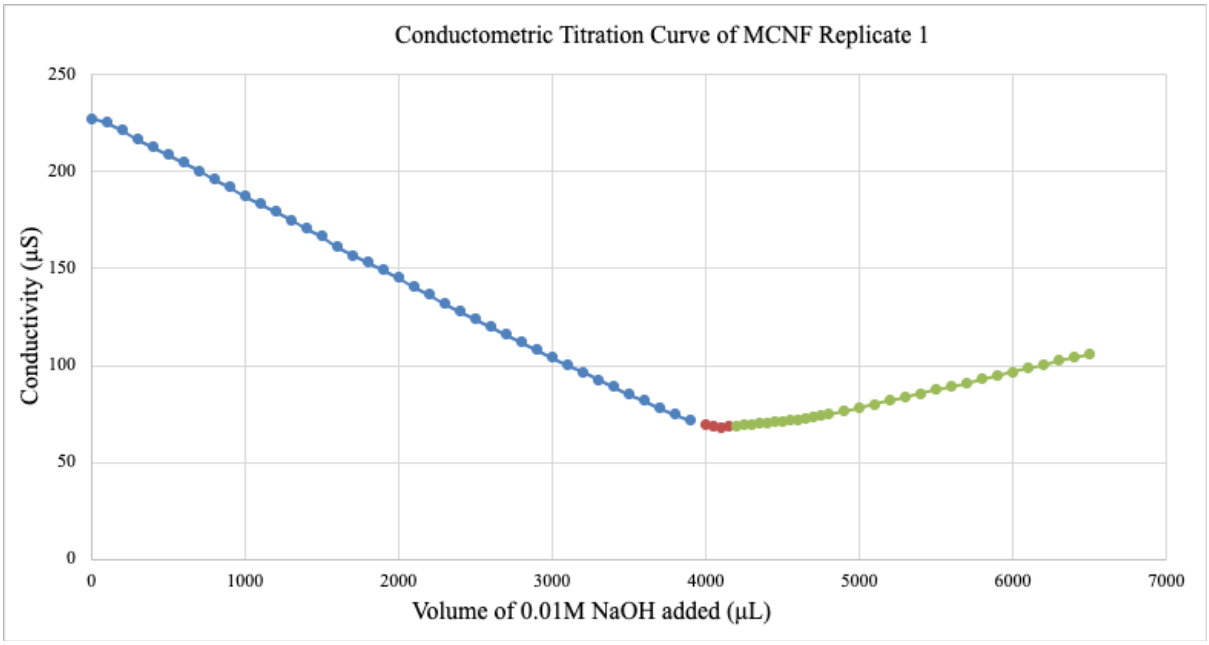


Figure A16. First replicate of conductometric titration curves used to calculate charge density of MCNF. It was calculated to be 160.94 µM/g.

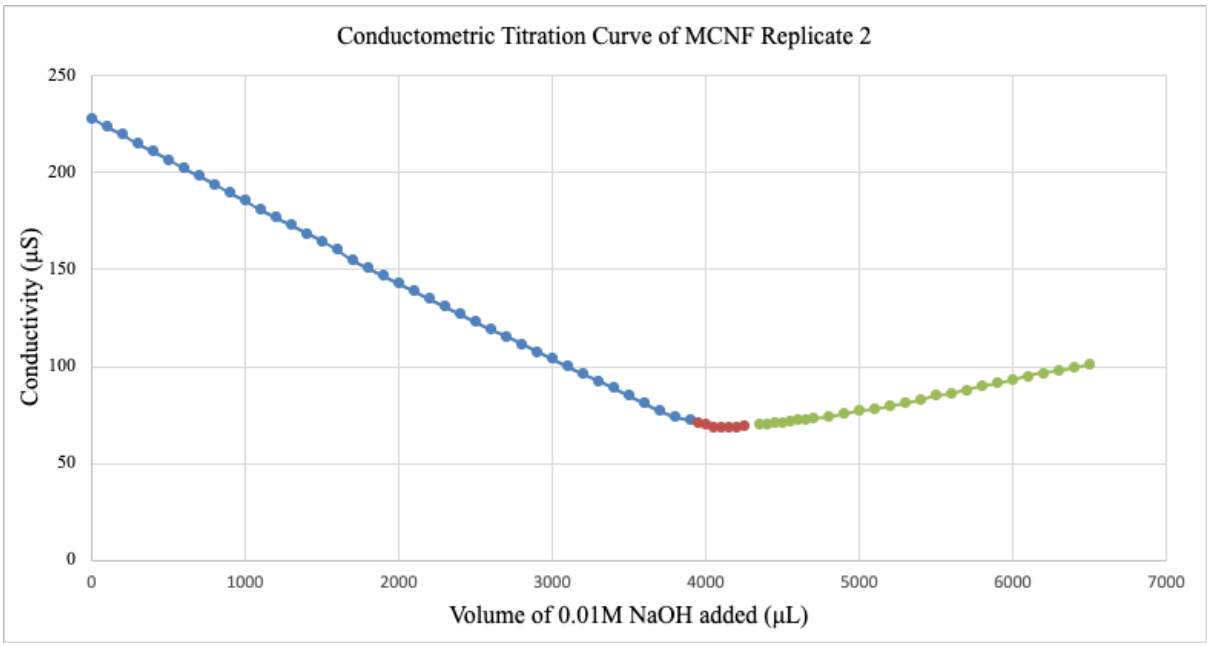


Figure A17. Second replicate of conductometric titration curves used to calculate charge density of MCNF. It was calculated to be 161.75 µM/g.

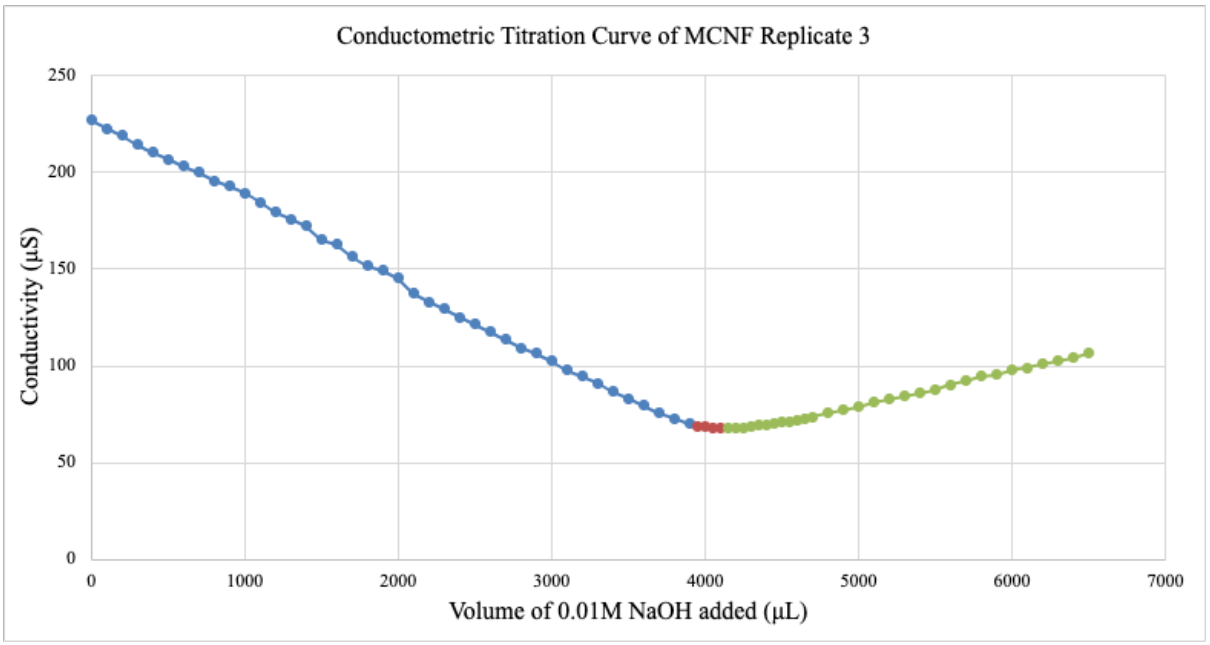


Figure A18. Third replicate of conductometric titration curves used to calculate charge density of MCNF. It was calculated to be 164.86 µM/g.

Film composition	CNF calculated (g)	CNF measured (g)	PVA calculated (g)	PVA measured (g)	Water calculated (g)	Water measured (g)
100% PVA	0.00	0.00	10.00	10.01	115.00	114.99
100% PVA	0.00	0.00	10.00	10.01	115.00	115.01
100% PVA	0.00	0.00	10.00	10.01	115.00	115.00
100% PVA	0.00	0.00	10.00	10.00	115.00	114.99
100% PVA	0.00	0.00	10.00	10.02	115.00	115.00
100% CNF	125.00	125.01	0.00	0.00	0.00	0.00
100% CNF	125.00	125.00	0.00	0.00	0.00	0.00
100% CNF	125.00	125.00	0.00	0.00	0.00	0.00
100% CNF	125.00	124.99	0.00	0.00	0.00	0.00
100% CNF	125.00	125.00	0.00	0.00	0.00	0.00
100% MCNF	125.00	125.00	0.00	0.00	0.00	0.00
100% MCNF	125.00	125.01	0.00	0.00	0.00	0.00
100% MCNF	125.00	125.01	0.00	0.00	0.00	0.00
100% MCNF	125.00	125.01	0.00	0.00	0.00	0.00
100% MCNF	125.00	125.01	0.00	0.00	0.00	0.00
95% CNF / 5% PVA	118.75	118.75	0.50	0.50	5.75	5.76
95% CNF / 5% PVA	118.75	118.75	0.50	0.51	5.75	5.74
95% CNF / 5% PVA	118.75	118.75	0.50	0.50	5.75	5.75
95% CNF / 5% PVA	118.75	118.75	0.50	0.51	5.75	5.77
95% CNF / 5% PVA	118.75	118.76	0.50	0.50	5.75	5.79
90% CNF / 10% PVA	112.50	112.50	1.00	1.02	11.50	11.53
90% CNF / 10% PVA	112.50	112.51	1.00	1.00	11.50	11.50
90% CNF / 10% PVA	112.50	112.50	1.00	1.00	11.50	11.54
90% CNF / 10% PVA	112.50	112.51	1.00	1.00	11.50	11.52
90% CNF / 10% PVA	112.50	112.51	1.00	1.00	11.50	11.51
85% CNF / 15% PVA	106.25	106.26	1.50	1.50	17.25	17.26
85% CNF / 15% PVA	106.25	106.24	1.50	1.52	17.25	17.24
85% CNF / 15% PVA	106.25	106.26	1.50	1.50	17.25	17.26

85% CNF / 15% PVA	106.25	106.25	1.50	1.52	17.25	17.33
85% CNF / 15% PVA	106.25	106.24	1.50	1.52	17.25	17.26
80% CNF / 20% PVA	100.00	100.01	2.00	2.00	23.00	23.03
80% CNF / 20% PVA	100.00	100.02	2.00	2.14	23.00	23.06
80% CNF / 20% PVA	100.00	100.02	2.00	2.02	23.00	23.04
80% CNF / 20% PVA	100.00	100.02	2.00	2.01	23.00	23.01
80% CNF / 20% PVA	100.00	100.00	2.00	2.01	23.00	23.00
95% MCNF / 5% PVA	118.75	118.75	0.50	0.52	5.75	5.77
95% MCNF / 5% PVA	118.75	118.75	0.50	0.51	5.75	5.77
95% MCNF / 5% PVA	118.75	118.76	0.50	0.53	5.75	5.77
95% MCNF / 5% PVA	118.75	118.75	0.50	0.51	5.75	5.77
95% MCNF / 5% PVA	118.75	118.76	0.50	0.52	5.75	5.77
90% MCNF / 10% PVA	112.50	112.50	1.00	1.01	11.50	11.82
90% MCNF / 10% PVA	112.50	112.51	1.00	1.01	11.50	11.50
90% MCNF / 10% PVA	112.50	112.49	1.00	0.99	11.50	11.52
90% MCNF / 10% PVA	112.50	112.51	1.00	0.99	11.50	11.52
90% MCNF / 10% PVA	112.50	112.51	1.00	1.07	11.50	11.50
85% MCNF / 15% PVA	106.25	106.25	1.50	1.49	17.25	17.27
85% MCNF / 15% PVA	106.25	106.26	1.50	1.53	17.25	17.28
85% MCNF / 15% PVA	106.25	106.25	1.50	1.49	17.25	17.25
85% MCNF / 15% PVA	106.25	106.24	1.50	1.50	17.25	17.27
85% MCNF / 15% PVA	106.25	106.26	1.50	1.50	17.25	17.90
80% MCNF / 20% PVA	100.00	100.00	2.00	1.99	23.00	23.02

80% MCNF / 20% PVA	100.00	100.00	2.00	1.99	23.00	23.00
80% MCNF / 20% PVA	100.00	100.00	2.00	1.98	23.00	23.00
80% MCNF / 20% PVA	100.00	99.99	2.00	1.99	23.00	23.00
80% MCNF / 20% PVA	100.00	100.02	2.00	2.02	23.00	23.01

Table A14. Calculated and measured amounts of CNF, MCNF, PVA, and DI water added to each replicate CNF/PVA composite film.

Film composition	Average thickness (µm)	Standard deviation
100% PVA	29.69	5.27
100% CNF	57.13	2.83
100% MCNF	56.36	1.65
95% CNF / 5% PVA	57.99	4.59
90% CNF / 10% PVA	53.29	2.10
85% CNF / 15% PVA	59.27	2.89
80% CNF / 20% PVA	62.49	3.41
95% MCNF / 5% PVA	60.09	2.88
90% MCNF / 10% PVA	57.30	1.58
85% MCNF / 15% PVA	57.20	2.14
80% MCNF / 20% PVA	59.43	3.77

Table A15. The average measured thickness of CNF, MCNF, and CNF/PVA composite films. Five films of each film composition were evaluated, and 10 thickness data points were measured per film.

Wavelength (nm)	Average transmittance % of 100% PVA film	Average transmittance % of 100% CNF film	Average transmittance % of 95% CNF / 5% PVA film	Average transmittance % of 90% CNF / 10% PVA film	Average transmittance % of 85% CNF / 15% PVA film	Average transmittance % of 80% CNF / 20% PVA film
800	91.69	73.62	82.69	85.74	86.46	85.68
795	91.50	73.33	82.80	85.88	86.52	85.52
790	91.72	73.44	82.81	85.84	86.61	85.65
785	91.61	73.38	82.66	85.72	86.42	85.52
780	91.42	73.13	82.50	85.59	86.31	85.35
775	91.70	73.33	82.53	85.66	86.35	85.53
770	91.72	73.27	82.55	85.71	86.41	85.52
765	91.35	72.89	82.68	85.85	86.56	85.39
760	91.62	73.05	82.57	85.73	86.48	85.44
755	91.61	73.04	82.66	85.80	86.51	85.51
750	91.71	73.06	82.43	85.64	86.37	85.41
745	91.63	72.89	82.33	85.48	86.24	85.29
740	91.65	72.86	82.35	85.59	86.28	85.34
735	91.60	72.76	82.09	85.31	86.03	85.19
730	91.73	72.81	82.20	85.42	86.17	85.30
725	91.69	72.75	82.11	85.38	86.06	85.21
720	91.73	72.70	82.18	85.47	86.15	85.24
715	91.70	72.59	82.04	85.34	86.04	85.15
710	91.54	72.43	82.16	85.48	86.16	85.09
705	91.74	72.50	82.04	85.35	86.06	85.13
700	91.62	72.37	81.97	85.32	86.00	85.02
695	91.64	72.32	81.92	85.28	85.98	84.98
690	91.60	72.21	81.87	85.25	85.92	84.94
685	91.64	72.16	81.87	85.24	85.94	84.98
680	91.62	72.07	81.84	85.21	85.93	84.90
675	91.50	71.92	81.77	85.18	85.85	84.78
670	91.59	71.91	81.67	85.06	85.76	84.78
665	91.62	71.87	81.68	85.11	85.79	84.78
660	91.64	71.80	81.61	85.06	85.75	84.74
655	91.55	71.64	81.59	85.05	85.73	84.65
650	91.61	71.62	81.49	84.97	85.65	84.61
645	91.59	71.53	81.38	84.88	85.54	84.55
640	91.53	71.38	81.32	84.83	85.50	84.46
635	91.56	71.33	81.23	84.74	85.40	84.43

630	91.53	71.20	81.23	84.78	85.45	84.37
625	91.54	71.13	81.10	84.68	85.33	84.31
620	91.50	71.00	81.06	84.62	85.28	84.22
615	91.56	70.96	81.02	84.62	85.26	84.22
610	91.58	70.86	80.93	84.54	85.18	84.14
605	91.46	70.66	80.86	84.48	85.12	84.01
600	91.55	70.63	80.78	84.44	85.06	84.00
595	91.53	70.51	80.65	84.33	84.95	83.90
590	91.49	70.39	80.56	84.26	84.88	83.82
585	91.49	70.28	80.50	84.22	84.81	83.74
580	91.56	70.22	80.40	84.13	84.74	83.70
575	91.48	70.05	80.32	84.06	84.67	83.59
570	91.51	69.93	80.24	84.00	84.58	83.51
565	91.50	69.80	80.14	83.93	84.51	83.42
560	91.59	69.76	80.07	83.88	84.46	83.40
555	91.58	69.62	80.02	83.86	84.43	83.33
550	91.56	69.48	79.96	83.82	84.39	83.24
545	91.58	69.35	79.79	83.66	84.23	83.14
540	91.53	69.18	79.69	83.59	84.14	83.01
535	91.56	69.05	79.59	83.52	84.06	82.93
530	91.51	68.87	79.44	83.38	83.92	82.78
525	91.50	68.71	79.35	83.32	83.86	82.67
520	91.49	68.55	79.19	83.19	83.71	82.54
515	91.50	68.41	79.03	83.04	83.57	82.42
510	91.45	68.20	78.91	82.96	83.48	82.28
505	91.45	68.03	78.78	82.85	83.35	82.15
500	91.48	67.87	78.60	82.69	83.20	82.01
495	91.43	67.64	78.45	82.56	83.05	81.84
490	91.44	67.45	78.33	82.45	82.93	81.70
485	91.40	67.21	78.10	82.26	82.72	81.50
480	91.28	66.91	77.92	82.11	82.54	81.25
475	91.29	66.70	77.69	81.91	82.33	81.06
470	91.33	66.48	77.48	81.75	82.14	80.88
465	91.27	66.18	77.26	81.56	81.93	80.63
460	91.27	65.89	77.02	81.33	81.68	80.39
455	91.23	65.50	76.71	81.07	81.38	80.04
450	91.28	65.16	76.40	80.80	81.08	79.75
445	91.14	64.65	76.07	80.50	80.74	79.31
440	91.14	64.19	75.64	80.13	80.36	78.90

435	91.13	63.66	75.14	79.69	79.86	78.39
430	91.10	63.06	74.71	79.29	79.40	77.89
425	91.07	62.40	74.07	78.72	78.79	77.25
420	91.10	61.67	73.46	78.19	78.19	76.62
415	91.07	60.83	72.70	77.46	77.42	75.84
410	91.07	59.87	71.86	76.71	76.60	74.94
405	91.02	58.74	70.80	75.71	75.53	73.85
400	90.86	57.37	69.63	74.63	74.37	72.57

Table A16. The average measured percent transmittance of CNF/PVA composite films. Five films of each film composition were evaluated, and five transmittance data points were measured at each of the following locations per film: top, bottom, center, left, and right.

Wavelength (nm)	Average transmittance % of 100% PVA film	Average transmittance % of 100% MCNF film	Average transmittance % of 95% MCNF/ 5% PVA film	Average transmittance % of 90% MCNF/ 10% PVA film	Average transmittance % of 85% MCNF/ 15% PVA film	Average transmittance % of 80% MCNF/ 20% PVA film
800	91.69	61.40	79.96	83.61	85.42	85.94
795	91.50	61.15	79.70	83.34	85.28	85.71
790	91.72	61.15	79.80	83.55	85.39	85.90
785	91.61	61.00	79.70	83.43	85.29	85.82
780	91.42	60.72	79.54	83.26	85.13	85.63
775	91.70	60.78	79.67	83.42	85.38	85.84
770	91.72	60.68	79.60	83.45	85.36	85.83
765	91.35	60.32	79.27	83.04	84.96	85.47
760	91.62	60.39	79.38	83.21	85.19	85.69
755	91.61	60.26	79.39	83.23	85.20	85.68
750	91.71	60.19	79.40	83.25	85.25	85.74
745	91.63	60.01	79.24	83.13	85.10	85.59
740	91.65	59.90	79.23	83.15	85.14	85.60
735	91.60	59.73	79.13	83.05	85.04	85.57
730	91.73	59.71	79.14	83.11	85.15	85.64
725	91.69	59.55	79.10	83.06	85.06	85.60
720	91.73	59.46	79.05	83.03	85.07	85.62
715	91.70	59.27	78.93	82.92	84.97	85.50
710	91.54	59.06	78.74	82.79	84.86	85.36
705	91.74	59.04	78.85	82.88	84.96	85.52
700	91.62	58.84	78.70	82.76	84.83	85.38
695	91.64	58.71	78.64	82.71	84.83	85.33
690	91.60	58.56	78.55	82.66	84.74	85.29
685	91.64	58.44	78.49	82.63	84.73	85.32
680	91.62	58.28	78.40	82.55	84.70	85.24
675	91.50	58.07	78.24	82.39	84.55	85.10
670	91.59	57.99	78.24	82.41	84.59	85.14
665	91.62	57.86	78.20	82.41	84.59	85.16
660	91.64	57.71	78.13	82.36	84.54	85.12
655	91.55	57.50	77.95	82.19	84.40	84.98
650	91.61	57.41	77.95	82.23	84.43	85.04
645	91.59	57.23	77.86	82.15	84.38	84.98
640	91.53	57.04	77.71	82.04	84.27	84.86

635	91.56	56.92	77.66	82.00	84.27	84.87
630	91.53	56.72	77.51	81.89	84.16	84.78
625	91.54	56.59	77.45	81.87	84.13	84.77
620	91.50	56.39	77.32	81.74	84.05	84.66
615	91.56	56.27	77.29	81.73	84.04	84.69
610	91.58	56.09	77.19	81.67	83.98	84.62
605	91.46	55.84	76.98	81.48	83.82	84.45
600	91.55	55.72	76.96	81.49	83.83	84.48
595	91.53	55.54	76.84	81.39	83.77	84.42
590	91.49	55.34	76.72	81.31	83.68	84.34
585	91.49	55.17	76.60	81.22	83.62	84.28
580	91.56	55.03	76.55	81.20	83.61	84.29
575	91.48	54.81	76.38	81.06	83.49	84.16
570	91.51	54.61	76.27	80.98	83.42	84.12
565	91.50	54.41	76.11	80.87	83.32	84.01
560	91.59	54.28	76.08	80.87	83.36	84.05
555	91.58	54.07	75.95	80.77	83.26	83.97
550	91.56	53.85	75.80	80.66	83.16	83.87
545	91.58	53.66	75.68	80.58	83.10	83.82
540	91.53	53.41	75.50	80.42	82.96	83.69
535	91.56	53.21	75.37	80.34	82.90	83.63
530	91.51	52.96	75.18	80.19	82.77	83.50
525	91.50	52.72	75.01	80.05	82.65	83.40
520	91.49	52.49	74.85	79.93	82.55	83.31
515	91.50	52.26	74.69	79.83	82.46	83.22
510	91.45	51.99	74.48	79.66	82.30	83.07
505	91.45	51.74	74.30	79.53	82.20	82.97
500	91.48	51.51	74.13	79.41	82.10	82.89
495	91.43	51.22	73.91	79.21	81.93	82.71
490	91.44	50.97	73.74	79.08	81.83	82.61
485	91.40	50.70	73.51	78.90	81.68	82.48
480	91.28	50.37	73.23	78.65	81.44	82.25
475	91.29	50.10	73.05	78.52	81.33	82.14
470	91.33	49.85	72.87	78.40	81.23	82.05
465	91.27	49.54	72.62	78.20	81.05	81.88
460	91.27	49.26	72.41	78.02	80.91	81.74
455	91.23	48.90	72.11	77.77	80.69	81.52
450	91.28	48.59	71.87	77.58	80.55	81.38
445	91.14	48.16	71.48	77.25	80.23	81.08

440	91.14	47.79	71.17	77.01	80.03	80.89
435	91.13	47.39	70.84	76.74	79.78	80.64
430	91.10	46.96	70.47	76.44	79.51	80.38
425	91.07	46.49	70.08	76.12	79.23	80.11
420	91.10	46.04	69.68	75.80	78.95	79.84
415	91.07	45.53	69.24	75.43	78.62	79.49
410	91.07	45.00	68.77	75.01	78.24	79.11
405	91.02	44.42	68.24	74.53	77.77	78.62
400	90.86	43.73	67.60	73.94	77.20	78.01

Table A17. The average measured percent transmittance of CNF/PVA and MCNF/PVA composite films. Five films of each film composition were evaluated, and five transmittance data points were measured at each of the following locations per film: top, bottom, center, left, and right.

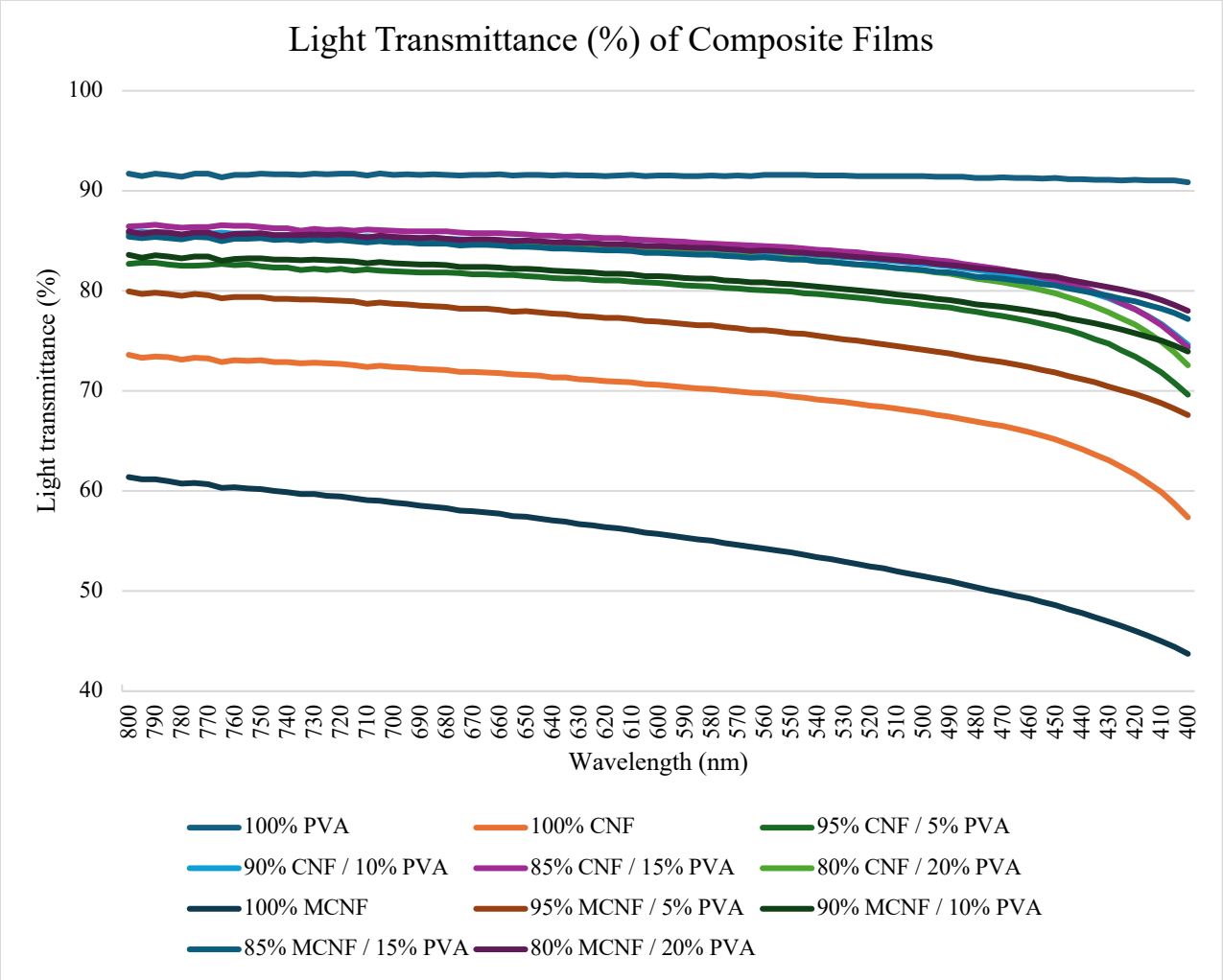


Figure A19. The average measured percent transmittance of CNF/PVA and MCNF/PVA composite films. Five films of each film composition were evaluated, and five transmittance data points were measured at each of the following locations per film: top, bottom, center, left, and right.

Film composition	Average transmittance % at 660 nm	Standard deviation
100% PVA	91.64	0.06
100% CNF	71.80	2.26
100% MCNF	57.71	0.93
95% CNF / 5% PVA	81.61	1.45
90% CNF / 10% PVA	85.06	0.85
85% CNF / 15% PVA	85.75	0.39
80% CNF / 20% PVA	84.74	1.58
95% MCNF / 5% PVA	78.13	3.33
90% MCNF / 10% PVA	82.36	0.97
85% MCNF / 15% PVA	84.54	0.04
80% MCNF / 20% PVA	85.12	0.11

Table A18. The average measured percent transmittance of CNF/PVA and MCNF/PVA composite films at a wavelength of 660 nm. Five films of each film composition were evaluated, and five transmittance data points were measured at each of the following locations per film: top, bottom, center, left, and right.

Film composition	Haze (%) of matte side	Diffuse luminous transmittance (%)	Y sample (light transmittance)	Y sample and instrument scatter	Y instrument scatter	Illuminant (A=1, C=2)	Std obs (2 or 10 degrees)
100% PVA	0.42	1.93	90.71	1.95	1.73	1	2
100% PVA	1.32	2.92	90.51	2.94	1.93	1	2
100% PVA	1.23	2.10	90.62	2.11	1.09	1	2
100% PVA	0.57	2.13	90.72	2.15	1.80	1	2
100% PVA	0.67	1.62	90.50	1.63	1.13	1	2
100% CNF	96.80	50.63	51.89	50.63	0.78	1	2
100% CNF	93.19	62.41	66.29	62.41	0.96	1	2
100% CNF	93.20	59.81	62.83	59.82	2.02	1	2
100% CNF	95.30	59.70	62.53	59.70	0.17	1	2
100% CNF	95.22	55.68	57.88	55.69	1.00	1	2
100% MCNF	95.07	53.02	54.59	53.03	2.08	1	2
100% MCNF	95.02	53.57	55.17	53.58	2.11	1	2
100% MCNF	94.98	53.06	54.69	53.07	2.06	1	2
100% MCNF	95.27	53.08	54.55	53.09	2.05	1	2
100% MCNF	95.24	54.16	55.74	54.17	1.94	1	2
95% CNF / 5% PVA	86.66	70.54	81.15	70.54	0.27	1	2
95% CNF / 5% PVA	85.25	70.29	82.18	70.30	0.29	1	2
95% CNF / 5% PVA	84.07	65.27	77.35	65.27	0.32	1	2

95% CNF / 5% PVA	85.72	70.06	81.56	70.06	0.17	1	2
95% CNF / 5% PVA	87.56	69.13	78.79	69.13	0.18	1	2
90% CNF / 10% PVA	79.47	67.95	84.95	67.95	0.52	1	2
90% CNF / 10% PVA	82.08	68.29	82.81	68.29	0.39	1	2
90% CNF / 10% PVA	75.74	63.04	82.80	63.04	0.40	1	2
90% CNF / 10% PVA	78.52	67.35	85.33	67.36	0.42	1	2
90% CNF / 10% PVA	75.28	62.40	82.40	62.40	0.46	1	2
85% CNF / 15% PVA	83.35	70.62	84.25	70.62	0.48	1	2
85% CNF / 15% PVA	74.67	63.65	84.69	63.65	0.49	1	2
85% CNF / 15% PVA	82.72	70.51	83.88	70.52	1.35	1	2
85% CNF / 15% PVA	78.86	67.26	84.55	67.26	0.69	1	2
85% CNF / 15% PVA	77.85	67.54	84.89	67.56	1.73	1	2

80% CNF / 20% PVA	78.13	67.22	84.36	67.23	1.56	1	2
80% CNF / 20% PVA	76.74	66.28	84.58	66.29	1.65	1	2
80% CNF / 20% PVA	78.43	66.55	83.15	66.57	1.62	1	2
80% CNF / 20% PVA	81.43	68.62	82.57	68.64	1.69	1	2
80% CNF / 20% PVA	77.35	65.77	84.40	65.77	0.57	1	2
95% MCNF / 5% PVA	77.02	62.02	78.80	62.03	1.69	1	2
95% MCNF / 5% PVA	79.42	62.29	76.88	62.30	1.61	1	2
95% MCNF / 5% PVA	82.91	62.66	73.71	62.68	2.12	1	2
95% MCNF / 5% PVA	77.68	61.99	78.23	62.00	1.58	1	2
95% MCNF / 5% PVA	84.89	62.61	72.40	62.62	1.60	1	2
90% MCNF / 10% PVA	71.56	59.17	80.70	59.18	1.78	1	2
90% MCNF / 10% PVA	76.15	61.54	79.01	61.55	1.76	1	2
90% MCNF /	81.13	62.92	76.02	62.94	1.66	1	2

10% PVA							
90% MCNF / 10% PVA	66.29	56.06	82.52	56.57	1.66	1	2
90% MCNF / 10% PVA	68.17	56.76	81.15	56.77	1.79	1	2
85% MCNF / 15% PVA	67.19	56.97	82.69	56.98	1.72	1	2
85% MCNF / 15% PVA	66.17	56.08	82.52	56.09	1.80	1	2
85% MCNF / 15% PVA	65.90	55.69	82.18	55.70	1.89	1	2
85% MCNF / 15% PVA	65.52	55.60	82.52	55.61	1.87	1	2
85% MCNF / 15% PVA	61.90	52.97	83.09	52.99	1.88	1	2
80% MCNF / 20% PVA	61.81	53.06	83.33	53.08	1.89	1	2
80% MCNF / 20% PVA	59.22	51.26	83.94	51.28	1.86	1	2
80% MCNF / 20% PVA	61.22	52.79	83.61	52.81	1.94	1	2
80% MCNF / 20% PVA	57.29	49.57	83.72	49.58	1.93	1	2

80% MCNF / 20% PVA	58.08	51.03	83.55	51.05	2.02	1	2

Summary		
Film composition	**Average haze (%) of matte side**	**Standard deviation**
100% PVA	0.84	0.41
100% CNF	94.74	1.55
100% MCNF	95.12	0.13
95% CNF / 5% PVA	85.85	1.33
90% CNF / 10% PVA	78.22	2.80
85% CNF / 15% PVA	79.49	3.59
80% CNF / 20% PVA	78.42	1.81
95% MCNF / 5% PVA	80.38	3.40
90% MCNF / 10% PVA	72.66	6.04
85% MCNF / 15% PVA	65.34	2.02
80% MCNF / 20% PVA	59.52	1.95

Table A19. The average measured percent haze of the matte side of CNF/PVA and MCNF/PVA composite films. Five films of each film composition were evaluated, and three data points were measured to calculate the percentage haze.

Film composition	Haze (%) of glossy side	Diffuse luminous transmittance (%)	Y sample (light transmittance)	Y sample and instrument scatter	Y instrument scatter	Illuminant (A=1, C=2)	Std obs (2 or 10 degrees)
100% CNF	95.36	51.65	53.11	51.66	1.92	1	2
100% CNF	89.34	66.52	72.60	66.54	2.31	1	2
100% CNF	94.40	56.81	59.03	56.82	1.85	1	2
100% CNF	91.03	65.04	70.10	65.05	1.77	1	2
100% CNF	94.26	57.41	59.94	57.41	1.53	1	2
100% MCNF	95.29	53.07	54.62	53.08	1.88	1	2
100% MCNF	95.05	52.11	53.67	52.12	2.07	1	2
100% MCNF	94.81	53.23	54.98	53.24	2.04	1	2
100% MCNF	95.20	53.12	54.62	53.13	2.07	1	2
100% MCNF	95.36	53.91	55.42	53.92	1.93	1	2
95% CNF / 5% PVA	85.14	70.17	82.15	70.17	0.28	1	2
95% CNF / 5% PVA	86.03	68.94	79.86	68.94	0.29	1	2
95% CNF / 5% PVA	84.61	63.71	75.02	63.71	0.32	1	2
95% CNF / 5% PVA	85.04	68.82	80.76	68.82	0.17	1	2
95% CNF / 5% PVA	86.40	69.72	80.54	69.72	0.17	1	2
90% CNF / 10% PVA	78.76	65.27	82.47	65.27	0.39	1	2

90% CNF / 10% PVA	81.14	66.46	81.50	66.46	0.40	1	2
90% CNF / 10% PVA	75.39	61.06	80.54	61.06	0.43	1	2
90% CNF / 10% PVA	79.90	65.73	81.84	65.73	0.41	1	2
90% CNF / 10% PVA	75.81	61.13	80.16	61.13	0.46	1	2
85% CNF / 15% PVA	83.22	67.28	80.39	67.28	0.47	1	2
85% CNF / 15% PVA	74.40	61.53	82.18	61.53	0.48	1	2
85% CNF / 15% PVA	83.95	67.89	80.40	67.89	0.49	1	2
85% CNF / 15% PVA	80.05	64.62	80.59	64.62	0.12	1	2
85% CNF / 15% PVA	78.37	64.14	81.26	64.15	0.57	1	2
80% CNF / 20% PVA	78.10	62.59	79.48	62.60	0.66	1	2
80% CNF / 20% PVA	77.50	64.25	81.17	64.26	1.67	1	2
80% CNF /	77.49	63.75	80.52	63.77	1.70	1	2

20% PVA							
80% CNF / 20% PVA	80.36	64.29	79.43	64.29	0.59	1	2
80% CNF / 20% PVA	76.19	61.47	79.81	61.48	0.83	1	2
95% MCNF / 5% PVA	79.74	62.11	76.49	62.12	1.48	1	2
95% MCNF / 5% PVA	79.30	61.90	76.58	61.91	1.55	1	2
95% MCNF / 5% PVA	84.56	59.00	68.12	59.02	2.08	1	2
95% MCNF / 5% PVA	75.75	61.15	79.01	61.16	1.66	1	2
95% MCNF / 5% PVA	83.57	60.09	70.55	60.10	1.62	1	2
90% MCNF / 10% PVA	73.45	60.05	79.98	60.07	1.65	1	2
90% MCNF / 10% PVA	75.33	60.50	78.26	60.51	1.99	1	2
90% MCNF / 10% PVA	82.54	62.66	74.37	62.68	1.74	1	2
90% MCNF / 10% PVA	67.52	55.73	80.43	55.74	1.79	1	2
90% MCNF / 10% PVA	73.90	58.91	77.94	58.93	1.71	1	2

85% MCNF / 15% PVA	66.40	56.18	82.45	56.20	1.76	1	2
85% MCNF / 15% PVA	65.77	55.18	81.68	55.19	1.80	1	2
85% MCNF / 15% PVA	65.23	55.20	82.29	55.22	1.87	1	2
85% MCNF / 15% PVA	68.20	56.37	80.43	56.38	1.90	1	2
85% MCNF / 15% PVA	62.01	52.73	82.54	52.74	1.90	1	2
80% MCNF / 20% PVA	62.40	52.86	82.29	52.87	1.85	1	2
80% MCNF / 20% PVA	62.23	52.93	82.44	52.95	2.00	1	2
80% MCNF / 20% PVA	61.98	53.00	82.80	53.01	2.05	1	2
80% MCNF / 20% PVA	58.84	50.43	83.00	50.45	1.93	1	2
80% MCNF / 20% PVA	59.23	50.44	82.27	50.46	2.10	1	2

Summary

Film composition	Average haze (%) of glossy side	Standard deviation
100% CNF	92.88	2.57
100% MCNF	95.14	0.22
95% CNF / 5% PVA	85.44	0.74

90% CNF / 10% PVA	78.20	2.52
85% CNF / 15% PVA	80.00	3.87
80% CNF / 20% PVA	77.93	1.53
95% MCNF / 5% PVA	80.58	3.55
90% MCNF / 10% PVA	74.55	5.37
85% MCNF / 15% PVA	65.52	2.26
80% MCNF / 20% PVA	60.94	1.75

Table A20. Average measured percent haze of the glossy side of CNF/PVA and MCNF/PVA films. Five films of each film composition were evaluated, and three data points were measured to calculate the percentage haze. Note, there is no glossy side of 100% PVA films as the two sides were undistinguishable.

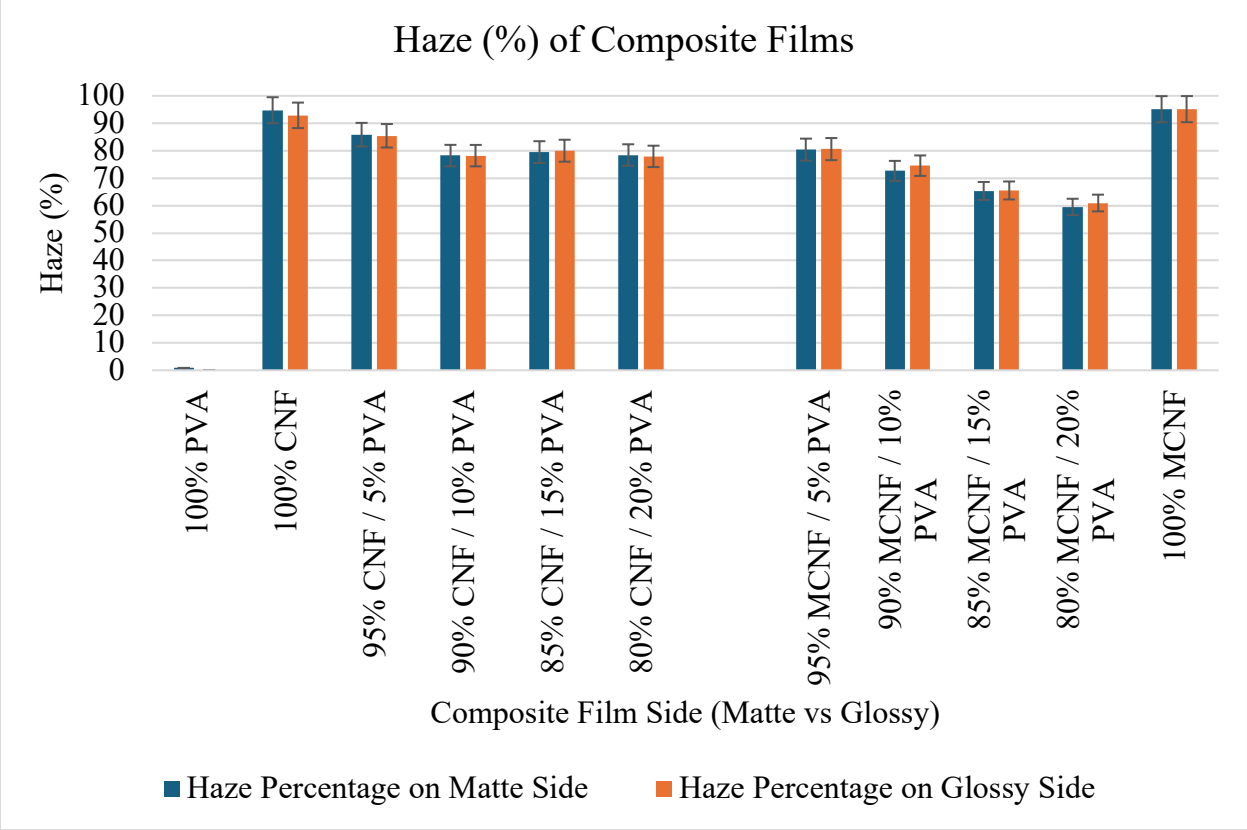


Figure A20. Comparison of the average measured percent haze of the glossy and matte sides of CNF/PVA and MCNF/PVA composite films. Five films of each film composition were evaluated, and three data points were measured to calculate the percentage haze. Note, there is no glossy side of 100% PVA films as the two sides were undistinguishable.

Film composition	Tensile strength (MPa)	Peak elongation (%)	Tensile energy absorption at maximum (J/m)	Tensile stiffness	Elastic modulus (MPa)
100% PVA	1009.43	2.34	14.76	0.04	2713.27
100% PVA	1197.23	2.28	16.87	0.04	2848.79
100% PVA	1032.90	5.57	45.74	0.03	1842.88
100% PVA	1854.53	3.23	37.75	0.05	2892.06
100% PVA	2300.56	3.31	50.16	0.07	4451.03
100% PVA	1889.74	2.60	31.27	0.07	2979.07
100% PVA	1819.32	3.11	36.51	0.05	2460.05
100% PVA	1044.64	2.62	17.30	0.04	2268.16
100% PVA	1091.59	2.18	14.69	0.04	2574.29
100% PVA	1349.82	2.12	17.43	0.05	3004.87
100% CNF	5950.93	5.46	220.54	0.16	4667.68
100% CNF	4213.77	5.09	135.89	0.11	3439.33
100% CNF	4530.69	3.19	92.06	0.14	4272.89
100% CNF	6009.62	5.69	228.55	0.15	4452.44
100% CNF	6220.89	5.25	218.15	0.15	4563.22
100% CNF	4812.39	3.90	124.08	0.14	4587.39
100% CNF	4518.95	2.94	84.14	0.16	5073.85
100% CNF	4155.09	3.59	96.14	0.13	4324.32
100% CNF	3861.65	3.09	75.63	0.13	4165.17
100% CNF	4835.86	3.50	108.76	0.15	4679.74
100% MCNF	7688.08	6.27	326.93	0.19	5970.76
100% MCNF	8439.28	6.53	368.87	0.17	5407.48
100% MCNF	8544.92	9.01	543.33	0.18	5632.80
100% MCNF	9718.67	11.47	789.10	0.17	5421.07
100% MCNF	10106.01	11.72	833.74	0.19	5702.99
100% MCNF	7899.36	6.29	331.51	0.19	5945.21

100% MCNF	5094.09	2.72	85.21	0.21	6862.86
95% CNF / 5% PVA	4929.76	6.61	205.46	0.09	2427.66
95% CNF / 5% PVA	4871.07	5.05	168.19	0.14	3953.31
95% CNF / 5% PVA	3568.21	3.16	72.01	0.12	3432.84
95% CNF / 5% PVA	5810.08	5.51	205.57	0.15	4316.83
95% CNF / 5% PVA	4624.59	2.89	82.28	0.14	4349.84
95% CNF / 5% PVA	5105.83	3.91	127.30	0.13	4152.56
95% CNF / 5% PVA	4213.77	2.60	67.06	0.15	5111.62
95% CNF / 5% PVA	4554.16	3.62	106.88	0.14	4849.09
95% CNF / 5% PVA	5023.66	3.23	103.27	0.16	4776.15
95% CNF / 5% PVA	6655.18	5.64	245.60	0.17	5029.03
90% CNF / 10% PVA	4741.96	3.26	99.23	0.15	5038.88
90% CNF / 10% PVA	5974.40	4.61	181.94	0.16	5093.60
90% CNF / 10% PVA	5387.53	4.15	139.75	0.13	4363.27
90% CNF / 10% PVA	5035.40	3.34	106.69	0.15	5092.06
90% CNF / 10% PVA	5739.65	4.58	170.31	0.16	5220.17
90% CNF / 10% PVA	4495.47	3.08	85.72	0.13	4355.39
90% CNF / 10% PVA	5246.68	4.05	137.03	0.15	5086.91

90% CNF / 10% PVA	4695.01	3.45	105.57	0.14	4372.11
90% CNF / 10% PVA	5457.95	4.06	148.21	0.15	4822.57
90% CNF / 10% PVA	6291.32	4.96	212.49	0.18	6175.01
90% CNF / 10% PVA	4295.94	2.95	78.88	0.14	4685.26
90% CNF / 10% PVA	4683.27	3.45	102.96	0.14	4676.04
85% CNF / 15% PVA	5117.56	3.27	106.72	0.15	4707.11
85% CNF / 15% PVA	5845.29	4.03	155.09	0.16	5052.56
85% CNF / 15% PVA	6126.99	4.16	163.68	0.18	5651.31
85% CNF / 15% PVA	6279.58	4.16	170.66	0.17	5313.39
85% CNF / 15% PVA	6009.62	4.76	190.14	0.16	4835.21
85% CNF / 15% PVA	5563.59	4.00	146.55	0.17	5224.32
85% CNF / 15% PVA	5692.70	4.32	166.17	0.17	5165.71
85% CNF / 15% PVA	4049.45	1.98	46.87	0.16	4719.59
85% CNF / 15% PVA	4824.12	2.51	74.57	0.17	4670.50
85% CNF / 15% PVA	4777.17	2.99	90.40	0.15	4489.43
80% CNF / 20% PVA	5129.30	4.86	167.34	0.12	3474.79
80% CNF / 20% PVA	4812.39	3.09	94.72	0.15	4204.06
80% CNF / 20% PVA	5997.88	5.01	200.56	0.15	4045.63

80% CNF / 20% PVA	5845.29	4.76	189.27	0.17	4410.79
80% CNF / 20% PVA	6584.75	4.78	204.88	0.17	5048.90
80% CNF / 20% PVA	6796.03	4.61	206.48	0.17	5152.83
80% CNF / 20% PVA	7641.13	4.79	240.07	0.20	5818.78
80% CNF / 20% PVA	4495.47	2.47	68.16	0.17	5032.29
80% CNF / 20% PVA	4178.56	2.24	55.78	0.15	4204.17
95% MCNF / 5% PVA	9530.87	11.82	808.79	0.18	5655.19
95% MCNF / 5% PVA	8568.40	9.88	629.70	0.20	5858.31
95% MCNF / 5% PVA	8944.00	10.93	694.36	0.18	5491.17
95% MCNF / 5% PVA	8533.18	10.07	608.69	0.16	4656.28
95% MCNF / 5% PVA	10728.10	12.31	944.92	0.21	6192.14
95% MCNF / 5% PVA	3474.31	1.19	22.89	0.19	5069.70
95% MCNF / 5% PVA	9037.90	9.75	633.42	0.18	5011.67
95% MCNF / 5% PVA	6303.05	4.31	183.50	0.17	5133.52

95% MCNF / 5% PVA	9366.55	9.45	638.82	0.22	6603.17
90% MCNF / 10% PVA	6901.67	5.40	262.74	0.19	5915.05
90% MCNF / 10% PVA	9120.06	9.70	638.50	0.20	6323.37
90% MCNF / 10% PVA	7500.28	7.24	385.72	0.19	5892.79
90% MCNF / 10% PVA	7054.26	6.52	325.86	0.16	5001.38
90% MCNF / 10% PVA	7406.38	7.18	385.17	0.17	5553.02
90% MCNF / 10% PVA	6678.65	3.72	163.54	0.21	6416.14
90% MCNF / 10% PVA	8662.30	10.13	627.09	0.19	5804.19
90% MCNF / 10% PVA	9765.62	12.75	872.23	0.18	5502.71
90% MCNF / 10% PVA	8803.15	9.52	595.23	0.19	5742.88
90% MCNF / 10% PVA	9425.24	9.07	606.52	0.21	6232.88
90% MCNF / 10% PVA	7441.59	4.08	191.74	0.21	6213.96

85% MCNF / 15% PVA	5751.39	5.22	215.13	0.17	4976.53
85% MCNF / 15% PVA	10035.59	10.48	754.58	0.22	6607.11
85% MCNF / 15% PVA	5399.26	2.82	96.89	0.19	5680.22
85% MCNF / 15% PVA	7993.26	7.90	454.68	0.18	5654.84
85% MCNF / 15% PVA	8263.22	9.36	565.36	0.19	6055.88
85% MCNF / 15% PVA	8005.00	8.80	498.74	0.17	5336.67
85% MCNF / 15% PVA	5739.65	3.67	140.21	0.18	5570.36
85% MCNF / 15% PVA	8087.16	9.41	549.87	0.16	5073.46
85% MCNF / 15% PVA	7065.99	5.48	271.41	0.18	5300.80
85% MCNF / 15% PVA	7875.88	6.96	379.35	0.17	5028.77
85% MCNF / 15% PVA	5704.44	2.82	100.35	0.20	6255.38
85% MCNF / 15% PVA	8814.89	10.14	646.08	0.20	6328.14

85% MCNF / 15% PVA	6209.15	3.27	128.27	0.21	6515.33
80% MCNF / 20% PVA	4248.99	1.50	35.41	0.19	5334.01
80% MCNF / 20% PVA	8005.00	9.51	547.42	0.16	4643.07
80% MCNF / 20% PVA	6784.29	3.87	167.89	0.21	6067.77
80% MCNF / 20% PVA	6866.46	5.80	284.17	0.18	5225.79
80% MCNF / 20% PVA	7148.16	9.43	480.78	0.14	4306.92
80% MCNF / 20% PVA	5258.41	2.77	92.79	0.20	6305.25
80% MCNF / 20% PVA	9108.32	10.11	665.67	0.20	6272.62
80% MCNF / 20% PVA	6737.34	4.13	183.03	0.20	5412.00
80% MCNF / 20% PVA	6514.33	3.61	151.49	0.21	5791.03
80% MCNF / 20% PVA	7523.76	4.45	214.03	0.21	5663.48

Summary

Film composition	Average tensile strength (MPa)	Standard deviation
100% PVA	48.20	14.31
100% CNF	86.30	12.05

100% MCNF	143.81	28.03
95% CNF / 5% PVA	85.30	14.16
90% CNF / 10% PVA	97.22	11.99
85% CNF / 15% PVA	93.59	14.51
80% CNF / 20% PVA	92.26	20.89
95% MCNF / 5% PVA	138.08	37.81
90% MCNF / 10% PVA	140.46	18.19
85% MCNF / 15% PVA	127.98	25.63
80% MCNF / 20% PVA	113.43	25.24
Film composition	**Average peak elongation (%)**	**Standard deviation**
100% PVA	2.94	1.02
100% CNF	4.17	1.08
100% MCNF	7.72	3.22
95% CNF / 5% PVA	4.22	1.38
90% CNF / 10% PVA	3.83	0.66
85% CNF / 15% PVA	3.62	0.89
80% CNF / 20% PVA	4.07	1.13
95% MCNF / 5% PVA	8.86	3.68
90% MCNF / 10% PVA	7.76	2.77
85% MCNF / 15% PVA	6.64	2.90
80% MCNF / 20% PVA	5.52	3.08
Film composition	**Average Young's modulus (MPa)**	**Standard deviation**
100% PVA	2575.32	599.12
100% CNF	4118.44	473.24
100% MCNF	5303.20	379.33
95% CNF / 5% PVA	4182.14	643.78
90% CNF / 10% PVA	4657.50	479.19
85% CNF / 15% PVA	4720.38	345.22
80% CNF / 20% PVA	4394.61	647.74
95% MCNF / 5% PVA	5258.06	735.48
90% MCNF / 10% PVA	5459.07	379.46
85% MCNF / 15% PVA	5356.00	523.64
80% MCNF / 20% PVA	5073.74	498.44

Table A21. Measured tensile data of CNF/PVA and, MCNF/PVA composite films. At least seven films of each PVA film composition were tested to calculate the average tensile strength, peak elongation and average Young's Modulus.

Film composition	Average mass decrease (%)	Standard deviation
100% PVA	11.97	5.59
100% CNF	24.20	9.24
100% MCNF	12.47	5.97
95% CNF / 5% PVA	20.86	5.70
90% CNF / 10% PVA	26.13	7.64
85% CNF / 15% PVA	36.08	7.00
80% CNF / 20% PVA	43.26	18.98
95% MCNF / 5% PVA	12.40	10.21
90% MCNF / 10% PVA	10.67	5.70
85% MCNF / 15% PVA	18.09	8.45
80% MCNF / 20% PVA	26.82	14.85

Table A22. The average measured percent mass decrease of CNF/PVA and MCNF/PVA composite films after eleven weeks because in soil at constant humidity. At least four samples of each film were measured weekly to calculate the average percent mass decrease.

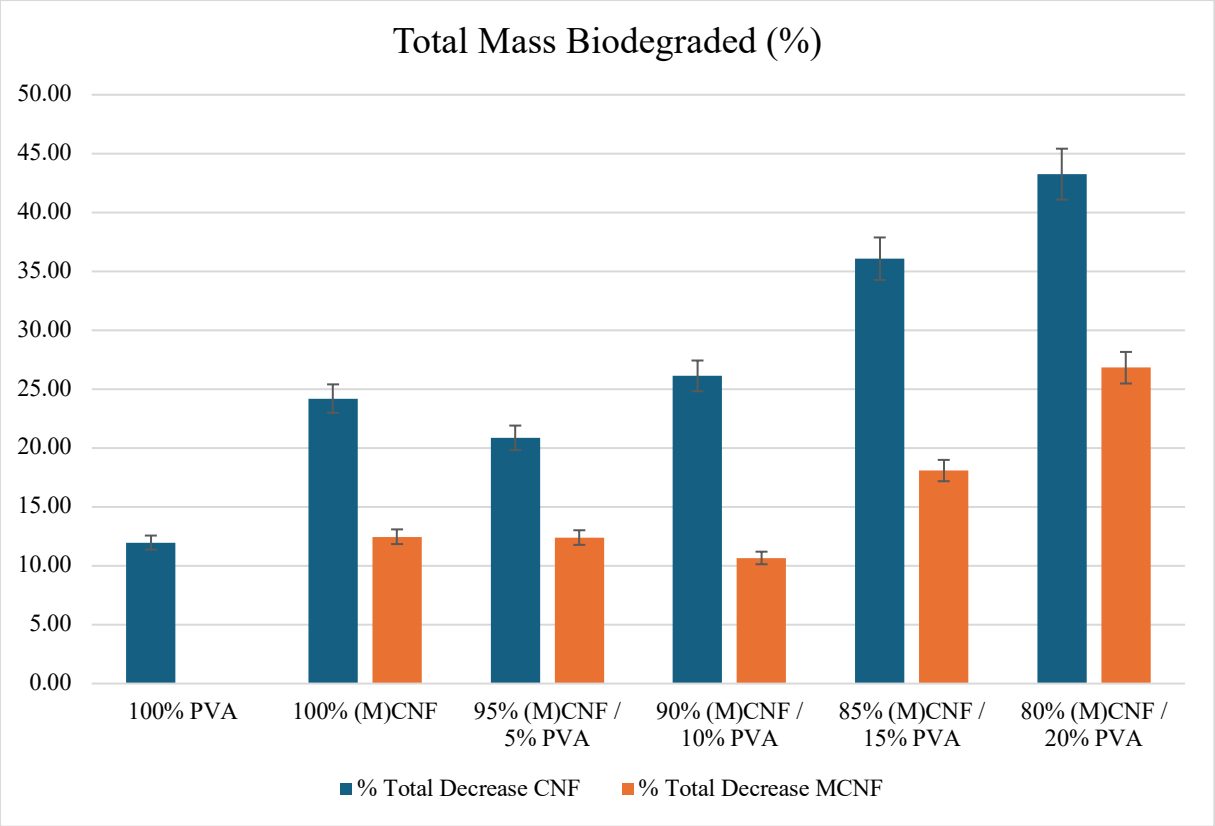


Figure A21. Comparison of the average measured percent mass decrease of CNF/PVA and MCNF/PVA composite films after eleven weeks because of in soil at constant humidity. At least four samples of each film were measured weekly to calculate the average percent mass decrease.

	Static contact angle (deg) over 10 minutes										
Time (s)	100 % PVA	100 % CNF	100% MCNF	95% CNF / 5% PVA	90% CNF / 10% PVA	85% CNF / 15% PVA	80% CNF / 20% PVA	95% MCNF / 5% PVA	90% MCNF / 10% PVA	85% MCNF / 15% PVA	80% MCNF / 20% PVA
0	16.7	56.0	46.2	52.0	61.2	51.7	54.3	40.5	49.2	43.5	34.9
30	17.0	54.8	47.5	59.5	56.9	51.7	54.1	37.4	49.6	42.1	34.5
60	17.1	52.0	46.4	45.2	53.9	50.6	55.7	36.8	51.7	41.3	33.7
90	16.4	52.2	45.6	53.6	55.3	50.8	53.4	37.5	49.4	40.1	33.6
120	15.8	51.7	45.1	50.8	54.1	50.4	55.0	36.0	49.9	38.8	33.1
150	15.5	51.7	44.6	54.0	53.3	51.0	54.6	32.1	47.6	37.9	33.0
180	15.5	49.0	44.1	45.2	51.1	51.3	56.3	33.5	45.3	37.2	32.1
210	15.4	49.8	43.6	45.7	52.9	50.9	57.5	34.0	43.9	36.4	32.1
240	15.4	47.8	43.1	44.7	52.5	50.6	57.0	32.9	43.1	35.9	31.5
270	13.5	46.4	43.0	44.9	51.5	50.0	60.1	27.9	42.6	35.5	31.3
300	0.0	46.5	42.4	49.6	50.5	49.8	56.1	31.7	42.0	33.9	30.6
330	0.0	45.5	41.9	48.1	50.1	49.6	55.0	30.1	41.6	34.4	30.1
360	0.0	45.7	41.3	44.0	48.5	49.0	53.5	32.1	41.1	34.0	30.0
390	0.0	45.1	41.6	44.0	51.6	48.7	54.3	31.3	40.6	32.7	29.5
420	0.0	44.3	39.4	52.9	48.2	48.3	53.4	29.0	40.2	31.8	29.1
450	0.0	43.4	38.5	47.3	46.9	47.7	53.5	30.1	40.0	31.8	29.0
480	0.0	43.8	37.5	42.3	46.3	47.3	52.9	29.0	39.2	31.3	28.4
510	0.0	42.8	37.1	49.7	51.1	46.8	52.6	26.3	38.7	30.3	28.1
540	0.0	42.2	36.6	51.8	45.7	46.4	51.8	26.4	38.0	30.8	27.7
570	0.0	41.4	36.1	46.6	50.5	45.8	51.9	27.7	37.7	30.2	27.0
600	0.0	41.6	35.6	46.6	45.1	45.4	51.1	26.6	37.1	29.1	27.0

Table A23. Measured static contact angle of CNF/PVA and MCNF/PVA composite films over 10 minutes. A contact angle measurement was calculated every 30 seconds.

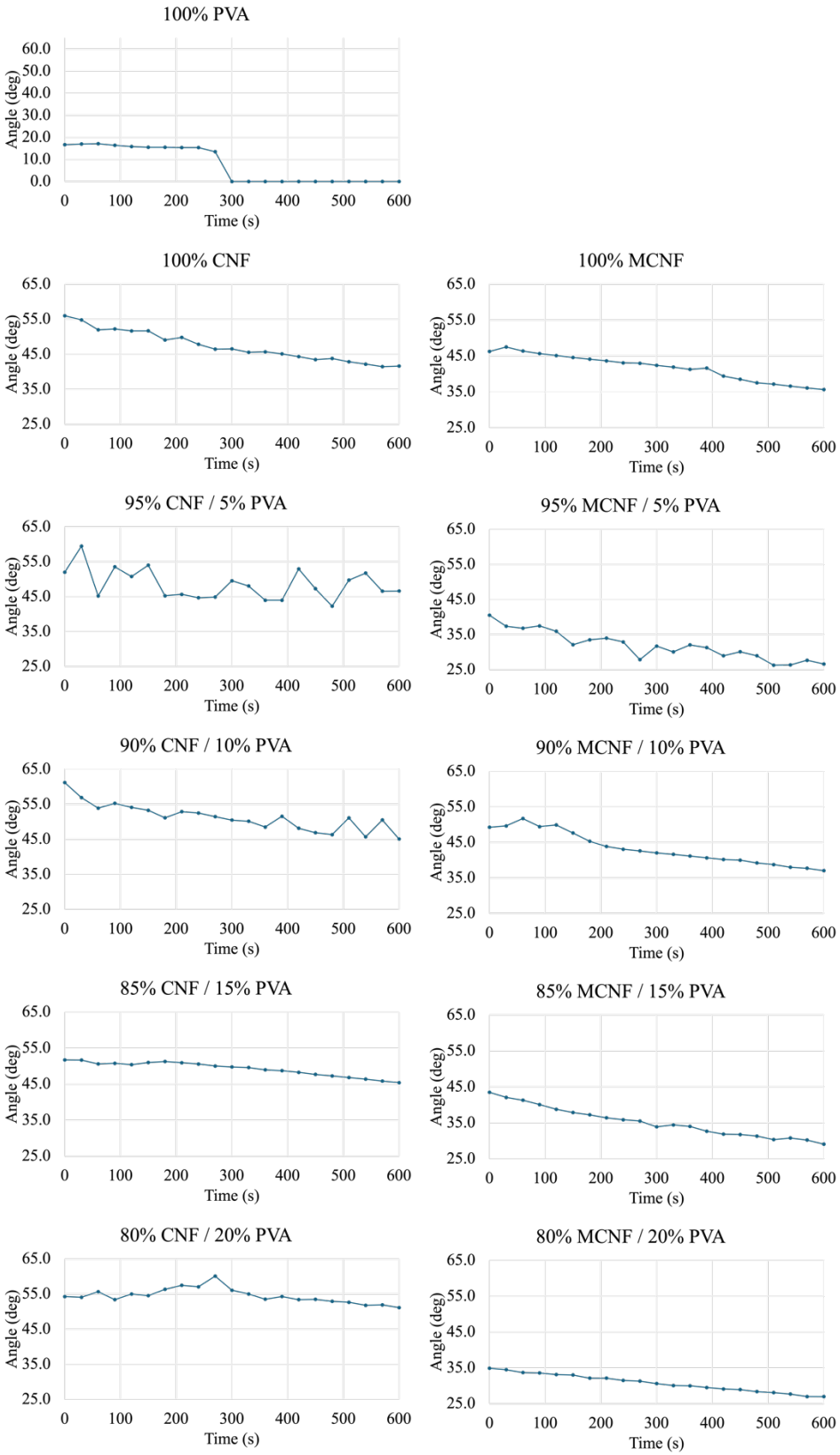


Figure A22. Comparison of measured static contact angle of CNF/PVA and MCNF/PVA composite films over 10 minutes. A contact angle measurement was calculated every 30 seconds.

Film composition	Average static contact angle of matte side (deg)	Standard deviation
100% PVA	19.64	2.89
100% CNF	55.25	1.48
100% MCNF	52.37	8.84
95% CNF / 5% PVA	49.28	3.67
90% CNF / 10% PVA	35.38	6.76
85% CNF / 15% PVA	40.31	3.10
80% CNF / 20% PVA	28.94	2.10
95% MCNF / 5% PVA	50.32	2.30
90% MCNF / 10% PVA	49.23	1.84
85% MCNF / 15% PVA	50.32	2.30
80% MCNF / 20% PVA	42.66	8.21

Table A24. Average measured static contact angle of the matte side of CNF/PVA and MCNF/PVA composite films. Three data points were measured to calculate the average contact angle.

Film composition	Average static contact angle of glossy side (deg)	Standard deviation
100% CNF	56.22	11.60
100% MCNF	35.98	0.77
95% CNF / 5% PVA	65.54	5.99
90% CNF / 10% PVA	45.28	6.58
85% CNF / 15% PVA	52.73	8.50
80% CNF / 20% PVA	46.15	2.66
95% MCNF / 5% PVA	47.01	7.78
90% MCNF / 10% PVA	50.01	2.13
85% MCNF / 15% PVA	41.60	11.64
80% MCNF / 20% PVA	46.76	2.57

Table A25. The average measured static contact angle of the glossy side of CNF/PVA and MCNF/PVA composite films. Three data points were measured to calculate the average contact angle. Note, there is no glossy side of 100% PVA films as the two sides were undistinguishable.

Film composition	Average advancing contact angle of matte side (deg)	Average receding contact angle of matte side (deg)	Hysteresis (deg)
100% PVA	19.08	0.00	19.08
100% CNF	77.63	56.71	20.93
100% MCNF	77.25	51.87	25.39
95% CNF / 5% PVA	44.81	34.47	10.35
90% CNF / 10% PVA	51.61	43.31	8.31
85% CNF / 15% PVA	68.98	45.06	23.92
80% CNF / 20% PVA	51.03	43.80	7.24
95% MCNF / 5% PVA	88.78	63.03	25.74
90% MCNF / 10% PVA	86.87	63.37	23.50
85% MCNF / 15% PVA	93.78	72.61	21.17
80% MCNF / 20% PVA	90.18	63.96	26.22

Table A26. Average measured dynamic contact angle of the matte side of CNF/PVA and MCNF/PVA composite films. Eight data points were measured to calculate the average advancing angle and at least five data points to calculate the average receding contact angle.

Film composition	Average advancing contact angle of glossy side (deg)	Average receding contact angle of glossy side (deg)	Hysteresis (deg)
100% CNF	55.97	32.51	23.47
100% MCNF	60.61	34.59	26.02
95% CNF / 5% PVA	55.71	44.05	11.66
90% CNF / 10% PVA	54.60	43.73	20.52
85% CNF / 15% PVA	59.59	42.23	17.36
80% CNF / 20% PVA	65.63	51.10	14.54
95% MCNF / 5% PVA	54.05	32.07	21.99
90% MCNF / 10% PVA	52.01	31.49	20.52
85% MCNF / 15% PVA	95.05	61.11	33.94
80% MCNF / 20% PVA	74.25	46.87	27.38

Table A27. Average measured dynamic contact angle of the glossy side of CNF/PVA and MCNF/PVA composite films. Eight data points were measured to calculate the average advancing angle and at least five data points to calculate the average receding contact angle. Note, there is no glossy side of 100% films as the two sides were undistinguishable.